

UNIVERSIDAD SAN FRANCISCO DE QUITO USFQ

Colegio de Ciencias e Ingenierías

**Design and Construction of a Human
Powered Vehicle**

**Francisco Xavier Plaza Calle
Mateo Nicolás Andrade Nicolalde
José Luis Paredes Dueñas**

Ingeniería Mecánica

Trabajo de fin de carrera presentado como requisito
para la obtención del título de
Ingeniero Mecánico

Quito, 13 de mayo de 2020

Universidad San Francisco de Quito USFQ

Colegio de Ciencias e Ingenierías

HOJA DE CALIFICACIÓN DE TRABAJO DE FIN DE CARRERA

Design and Construction of a Human Powered Vehicle

**Francisco Xavier Plaza Calle
Mateo Nicolás Andrade Nicolalde
José Luis Paredes Dueñas**

Calificación:

A

Nombre del profesor, Título académico

**Juan Sebastián Proaño Avilés,
Ingeniero Mecánico, PhD**

Quito, 13 de mayo de 2020

DERECHOS DE AUTOR

Por medio del presente documento certifico que he leído todas las Políticas y Manuales de la Universidad San Francisco de Quito USFQ, incluyendo la Política de Propiedad Intelectual USFQ, y estoy de acuerdo con su contenido, por lo que los derechos de propiedad intelectual del presente trabajo quedan sujetos a lo dispuesto en esas Políticas.

Asimismo, autorizo a la USFQ para que realice la digitalización y publicación de este trabajo en el repositorio virtual, de conformidad a lo dispuesto en el Art. 144 de la Ley Orgánica de Educación Superior.

Nombres y apellidos: Mateo Nicolás Andrade Nicolalde

Código: 00124590

Cédula de identidad: 1003199229

Lugar y fecha: Quito, mayo de 2020

DERECHOS DE AUTOR

Por medio del presente documento certifico que he leído todas las Políticas y Manuales de la Universidad San Francisco de Quito USFQ, incluyendo la Política de Propiedad Intelectual USFQ, y estoy de acuerdo con su contenido, por lo que los derechos de propiedad intelectual del presente trabajo quedan sujetos a lo dispuesto en esas Políticas.

Asimismo, autorizo a la USFQ para que realice la digitalización y publicación de este trabajo en el repositorio virtual, de conformidad a lo dispuesto en el Art. 144 de la Ley Orgánica de Educación Superior.

Nombres y apellidos: Francisco Xavier Plaza Calle

Código: 00130030

Cédula de identidad: 1722827233

Lugar y fecha: Quito, mayo de 2020

DERECHOS DE AUTOR

Por medio del presente documento certifico que he leído todas las Políticas y Manuales de la Universidad San Francisco de Quito USFQ, incluyendo la Política de Propiedad Intelectual USFQ, y estoy de acuerdo con su contenido, por lo que los derechos de propiedad intelectual del presente trabajo quedan sujetos a lo dispuesto en esas Políticas.

Asimismo, autorizo a la USFQ para que realice la digitalización y publicación de este trabajo en el repositorio virtual, de conformidad a lo dispuesto en el Art. 144 de la Ley Orgánica de Educación Superior.

Nombres y apellidos: José Luis Paredes Dueñas

Código: 00124173

Cédula de identidad: 1715418750

Lugar y fecha: Quito, mayo de 2020

ACLARACIÓN PARA PUBLICACIÓN

Nota: El presente trabajo, en su totalidad o cualquiera de sus partes, no debe ser considerado como una publicación, incluso a pesar de estar disponible sin restricciones a través de un repositorio institucional. Esta declaración se alinea con las prácticas y recomendaciones presentadas por el Committee on Publication Ethics COPE descritas por Barbour et al. (2017) Discussion document on best practice for issues around theses publishing, disponible en <http://bit.ly/COPETHeses>.

UNPUBLISHED DOCUMENT

Note: The following capstone project is available through Universidad San Francisco de Quito USFQ institutional repository. Nonetheless, this project – in whole or in part – should not be considered a publication. This statement follows the recommendations presented by the Committee on Publication Ethics COPE described by Barbour et al. (2017) Discussion document on best practice for issues around theses publishing available on <http://bit.ly/COPETHeses>.

RESUMEN

La búsqueda de nuevas formas de transporte es un tema relevante en la investigación ingenieril actual. Las personas están cambiando sus patrones de consumo hacia formas de transporte más sostenibles y limpias. Con esto en mente, la Asociación Americana de Ingenieros Mecánicos propone un concurso regional anual para la construcción de un vehículo de tracción humana. Se ha propuesto representar a la USFQ en el concurso del 2020 en la universidad UNAM. Este tipo de vehículo es una solución apropiada para viajes de distancias intermedias en áreas urbanas. Por esto, el siguiente trabajo detalla la etapa de diseño del primer prototipo desarrollado por la universidad. Esté cubre temas como la descripción del problema y análisis del mismo, metodologías de selección, el diseño del concepto, el diseño de detalle, simulaciones de elementos finitos de componentes críticos, y plan de pruebas y de manufactura. El diseño elegido fue el de una bicicleta semi reclinada con dos llantas frontales hecha de acero estructural ASTM A500. Se decidió sacrificar el peso del vehículo al usar un acero común fácil de encontrar en el país para reducir el presupuesto de prototipaje del vehículo y mejorar sus propiedades de mecanizado. Los componentes externos seleccionados para este vehículo son Shimano. El trabajo futuro se relaciona al plan de manufactura y pruebas para futuras optimizaciones del diseño.

Palabras clave: Vehículo de Tracción Humana, ASME, Análisis de Elementos Finitos, Diseño Mecánico, Sistema de Dirección, Chasis, Sistema de Tracción

ABSTRACT

Nobel alternatives for transportation has been a trending topic within engineering research. People is shifting to cleaner and sustainable ways to transport. Within this effort, the American Society of Mechanical Engineers proposes annually a regional contest to develop a Human Powered Vehicle. We have proposed to represent USFQ in the 2020 contest in UNAM university. This type of vehicle seems to be an appropriate solution for mid-distance travel and daily commutes in urban areas. Therefore, the following paper details the design stage of the first prototype developed. It covers the problem's framing and analysis, selection methodologies, concept design, detail design, finite element analysis of its critical components, manufacturing, and testing plans. The design choice was a tadpole semi-recumbent bike made of ASTM A500 structural steel. It was decided to sacrifice the vehicle's weight by using common structural steel alloy to reduce prototyping budget and gain manufacturing easiness. Shimano external components were selected to be used in this trike. Future work will be related to manufacture and test this design for later optimizations.

Key Words: Human Powered Vehicle, ASME, Finite Element Analysis, Mechanical Design, Direction System, Chassis, Drivetrain

TABLE OF CONTENTS

LIST OF FIGURES	12
LIST OF TABLES	16
INTRODUCTION	17
Problem Statement	18
In-use purposes and market	19
Unintended uses	19
Special feature.....	19
Service environment	20
Safety	20
Problem Specification.....	21
Objective	21
Requirement List.....	21
Design Constrains	21
State of the Art.....	23
Design Concepts & Selections.....	25
Design Constrains	25
Topics.....	26
Analysis.....	27
Project Management	39
Budget.....	39

	10
Schedule	40
Engineering Standards	41
MATERIALS AND METHODS	43
Material and Component Selection.....	43
Gearing.....	43
Design for Manufacturing.....	49
Manufacturing Pan.....	49
Assembly.....	50
Cost	50
Maintenance.....	50
Life Cycle Assessment.....	50
RESULTS AND DISCUSSION	52
Design Report	52
Prototype Test Plan.....	54
Safety Through Design	58
Results, discussion, and conclusions	60
Future Work.....	61
References.....	63
APPENDIXES	65
Appendix A - Engineering drawings and detailed calculations.....	65
Drawing List	65

	11
Assembly Drawings	66
Chassis Drawings.....	70
Direction System Drawings	86
Engineering Analysis	91
Automatic Control	142
Matlab Codes	146
Arduino Codes	170
Appendix B – Project Management	171
Material and Component Selection Tables	171
Design for Manufacturing.....	178
Gantt Chart.....	179
Budget and Expenses Report	180
Appendix C – Maintenance and Operating Manual	181
Operation Manual	181
Maintenance Manual.....	183

LIST OF FIGURES

Figure 1 Safety Brake Example	29
Figure 2 Automatic shifting	29
Figure 3 Electric engine with energy regeneration system (Taris Keiper, 2020)	30
Figure 4 Slope Assistant Sketch (Archibald, 2016).....	30
Figure 5 Front Wheel Drive.....	31
Figure 6 Simple Rear Wheel Drive.....	32
Figure 7 All Wheel Drive	33
Figure 8 Complex Chain Wheel Drive (Archibald, 2016).....	33
Figure 9 Front Wheel Steer (Ihsen, 2019)	34
Figure 10 Hovercraft Rear Steering	35
Figure 11 All Wheel Steering (Moog, 2018).....	35
Figure 12 Tadpole Concept (Mahmood, 2015).....	36
Figure 13 Delta Concept (Mustain, 2019)	37
Figure 14 Quad Concept (Hinsenkamp, 2017)	37
Figure 15 Handlebar (De Silvestri, 2019).....	38
Figure 16 Steering Levers (Mahmood, 2015).....	38
Figure 17 Steering Wheel (Laaribi, 2019)	39
Figure 18 Ilalo's Budget Distribution Within Subsystems.....	40
Figure 19 ISO Tire Size Interpretation (Archibald, 2016).....	43
Figure 20 Gearing Information	46
Figure 21 Equivalent Gearing Developments.....	47
Figure 22 Speed Ranges for Each Gear.	47
Figure 23 Design for manufacturing.....	49
Figure 24 Ilalo Prototype Final Render	53

Figure 25 HPV Basic linear dimensions.....	53
Figure 26 Shimano Alivio FC-M4050.....	91
Figure 27 Decomposition of force in the rotation (Höchtl, 2010).....	92
Figure 28 Distribution of pedaling force along the rotation (Höchtl, 2010).....	92
Figure 29 Adaption of the tangential and radial force along the rotation (Höchtl, 2010)	93
Figure 30 Pedaling force application	94
Figure 31 7% proportional mesh.....	95
Figure 32 5% proportional mesh.....	95
Figure 33 3% proportional mesh.....	95
Figure 34 1% proportional mesh.....	96
Figure 35 Maximum stress polar graph.	96
Figure 36 Von Mises stress distribution on a critical scenario.	97
Figure 37 Stress concentrator in a critical scenario.	98
Figure 38 Displacement distribution on a critical scenario.	99
Figure 39 Static Loads Under Different Slope Grades.	101
Figure 40 Traction Force Steady State Slopes.....	102
Figure 41 Max Acceleration Force Study.....	104
Figure 42 Max Vehicle Acceleration Study.....	104
Figure 43 Front Wheel Turning Reaction Force.....	106
Figure 44 Rear Wheel Turning Reaction Force.....	106
Figure 45 Centripetal Force for Different Turning Velocities.....	107
Figure 46 First Chassis Concept	109
Figure 47 FEA Set-up.	111
Figure 48 FEA Critical Scenario Display.	112
Figure 49 Final Chassis Design Concept.....	113

Figure 50 Bottom Bracket Mount.....	115
Figure 51 Rear Wheel Caliper Mount.....	116
Figure 52 Rear Wheel Right & Left Dropouts.....	116
Figure 53 Seat Design in context with the full assembly.....	117
Figure 54 Final Chassis Design	118
Figure 55 Final Chassis Mesh (9332 elements).....	119
Figure 56 Mesh Independence Identification.	119
Figure 57 SimSolid Drop Test Result.....	121
Figure 58 SimSolid Back Crash Load Case Simulation.	121
Figure 59 Rear Wheel Dropout FEA Analysis.	122
Figure 60 Caliper Mount FEA.	123
Figure 61 Critical Weld Scenario Simplification Sketch.....	124
Figure 62 Side definition of the vehicle terms.....	126
Figure 63 Front definition of the vehicle terms (Archibald, 2016).....	126
Figure 64 Ackerman Steering Angle for Tadpole Design (Archibald, 2016).....	127
Figure 65 Track Rod Mechanism Neutral Steer (Archibald, 2016).....	128
Figure 66 Track Rod Mechanism 30 degrees Steer (Archibald, 2016)	128
Figure 67 Track Rod Parameters (Archibald, 2016).....	129
Figure 68 Kinematic Diagram of Steering Mechanism.	131
Figure 69 Track Rod Steering Angle Error.....	131
Figure 70 Track Rod Steering Angle.....	132
Figure 71 High Speed Cornering Parameters (Archibald, 2016).....	136
Figure 72 Understeer Gradient.....	137
Figure 73 Steer Angle vs Speed and Rollover Threshold.....	138
Figure 74 Lateral Acceleration vs Speed.....	138

Figure 75 Kinematic Diagram of Six Bar Steering Mechanism.....	140
Figure 76 Six Bar steering Angle for Outside Wheel.....	140
Figure 77 Six Bar Steering Angle Error for Outside Wheel.....	141
Figure 78 Automatic Control Schematic	143
Figure 79 Switch Simulation	144
Figure 80 App Interface	145

LIST OF TABLES

Table 1 Engineering Standards	41
Table 2 Engineering Analysis Plan.....	52
Table 3 Summary of the test planification.....	54
Table 4 Risk Analysis	58
Table 5 Preliminary FEA Results.	112
Table 6 Ilalo External Components Selection	114
Table 7 ANSYS chassis FEA Analysis.	120
Table 8 Cornering Tire Properties (Archibald, 2016).....	136

INTRODUCTION

The following senior project consists in the development of a Human Powered Vehicle to compete in the annual HPVC (Human Powered Vehicle Challenge) contest organized by ASME LATAM in Mexico. A human powered vehicle can be defined as a vehicle whose sole power input is human generated. The relevance of this project regards sustainable transportation alternatives for urban areas. Therefore, this vehicle must fit a single average Ecuadorian male and female rider for commuting and daily use in an urban area and be safe enough to ride at medium speeds. Within the most important design parameters considered were weight, manufacturability, production cost and ergonomics. With this consideration, we have decided to develop a structural steel semi-recumbent tadpole trike with rear power transmission.

The vehicle designed was divided into three subassemblies. The powertrain or transmission is concerned in the component selection for appropriate power transmission from the user to the rear wheel. The structural or chassis subassembly design the main structure of the vehicle. Its job is to give an efficient and lightweight support for the functional subassemblies. The direction or drivetrain subassembly regards the vehicle maneuverability.

In the following document, a detail explanation of the design process for each subassembly is presented. Shimano components of medium tier were selected due to price and performance. For the chassis, three different round tube profiles were selected to achieve lightweight and stiff characteristics. A track rod mechanism was selected to control the vehicle. The benchmark for a first-generation prototype was reached in this design. The expected prototyping cost will be around \$1800.

Regarding manufacturing, it is expected to start the construction of the prototype as soon the sanitary emergency is over. Once the vehicle is built, the test plan presented below should be executed. This will assist the team on validating the design and understanding better loading scenarios. Information on the vehicle stress conditions and stiffness will help to optimize the design for future iterations.

For future work, the team should focus on reducing the vehicles weight and improving its stiffness. Also, iterating to achieve maximum user comfort will be crucial for the project success in the market. This should include the implementation of weather protection systems, IoT and E-bike modularity, and night drive lights.

Problem Statement

According to the ASME HPVC rulebook, the objective of the contest is to apply sound engineering principles towards the development of practical, efficient, and sustainable human-powered vehicles. Global warming and increasing pollution levels have shifted research into sustainable ways of transportation. Also, rising traffic in rural areas due to daily commute made them bet on different transportation techniques such bicycles. European cities such Amsterdam and Copenhagen are good examples of this transition. Also, share riding platforms, such Uber, have presented its own solution to this issue. Uber Bike and Bird are apps that offer alternative transportation methods to address mobility issues and traffic in big rural areas. The problem that these solutions have in common is that bicycles, and other human powered vehicles proposed, were not designed to share lanes with cars and they are not safe to use in traffic. Although some cities may have the budget to invest in the construction for specific lanes for bicycles, that is not the case for Ecuador. Therefore, the necessity of developing an alternative transportation way for daily use in rural areas that is environmentally friendly and safe to use.

This vehicle shall win the ASME E-Fest 2020. It should provide reliable year-round single-person transportation in an uneven urban area. Expected usage includes personal transport, commuting, shopping, and recreation. The operator must be provided reasonable protection against the elements, and vehicle maintenance should be minimized. The vehicle should be comfortable, easy to operate and easy to propel. Expected environmental conditions are wind and sunlight within temperatures from 5 to 25 °C. The vehicle should be safe to drive at night and comfortable to ride in hilly areas.

In-use purposes and market

To provide clean, cheap, and efficient personal transportation for typical daily tasks in an urban area.

Unintended uses

- Operating in rough terrain
- Operate in heavy weather conditions

Special feature

- Light system for safety when riding in the night
- Cargo space for daily tasks.
- Interactivity vehicle-user through IoT.
- Parking lock included
- Reduce maintenance and no exposed dynamic components

Competitor

- Public and private motorized transportation
- Regular bicycles available in the market
- Kratos EAFIT previous winner of HPVC ASME E-Fest

Service environment

Region: The vehicle should provide comfortable and safe transport in temperate climates in urban areas day and night.

Road Surface: The vehicle shall be operable without significant service or life penalty on road surfaces ranging from smooth asphalt, concrete, stone pavement and broken asphalt.

Weather: The vehicle shall be operable in rain, wind, and slush. It should be corrosion resistance to ride in wet conditions.

Temperature: The vehicle should be safe and operable in temperature ranging from 5 to 30 Celsius.

Safety

Hazards: There should be no hazards such sharp edges, open tubes, or pinch-points that could harm the operator in normal vehicle operations.

Crashworthiness: The vehicle shall be able to sustain a head-on collision from 1.3 m/s with no permanent deformation. Vehicle fairings should withstand normal handling of the vehicle, including a person leaning of the fairing.

Problem Specification

Objective: To design, build, and test an innovative, efficient, practical, and sustainable Human Powered Vehicle (HPV).

Requirement List: The requirement list is found in the rule book of ASME 2020 HPVC competition.

Design Constrains

Must

1. The vehicle must be able to fit a single driver of height up to 1.85 meters.
2. The vehicle should weigh less than 25 kg.
3. The vehicle should cost to prototype less than 1500 USD.
4. The vehicle size should be less than 2.5 meters L, 1.5-meter W, and 1.5-meter H.
5. The vehicle must have a minimum turning radio of 8 meters.
6. The vehicle must be able to drive 30 meters on a straight line at a speed of 5-8 km/h on a flat paved road.
7. The vehicle must be able to make a 3 second full stop without external intervention.
8. The vehicle must have a minimum clearance from the ground of 0.10 meters.
9. The vehicle must have space to paste two stickers of dimensions 35x30 cm.
10. The vehicle must be easy to access for an average Ecuadorian user.
11. The vehicle must have a Roll Over Protection device that keeps the driver away from the floor at all circumstances.
 - a. It must hold a 2670 N load at 12 degrees from the vertical axis.
 - b. It must hold a 1330 N horizontal load applied at shoulder height.
12. The vehicle must have a safety harness of minimum 4 points with safety certification.

13. The vehicle must be free of sharp edges, and all internal gear should not contact the user at any circumstance.
14. The vehicle must have storing space enough to fit a box of 13x8x15 inches.
15. The vehicle must reach 40 km/h within 10 seconds.
16. The vehicle must be able to full stop from 25 km/h within 6 meters.
17. The vehicle must have any form of automatic control.
18. The vehicle must be able to fit in a pits area of 2.6x4.9 meters with full maintenance team and equipment.
19. The vehicle must be able to drive up a slope of 5% and drive down a 7% slope with average human power and safety conditions.
20. The vehicle must be able to give maintenance by a single person.
21. The vehicle should follow the minimum aesthetic requirements presented by the marketing team.

Maybes

1. The vehicle should have a drag coefficient of less than 0.25.
2. The vehicle should provide protection from rain, wind, and sunlight to the user.
3. The vehicle may have a trailer linkage of 2in ID.
4. The vehicle may be able to support a second passenger.
5. The vehicle may have an Automatic Braking System (ABS)
6. The vehicle may have a Generative Breaking System.
7. The vehicle may have an electric motor to aid transportation in Cumbayá.
8. The vehicle may have an automatic lock system.
9. The vehicle may have an audio Bluetooth system upgrade capability.

Constrains

1. Security
2. User comfort
3. Price
4. Manufacturing time
5. Aesthetics
6. Feedback to the user
7. IoT Upgrade Capability
8. Maintenance easiness
9. Modularity
10. Monitorability
11. Environmentally friendly
12. Efficiency

State of the Art

Human Powered Vehicles will become a novel, trending solution for urban mobility in the new century. With the appearance of E-Bikes as an environmentally friendly, non-expensive solution for travelling medium distances, some developed cities have adapted their policies to be more biking friendly. Moreover, information technologies rising from the 5G industry will create new opportunities for transportation technologies connected to the grid. This paper will explore why Human Powered Vehicles will be important in the future for human transportation analyzing E-Bikes and current trends in non-motorized transportation systems.

Human Powered Vehicles assisted with E-Bike technologies are the future of transportation. According to Hung & Lin, some countries will ban fossil fuel motorized vehicles by 2040 because of its GHG emissions. Also, this is sustained by the fact that in the

last 10 years E-bikes usage have increased in more than 100 times (Hung & Lim, 2020). This fast adoption of this transportation method is due to its size, it is small and traverse a variety of grounds. They also allow people to avoid traffic jams, and they do not have mayor legal restrictions in the cities (Hung & Lim, 2020). Nonetheless, pollution of these kind of vehicle can also be significant due to its product life cycle and well-to-wheel emissions. To avoid this last type of pollution, driver should be willing to drive in temperature bellow 10 C. Human Powered Vehicles can address this issue giving better weather isolation than E-Bikes to drivers. There exist three different types of E-Bikes: pure E-Bikes, Powered-assistance, and mixed. The pure ones do not require pedaling, the Powered-assisted aid the cycles pedaling according to the load exert, and the mixed ones do a fusion of both previous types. For H.P.V, the powered isolation modeled seem to be the more optimal. Although there are no major regulations, the power-size of electric motors is restricted to less than 750W in Unite States and 250W in Europe, India, and Japan.

On the other hand, Smart Cities will create opportunities for new ways of transportation. These are cities where 5G communication technologies allows interactivity between city planners, users, and products. This will allow better communication and transportation efficiently, but it will also require major improvements in transportation products. For the year, 2050 it is predicted that more than 70% of population will live in urban areas. A clear example in the bicycle fleet in Copenhagen with GPS and a tablet in the handlebar. The idea is to implement big data in this transportation technology. The issues are the privacy lost that this kind of technologies cause (Frauke, 2016).

Because of these coming changes in urban planning and environment concerns, Human Powered Vehicle well designed can be the perfect breach between comfort transportation, efficiency, and sustainability. Although, a lot of studies are yet to be done in muscle performance and comfort in this kind of vehicles.

Design Concepts & Selections

Design Constrains

To select the adequate design alternatives for our Human Powered Vehicle, the following constrains have been define based on its relevance to the project.

Cost

The monetary cost of pursuing the design alternative. This includes cost of raw materials, manufacturing and assembling.

Manufacturability

The easiness of the materials and parts to be manufactured. As college students we do not have access to expensive, complicated manufacturing techniques.

Weight

The overall extra weight the alternative will add to the prototype. This is important because we are pursuing a lightweight, efficient human powered vehicle.

Efficiency

The efficiency of transferring torque from the cranks to the wheel.

Maintenance

The level of maintenance that will be required of the questioned alternative is selected. It is important to be quick in repairments and troubleshooting during the race.

Durability

The resistance of the alternatives to wear off. This is important due to the long lifetime requirement of our vehicle.

Stability

The stability of the selected alternative. This is important because we want to accomplish to design a vehicle easy to operate at low speeds.

Benefit to the user (BtU)

The added value that the alternatives will give to the end of user of the vehicle. We want to design a product practical for urban daily transport.

Comfort

The level of comfort that the alternative will bring to the user. This is important for a product design perspective.

Topics***Materials***

The materials to be considered are: Steel 1018, Steel 4130, Aluminum and Bamboo.

Traction

The traction systems to be considered are: FWD (Front Wheel Drive), SRWD (Simple Rear Wheel Drive), AWD (All Wheel Drive) and CRWD (Complex Chain Rear Wheel Drive).

Direction

The direction systems to be considered are: FWS (Front Wheel Steering), RWS (Rear Wheel Steering) and AWS (All Wheel Steering).

Automatic Control

The automatic control Systems to be considered are: Safety Brake, Automatic Gear Change, Slope Assist and Electric Engine with Energy Regeneration System.

Chassis Configuration

The chassis configuration to be considered are: Tadpole, Delta, and Quad.

Interface

The interface systems to be considered are: Steering Levers, Steering Wheel, and Handlebar.

Analysis

The tables used in the analysis of the different options can be found in Appendix A.

Materials

For the materials analysis, the main constrains selected were cost, manufacturability, weight, and endurance. These together sum up the most important criteria that a material should have in order to be considered for chassis design.

- Steel AISI 1018: This is the most common inexpensive steel. It is easy to manufacture and weld. It is more heavy than other alloys such aluminum, but similar in weight to low alloy steels such 4130. The biggest drawbacks are the tendency to corrode and its relatively high density (M. Archibald, 2016).

- Steel AISI 4130: This is a higher quality steel for frames that use a chromium-molybdenum steel. It has higher strength, good weldability. However, this is harder to obtain in the country. There are a variety of different tube diameters of this material. It has high tensile strength, but it is harder to bend although it is possible for smaller diameters. During welding it is important to avoid fast cooling of this material because it can become brittle. It is harder to process, and just a little more expensive than AISI 1018 (M. Archibald, 2016).
- Aluminum Alloys: This are more expensive than steel alloys although they have a smaller density. It is harder to manufactured, and its mechanical properties are lower than alloy steels (M. Archibald, 2016).
- Bamboo: This is a non-metallic material for structures. It has inferior mechanical properties than metallic components, however it has a comparable price with low-carbon steels and significant lower density. Bamboo can have high performance with relative low cost (M. Archibald, 2016). It has a less manufacturing freedom than steel.

The selection chart is in Appendix A. It is important to mentioned than lower prices, low density, high manufacturability, and high durability are consider beneficial for the project.

Automatic Control

The automatic control component of our product is key for our senior project. We have determined that a Safety Brake, Automatic Gear shifts, Slope Assist and Electric Engine with Energy Regeneration System. Our design constrains for these are price, manufacturability, maintenance, weight, and user benefit.

- Safety brake: This option refers to a parking automatic brake controlled by an interface that secures the vehicle in public places when it is not in use. This is a low cost, easy to implement control solution. It is also easy to give maintenance, and it can be lightweight.

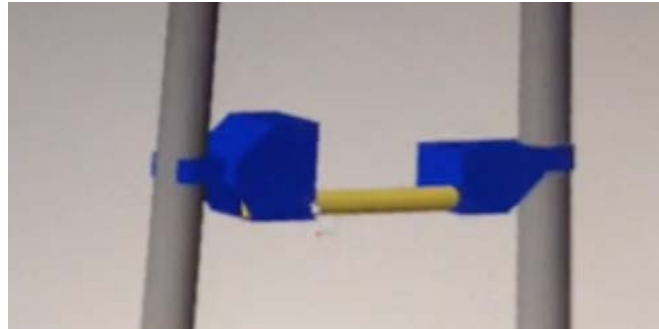


Figure 1 Safety Brake Example

- Automatic gear shift: This technology has been developed in a high level by Shimano, and it has proof to be extremely useful in avoiding wear-off of components. This has a more complex implementation, but it is also lightweight in comparison.



Figure 2 Automatic shifting

- Electric Engine with Energy Regeneration System: This is by far the most useful but more complex solution. Studies on E-Bikes have shown the wide application of pedaling assisting motors. The implementation is more complex, and it add more weight to the system. However, when it is charge, it significantly benefits the rider.

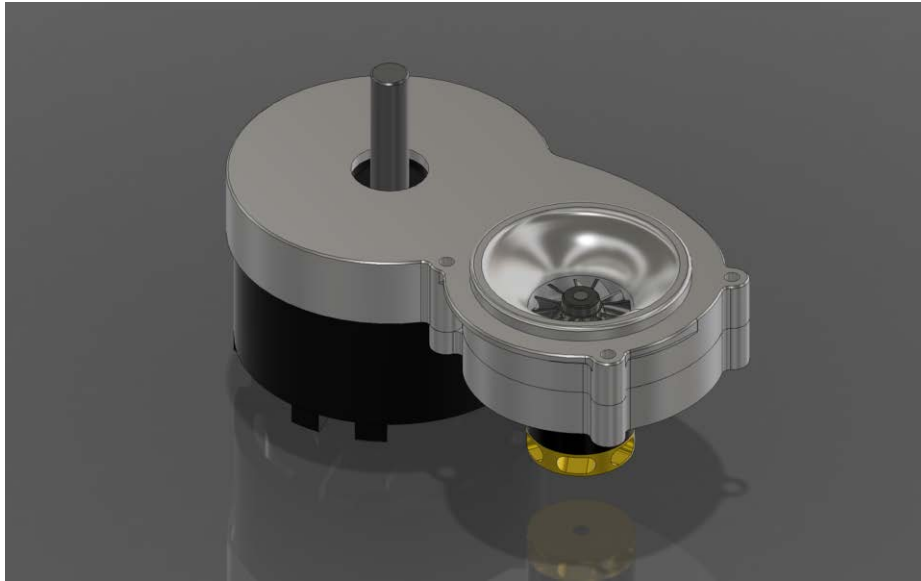


Figure 3 Electric engine with energy regeneration system (Taris Keiper, 2020)

- Slope assistance: This solution is useful for starting pedaling in slopes. It is a mechanism that slowly releases the brakes, so the bicycle does not roll down before getting enough torque. This implies an intermedium level implementation, and not too much extra weight.

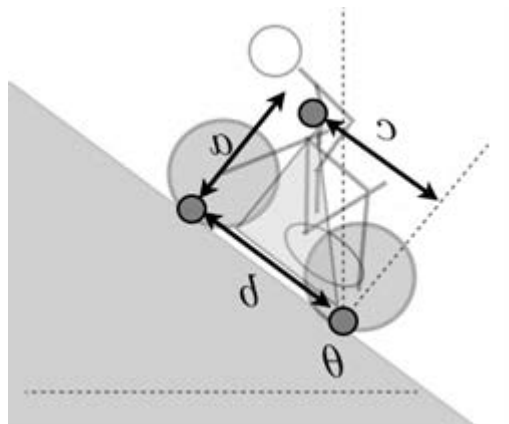


Figure 4 Slope Assistant Sketch (Archibald, 2016)

The weighted matrix of selection is in Appendix A.

Traction

For the traction analysis, the criteria *Cost*, *Manufacturability*, *Maintenance*, *Durability*, *Weight*, and *Efficiency* were considered. These all evaluate the optimal system to be able to transmit power from the vehicle pedals to the wheels.

- FWD: The Front Wheel Drive is seemingly simple traction system, in which a chain is used to transmit power from the pedals to the front axle or wheel(s). Its benefits are that it takes less space than other systems, requires less components and has a relatively simple distribution due to the proximity of the front axle to the pedals, with little chance of other vehicle components interrupting the chain path. Its downside is that its implementation is complicated depending on the suspension that is being used, as well as the possibility of a frontal directional system. These could make an FWD a complex matter to design, produce, assemble, and maintain. It can cause understeer.

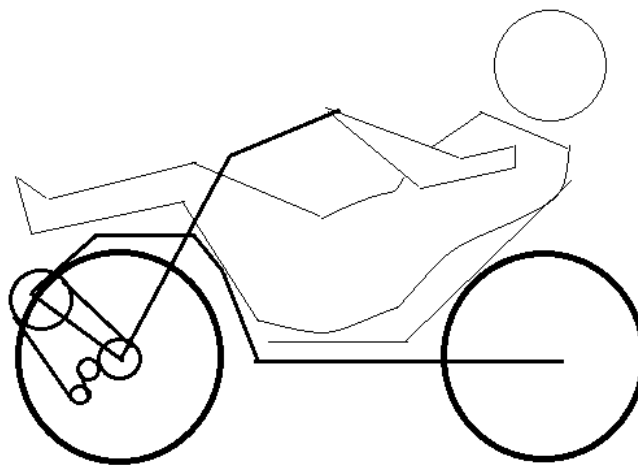


Figure 5 Front Wheel Drive

- SRWD: The Simple Rear Wheel Drive consists of a simple distribution of power from the pedals to the rear axle or wheel(s). It is characterized by its long, single chain that is distributed along the bottom of the chassis with the help of tension and chain direction mechanisms. Its benefits are relative to the FWD, but with a longer chain but

a simple setup. The downside would be that a longer chain is more exposed to damage and derailing. This also means more weight, as well as the challenges of setting up the inclination changes along the chassis.

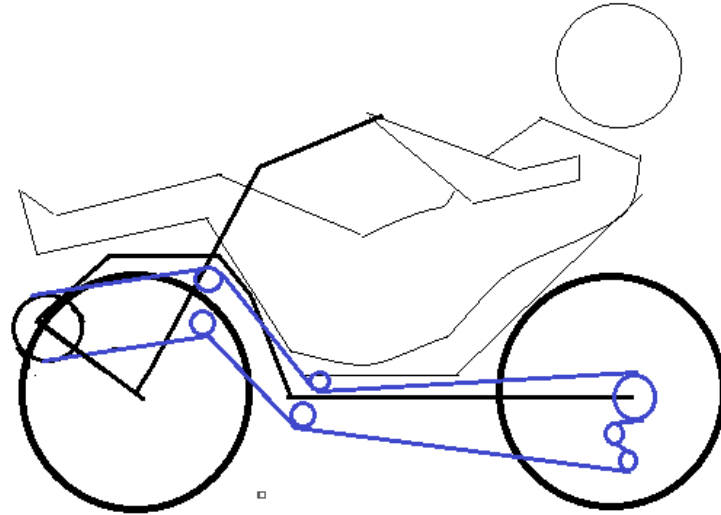


Figure 6 Simple Rear Wheel Drive

- AWD: The All-Wheel Drive is the most complex possibility, with a system of chains providing power to every wheel in the vehicle. While it has the most potential torque (depending on the final design), and more overland uses, the AWD has so many delicate components and difficulties in assembly so it is not a common design choice among the ASME competitors.

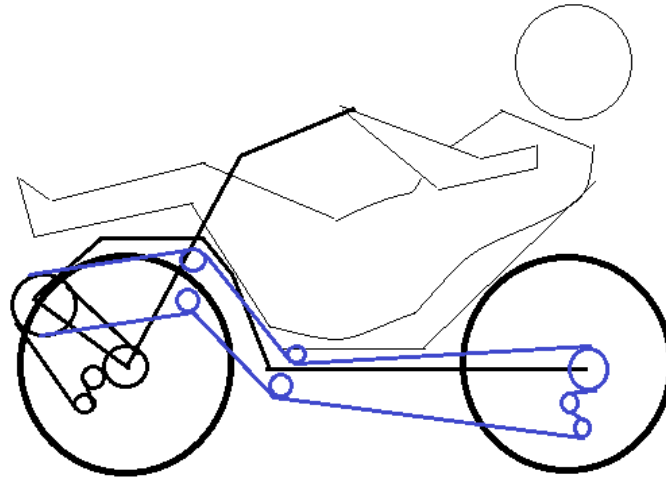


Figure 7 All Wheel Drive

- CRWD: The Complex Chain Rear Wheel Drive has a similar configuration to the SRWD, but instead of being a single chain, it is composed of two chains connected by a gear or disk. The benefits of this system would be to avoid the complex changes in inclination for the chain and adding the possibility of including a velocity change for the chains (if the gears that connect them are of different diameters). The downside of the system is that it becomes prone to malfunction under high stress and prolonged usage, as well as a slightly more complex design and development.

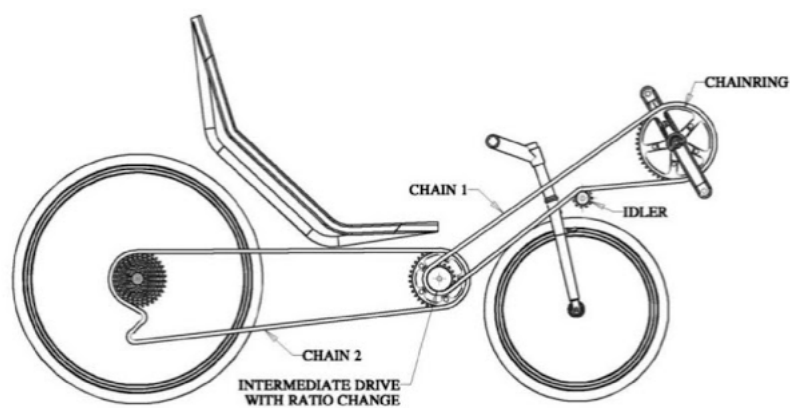


Figure 8 Complex Chain Wheel Drive (Archibald, 2016)

Direction

For the direction analysis, the criteria *Cost*, *Manufacturability*, *Weight*, *Maintenance*, and *Stability* were considered. These all evaluate the optimal system to be able to transmit force from the driver arm to steer the vehicle.

- FWS: The Front Wheel Steer is seemingly simple steer system; two arms and four attachment points are used to transmit force from the driver to the front wheels. Its benefits are that it takes less space than other systems, requires less components and has a relatively simple distribution due to the proximity of the front axle to the driver arms, with little chance of other vehicle components interrupting the steering arms travel. Its downside is that it is not the most efficient way to steer the vehicle.

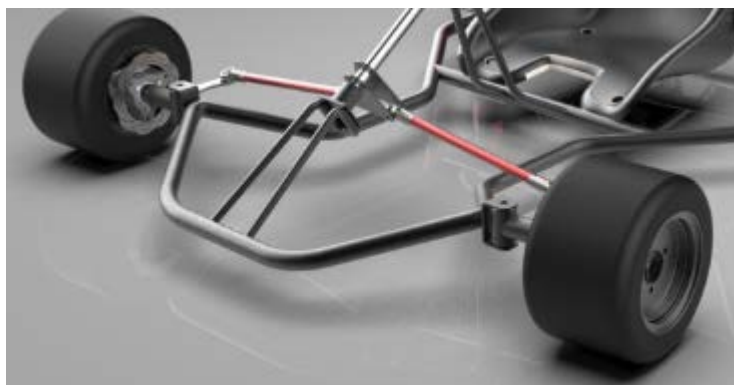


Figure 9 Front Wheel Steer (Ihsen, 2019)

- RWS: The Rear Wheel Steer is a bit more complicated to build and design, two arms and two attachment points are used to transmit force from the driver to the front wheels. Its benefits are that it takes less space on the front axle than other systems, but requires more components and has a complex distribution due to the proximity of the rear axle to the driver arms, it has a bigger chance of other vehicle components interrupting the steering arms travel and the steering angle of the rear tire would be quite small, and produces a hover-craft like handling with too much oversteer.

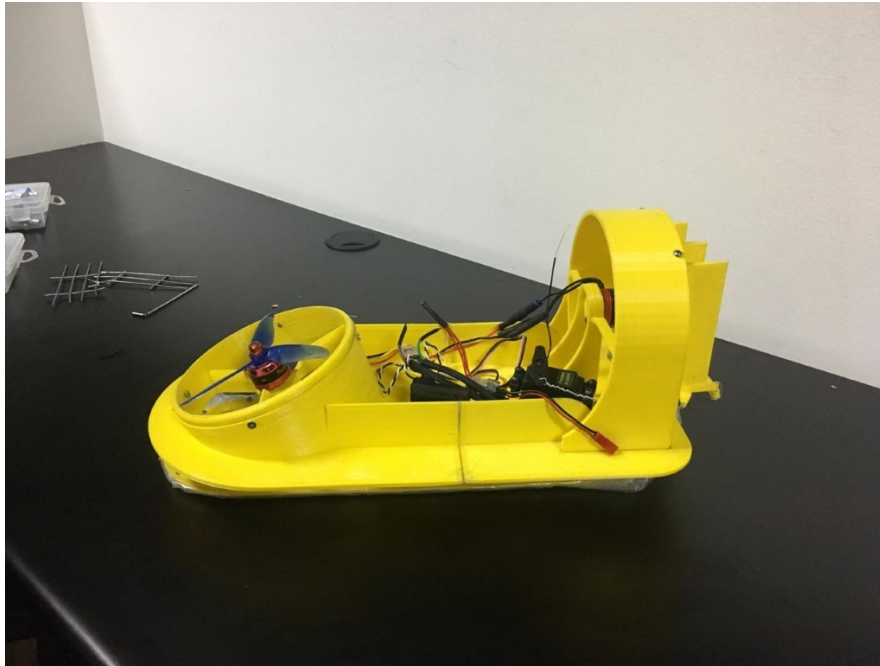


Figure 10 Hovercraft Rear Steering

- AWS: The All-Wheel steering is the most complex possibility, with a system of arms providing force to every wheel in the vehicle. While it has the most precise steering capability, and more low speed uses, the AWS has so many delicate components and difficulties in assembly, so it is not a common design choice among the ASME competitors.

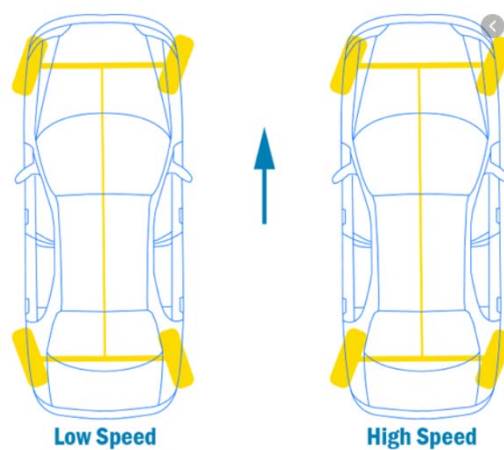


Figure 11 All Wheel Steering (Moog, 2018)

Configuration

The configuration refers to the chassis type that will be used for the main body of the vehicle. It is assumed that a recumbent system will always be used. A bicycle system is not considered because of its complete lack of stability. The criteria applied to this analysis are *Cost, Manufacturability, Weight, and Stability*.

- Tadpole: A tadpole design refers to the configuration with two wheels on a front axle and one wheel on a rear axle. This is the most widely used configuration in competitions.

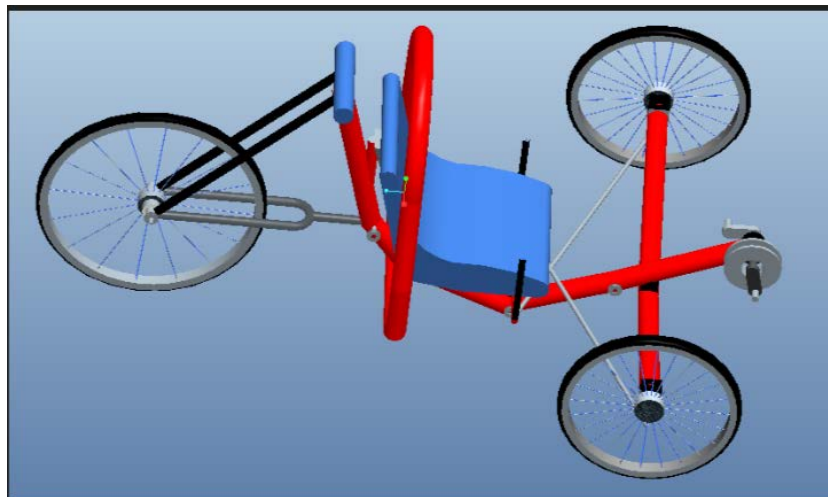


Figure 12 Tadpole Concept (Mahmood, 2015)

- Delta: The delta design is made up of one wheel in the front axle and two wheels in the rear axle. This is similar to the tadpole but has a different weight distribution.



Figure 13 Delta Concept (Mustain, 2019)

- Quad: The Quad configuration is composed of two wheels on the front axle and two wheels on the rear axle. It is not commonly used due to its increased weight.

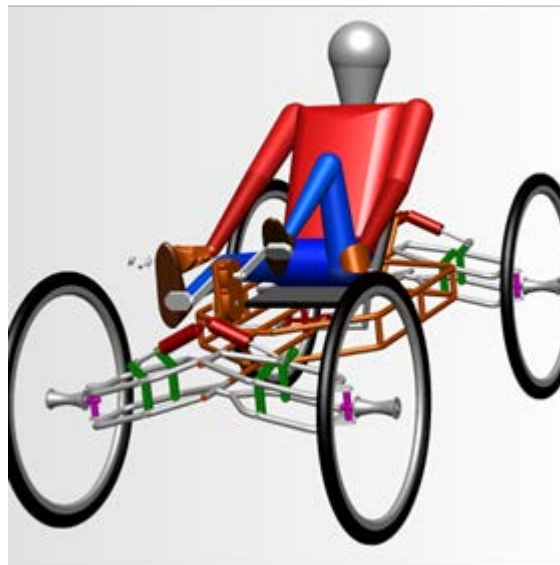


Figure 14 Quad Concept (Hinsenkamp, 2017)

Interface

The interface refers to the steering type that will be used for the main body of the vehicle. It is assumed that the driver comfort will be on play. The criteria applied to this analysis are *Cost*, *Manufacturability*, *Comfort*, and *Weight*.

- Handlebar: A handlebar refers to a bicycle like input on the direction, using a main center steering column and a handlebar, located between the driver legs.



Figure 15 Handlebar (De Silvestri, 2019)

- Steering Levers: The steering levers refers to two levers located on the side of the driver, where the vehicle could be steered with one or two of the levers, the driver will not have any problem with the legs or with the knees. This is the most widely used configuration in competitions.

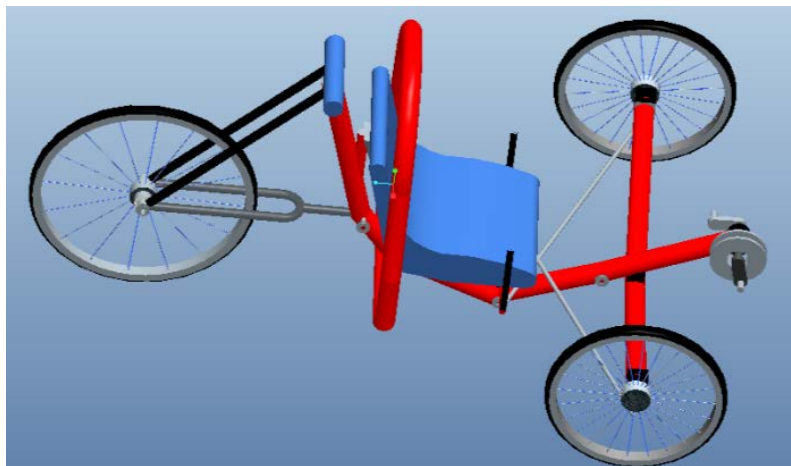


Figure 16 Steering Levers (Mahmood, 2015)

- **Steering Wheel:** A steering wheel refers to a car or go-kart like input on the direction, using a main center steering column and a steering wheel, located between the driver legs.

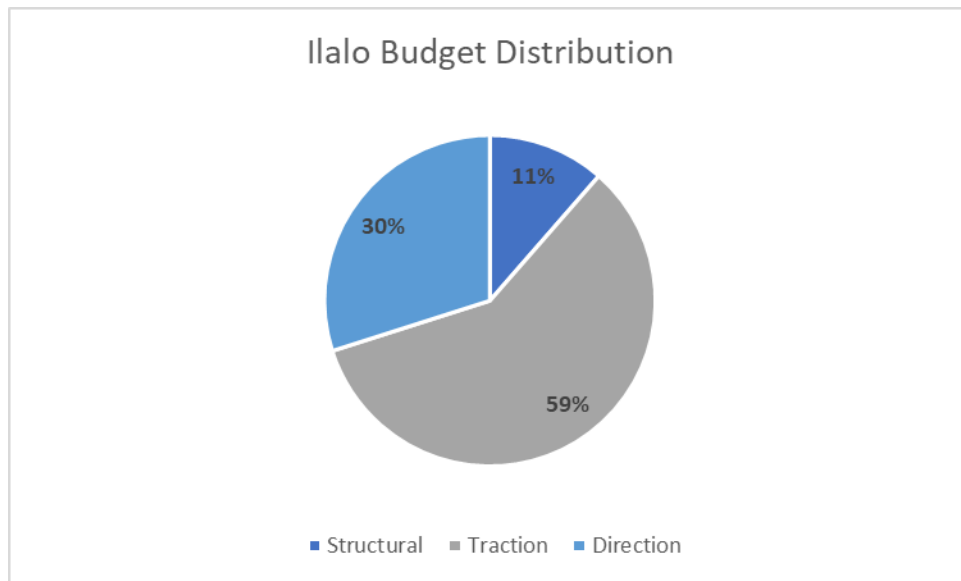


Figure 17 Steering Wheel (Laaribi, 2019)

Project Management

Budget

The initial budget for the project consists of 300 USD, provided by USFQ's Department of Mechanical Engineering. Presumably, the cost of developing the whole project is estimated around 1800 USD which is why a cash injection from the team members will eventually be necessary. That course of action will be evaluated further and implemented when needed once the initial budget starts to deplete. A detail analysis of our budget can be found in the Appendix B. The graph below shows the percentage of the total weight for each subsystem in the design. The structural subsystems require only 11% of the total budget, and the powertrain subsystem requires 59% of the overall budget.



*Figure 18 Ilalo's Budget Distribution Within Subsystems.
The biggest percentage of the prototype's budget is allocated to the powertrain components*

Schedule

The detailed timeframes for the project are detailed in the annexed Gantt Diagram. It includes information regarding the time expectations for research, the design and manufacturing of the different foreseen prototypes, simulations, and evaluations, as well as the preparation for the ASME competition. These dates were modified because of the Covid-19 Pandemic subject to modification in relation to the project progress, project changes, evaluations, and general market landscape.

Engineering Standards

Table 1 Engineering Standards

Standard	Detail	Cost
ISO 4210-2:2015	Cycles — Safety requirements for bicycles — Part 2: Requirements for city and trekking, young adult, mountain and racing bicycles	\$ 141,55
ISO 4210-3:2014	Cycles — Safety requirements for bicycles — Part 3: Common test methods	\$ 59,49
ISO 4210-4:2014	Cycles — Safety requirements for bicycles — Part 4: Braking test methods	\$ 141,55
ISO 4210-5:2014	Cycles — Safety requirements for bicycles — Part 5: Steering test methods	\$ 90,26
ISO 4210-6:2015	Cycles — Safety requirements for bicycles — Part 6: Frame and fork test methods	\$ 121,04
ISO 4210-8:2014	Cycles — Safety requirements for bicycles — Part 8: Pedal and drive system test methods	\$ 59,49
ISO 6695:2015	Cycles — Pedal axle and crank assembly with square end fitting — Assembly dimensions	\$ 38,98
ISO 6692:1981	Cycles — Marking of cycle components	\$ 38,98
ISO 10230:1990	Cycles — Splined hub and sprocket — Mating dimensions	\$ 38,98
ISO 6697:1994	Cycles — Hubs and freewheels — Assembly dimensions	\$ 38,98
		\$ 769,30

The standard ISO 4210-2:2015 is applied on the safety test section of the vehicle, the main concern to be covered with this standard is the main frame rigidity and safety.

The standard ISO 4210-3:2014 is applied on the common test methods of: brakes, steering system, pedal, and drive system.

The standard ISO 6695:2015 is applied on the assembly of the pedal axle and crank using a square end fitting.

The standard ISO 6692:1981 is applied on the main design to know all the components needed to build a bicycle

The standard ISO 10230:1990 is applied on the design of the direction component, hubs.

The standard ISO 6697:1994 is applied is applied on the design of the freewheels and hubs.

MATERIALS AND METHODS

Material and Component Selection

The materials selection was explored in a previous section.

Gearing

The Gear Development is the main factor to consider when selecting a gearing setup. It represents the distance in meters that a vehicle can advance during a single revolution from the powered wheel. Complex gear combinations create the possibility of having several different gear developments, each suited to different tasks. Parting from this factor, a relative coherence of the system can be analyzed, as well as the different speed ranges in each gear configuration. The purpose of these computations is to evaluate the gearing information to ensure optimal performance for the proposed needs of the HPV. The results of this study aim to prove that the chosen transmission components are viable for the performance objectives of the project.

Sketch

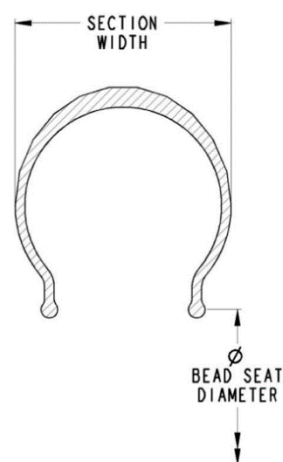


Figure 19 ISO Tire Size Interpretation (Archibald, 2016)

Assumptions/Data

All the data used in this section is based upon several assumptions. A regular performance is implied, meaning that the cadence would be constant. Cadence values, where taken from the literature review made on the subject (from papers from previous competitors from other universities, as well as ASME literature on the subject). The chosen components are the set of the Shimano Alivio M4000 Series.

- Tire Section Width = 54 [mm]
- Bead Seat Diameter = 559 [mm]
- Nominal Cadence = 90 [rpm]
- Maximum Cadence = 135 [rpm]
- Minimum Cadence = 50 [rpm]
- 3 Chainring sizes (FC-M4050)
 - 40 teeth
 - 30 teeth
 - 22 teeth
- 9 Freewheel Cogs (CS-HG400-9)
 - 25 teeth
 - 23 teeth
 - 21 teeth
 - 19 teeth
 - 17 teeth
 - 15 teeth
 - 13 teeth
 - 12 teeth
 - 11 teeth

Development

Since there are 27 different gearing combinations, all the calculations were made using the power of MATLAB. The gear development was obtained using the following expressions, obtained from the *Overview of Human-Powered Vehicles* (M. Archibald, 2016).

$$G = \frac{N_{CH}}{N_w} \times D \times \pi$$

$$D = \frac{BSD + (2 \times SW)}{1000}$$

Where:

G = Gear Development [m]

D = Wheel Outer Diameter [m]

NCH = Teeth on the Chainring

Nw = Teeth on the rear wheel cog

BSD = Band Set Diameter [mm]

SW = Tire Section Width [mm]

By combining the obtained gear developments with the cadence values (which express minimum, maximum, and nominal RPM's at which the vehicle operates), the speed ranges for each gear can be found:

$$V = \frac{G \times Cad}{60}$$

Where:

V = Speed [m/s]

Cad = Cadence Value [rev/min]

Solution

BICYCLE GEAR CALCULATOR

VEHICLE: Ilalo
 DRIVE WHEEL: 54-559 ISO
 LOW GEAR: 1.8 meters
 HIGH GEAR: 7.6 meters
 RANGE: 4.13

CHAINRING TOOTH NUMBERS:
 40 30 22

CASSETTE TOOTH NUMBERS:
 25 23 21 19 17 15 13 12 11

GEARS (meters)

	HIGH	MID	LOW
	3.4	2.5	1.8
	3.6	2.7	2.0
	4.0	3.0	2.2
	4.4	3.3	2.4
	4.9	3.7	2.7
	5.6	4.2	3.1
	6.4	4.8	3.5
	7.0	5.2	3.8
	7.6	5.7	4.2

Figure 20 Gearing Information

The obtained gearing values represents the whole gear development range in meters. On the lowest gear, the vehicle will advance 1.8 meters per wheel revolution, while on the highest gear the values increase to 7.6 meters. This means that, according to the literature, the gearing range chosen is suitable for a wide variety of applications, from steep hills with heavy loads, to high speeds or downhill runs (M. Archibald, 2016). The Gears matrix shows detailed information on the development on each combination, categorized as high, mid and low gears according to the 3 main chainrings.

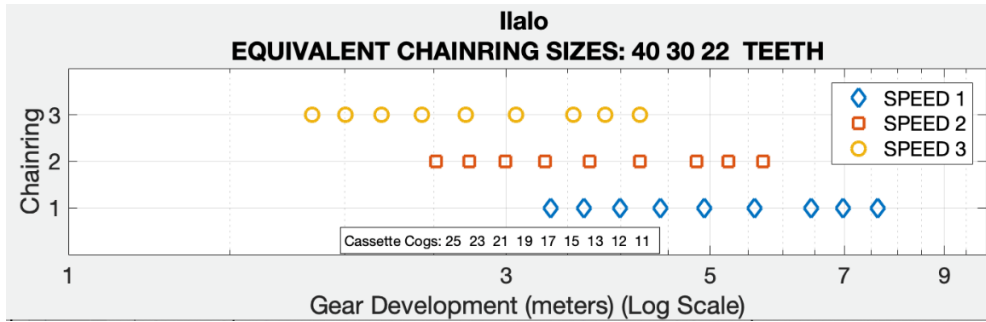


Figure 21 Equivalent Gearing Developments.

Distributions show no noticeable effort spikes when changing gears

The graph (Figure 21) shows a logarithmic layout of the gear development for all the combinations. This helps visualize and compare the different combinations. Each mark on the graph represents a specific gearing combination. Since most of the gears show a similar spacing between them, it can be assumed that there will not be any noticeable effort spikes when changing gears, which is good for the comfort of the driver. It is also relevant to point out that there are some seemingly unnecessary gearing combinations since several ones share a similar development. The benefit of having them is that they allow for a smoother gearing transition, even though they do not provide any significant case gain.

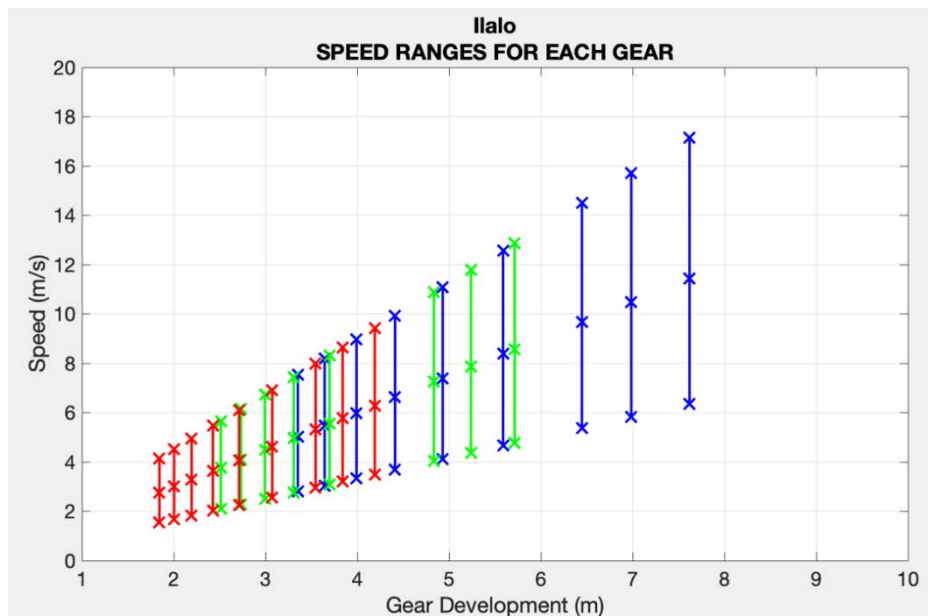


Figure 22 Speed Ranges for Each Gear.

Maximum possible speed of 17 [m/s]

The graph on figure 22 demonstrates all the tentative speed ranges for each gear, on the three different cadence values assumed. All the red lines represent the Low Gears, the green ones correspond to the Mid Gears, while the blue ones provide information on the High Gears. It is important to clarify that even though the maximum speed shown would be of about 17 [m/s] (almost 60 km/h), these calculations are only tentative. They do not take into consideration the drive train efficiency, or other important values such as the vehicle weight and other potential losses. The actual achieved speeds will be considerably lower, but this first calculation gives a good analysis on the behavior of the gearing, the relation between different gearing combinations. Even assuming a 75% final efficiency (usually recumbent tadpole tricycles have a drivetrain efficiency of around 90%), the maximum speed with this gearing choice would be over 45 [km/h], which is a desired outcome.

These results prove that the gearing development and range provided by the chosen components are right in the desired values, which will provide a decent balance between comfort for the user and a good performance in varied situations. Therefore, the chosen components are valid to accomplish the project's objectives.

Design for Manufacturing

Manufacturing Plan

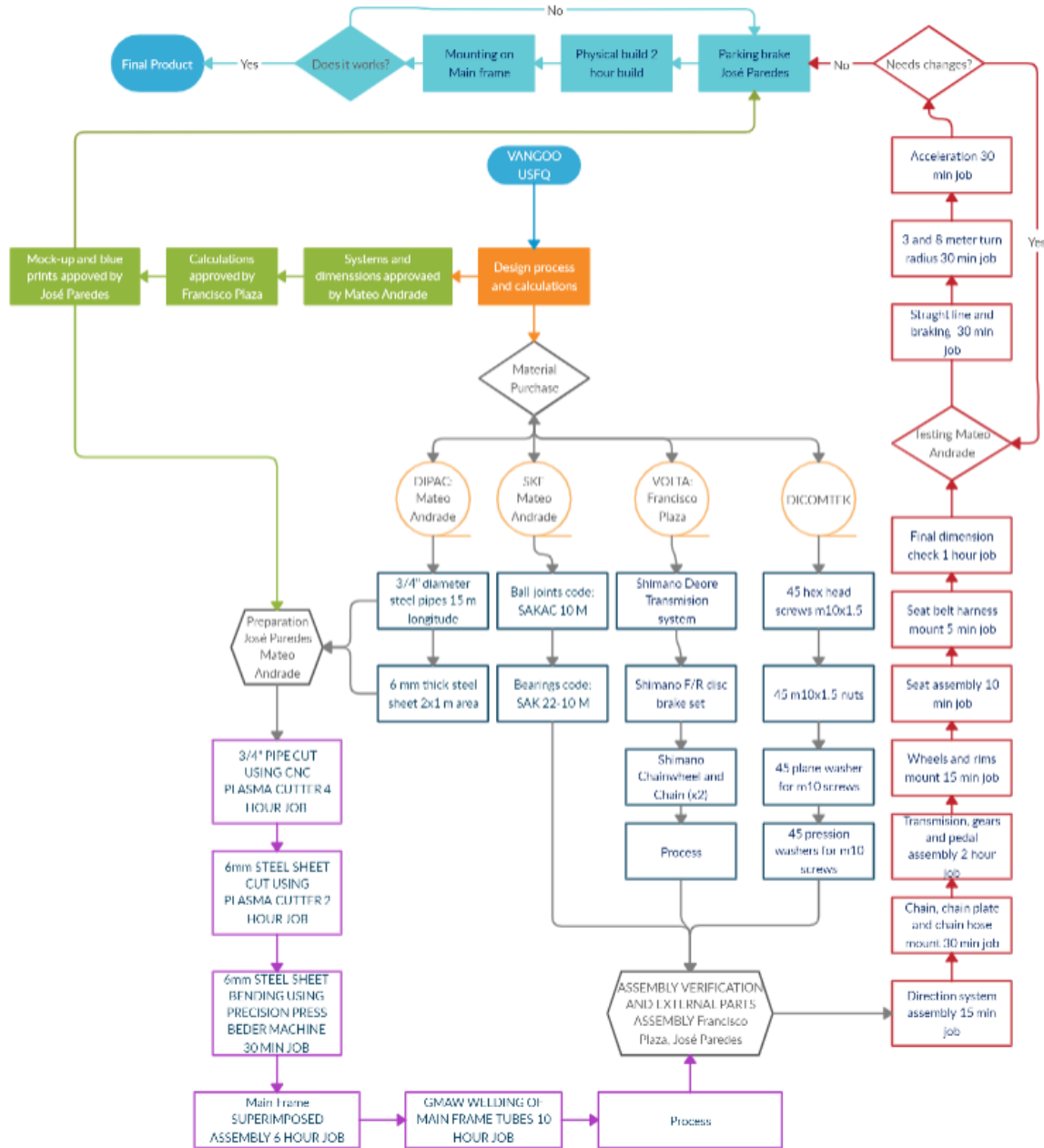


Figure 23 Design for manufacturing

A full-size version of the diagram can be found on ANNEX-B

Assembly

The assembly of the vehicle is to be done by the team members, following the steps assigned by the manufacturing plan, as well as the detailed assembly instructions included with each of the drivetrain components, which will be bought externally. To ensure there is a perfect fit of the welded joints in the chassis, within the set tolerances and without the tubes bending, a frame will be used to keep the tubes in place securely throughout the welding process.

Cost

The cost of each component is detailed in the *Budget* section in Annex B. The total cost of the project, taking into account all the materials and work needed is 1742.84 \$. To reduce costs, external manufacturing help was not used for the plan.

Maintenance

The steps and factors to take into account regarding the maintenance of the vehicle and its components is detailed in the *Maintenance and Operation Manual*.

Life Cycle Assessment

The life cycle of the vehicle begins with the purchase of its components and materials. All the drivetrain components will come from external manufacturers (Shimano) as brand new. The tubes will also be brand new (no recycled products to ensure initial quality), as well as the plaques that will be used to manufacture parts such as the brake calipers. The anticorrosive paint layer that will be applied to most parts of the vehicle, as well as the quality workmanship and procedures, the high-quality drivetrain components and the properties of the used materials will help extend the product's normal life cycle. It is expected that the vehicle could be

operational for 15 years as long as all the instructions detailed in the *Maintenance and Operation Manual* were followed accordingly, and the vehicle was not involved in major crashes, or unexpected abuse. After the product has spent its expected usability, the life cycle continues in the treatment of the components. The whole chassis and the parts in the direction system can be easily recycled in steel manufacturing plants, the driver seat can be used in different products, and the drivetrain components can be reused for other products or recycled through Shimano's waste project. The only part that would not be easy or safe to recycle would be the seat belt, which would go to waste.

RESULTS AND DISCUSSION

Design Report

The following section will explore in detail the engineering analysis performed to design the human powered vehicle. The design was divided into three main subsystems: transmission, direction, and chassis. The former includes the structural analysis of the vehicle's body and design subcomponents. It also takes in consideration the proper mounts required to assembly the other subsystems. The direction subsystems focus on driving and maneuverability of the vehicle. It includes all the direction subcomponents design, wheels, and user interface. Last, the transmission subsystems focus on how to proper power the vehicle. It includes the component selection, chain path, and braking systems. The following studies were performed under each subsystem. The in-depth engineering analysis can be found in the Appendix A.

Table 2 Engineering Analysis Plan

Plan of Engineering Analysis		
Chassis	Direction	Transmission
Preliminary FEA to size chassis frame and material	Ackerman design calculations	Component validity analysis
Detail Component design	Track rod analysis	Crank FEA
Detail Component FEA	-	-
FEA Validation	-	-
Weld Design	-	-

Figure 24 show the vehicle final design appearance and figure 25 shows the main design dimensions.



Figure 24 Ilalo Prototype Final Render

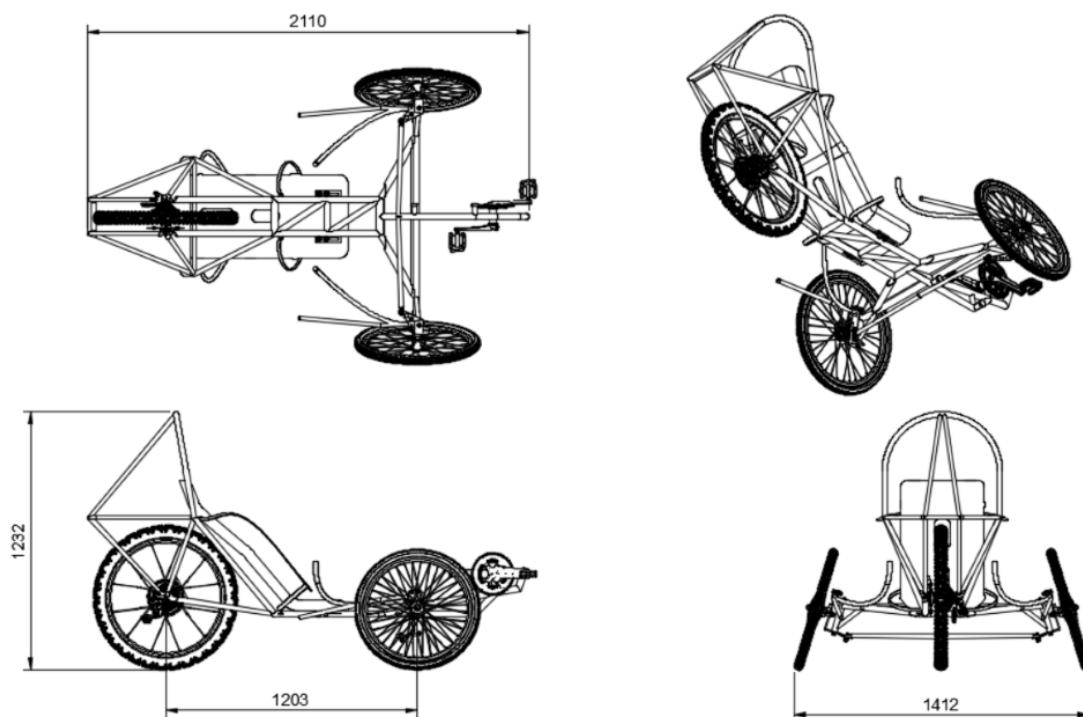


Figure 25 HPV Basic linear dimensions.

The overall dimensions of the vehicle are 2110 [mm] x 1412 [mm] x 1232 [mm]

Prototype Test Plan

This plan was designed to validate the *Ilalo* HPV performance respect to its design parameters. Also, it will assist in gaining insights of several performance aspects regarding weight, size, user comfort, and power efficiency for future iterations of the design.

Minimum Required Instrumentation:

- Measuring tape
- Weight
- 3 axis Strain gages in the critical components of the vehicle.
- Video recording device
- Tachometer placed in the rear wheel and crankset.
- DAQ

Next, a table that summarizes the test planned to be performed once the vehicle is built.

Table 3 Summary of the test planification

Prototype Test Plan	
Test	Method for Validation
Weight the prototyp	Weight less than 25 kg
Measure prototype dimensions	Less than 2.5m L * 1.5m W * 1.5m H
Measure vehicle clearance from the ground	The vehicle should be able to ride above a 10cm tall obstacle
Measure vehicle cargo space	Able to fit a 13x8x15 inches rectangular box
Measure vehicle's critical component stress and strain	Use straingages for data acquisition
User comfort	User's Satisfaction Survey
User power input	Measure power input in the cranksset
Acceleration test	100m sprint race
Braking test	Braking distance less than 6m from 25km/h
Turning test	3.0 and 6.0 turning radii at 5km/h
Vehicle stability	Travel 30m in a straight line at 5 & 8 km/h
Roll Over 2670 N @12° from the vertical	Deformation less than 5cm
Roll Over 1330N Horizontal Load	Deformation less than 3.8cm
Overall Roll Over Performance	The tallest rider should not touch the exterior of the vehicle
Field of View	The field of view needs to be at least 180 °
Parking break	The parking break should not yield at slopes from -7% to 5%

1. Geometric validation

- a. The vehicle will be weight using a car scale to compare with the design specification.
- b. The vehicle will be measured to compared with the design specifications.
- c. The vehicle clearance respect from the ground will be measured.
- d. The vehicle's cargo space will be measured to cross checked with the design specification.
- e. The vehicle's stress distribution in frame members under all the experiments will be study for the critical components determined during the manufacturing stage by the team. This will assist in reducing weight in future iterations and gaining insights in the real load the vehicle will be exposed. This will be use by the CAE engineers in the team to improve the concepts design.

2. General performance

- a. The vehicle will be tested by different riders of different body mass, height, gender, and age. Vehicle speed and torque will be measured to study the performance of the prototype under different scenarios. All this test will be performed in the same flat testing location to reduce the experiment error. Annotation on overall user comfort, first impressions on the prototype, and comments should be recorded for a qualitative analysis of the vehicle.
- b. Acceleration test will be conducted to understand the top acceleration reachable with the prototype. A male a women rider will be instructed to sprint the vehicle from rest for 100m. Final speed and time will be measured. This study will be performed 10 times under different days so muscular fatigue will be minimum.

3. Performance Safety Requirements

a. The vehicle's breaking performance will be tested on a flat surface. The breaking distance must be 6.0 m or less, starting at a speed of 25 km/h and ending at 0 km/h. 10 tests will be necessary to show a real value of the breaking distance.

i. The same test under wet surface conditions will be performed to revise the vehicle's performance under rainy conditions.

b. The vehicle's steering performance will be tested on a flat surface and with a turning radius of 3.0 m and 6.0 m at a constant speed of 5 km/h. 10 tests will be necessary to show a real value of the steering performance and driver feedback.

c. The vehicle's stability performance will be tested on a flat surface. The vehicle should travel 30.0 m in a straight line at a speed of 5 km/h to 8 km/h. 10 tests will be necessary to show a real value of straight-line stability.

4. Rollover Protection System.

a. The top load strength of the vehicle will be tested on the lab, placing a 2670 N load in the top of the roll bar, this load will be directed downward at an angle of 12° from the vertical towards the rear of the vehicle. The roll bar will be accepted if: there is no plastic deformation, delamination or fracture, the maximum elastic deformation accepted is 5.1 cm, and that deformation shall not touch any part of the driver's body.

b. The side load strength of the vehicle will be tested on the lab, placing a 1330 N load in the side of the roll bar at shoulder height, and the reactant force to the harness or to the seat. The roll bar will be accepted if: There is no plastic deformation, delamination or fracture, the maximum elastic deformation accepted is 3.8 cm, and that deformation shall not touch any part of the driver's body.

c. To test the effectiveness of the roll over protection system, the vehicle will lay on its side and will be inverted as well with the driver inside, with the safety helmet and harness adequately secured, once the vehicle is laying on its side and its inverted the driver should not touch the ground with any part of the body.

5. Field of View

a. The vehicle should provide the driver a horizontal FOV (Field Of View) of at least 180° wide. This will be tested placing color tapes around the vehicle according to the different angles.

6. Parking brake

a. The electric parking brake will be tested on different slope grades from -7% to 5%. The vehicle will be parked properly, and the parking brake will be activated. The test will verify the stability of the brake for different loading scenarios of the vehicle.

Safety Through Design

Table 4 Risk Analysis

Code	Description	Priority Impact*Prob	Responsible	Decision taken	Status	Observations
VNG-001	Lack of budget	4*5 = 20	Francisco Plaza	Share: Add capital by each member of the group	Active	Analyze sponsor plan
VNG-002	Chassis design flaws	3*5 = 15	José Paredes	Avoid: Work with cross check design	Active	Advisory by Patricio Chiriboga and Paul Arauz
VNG-003	Injury by moving parts	4*3 = 12	Mateo Andrade	Reduce: Use PPE	Active	Check that PPE is used
VNG-004	welded joints failure	5*2 = 10	Francisco Plaza	Transfer: Qualified workforce for the job	Active	Check the status of construction blue prints
VNG-005	Schedule non-compliance	4*4 = 16	José Paredes	Prepare: Plan the schedule with extra time	In process	Have one or more weekly schedule reviews
VNG-006	communication problems	4*2 = 8	Mateo Andrade	Reduce: count with organizational support of the human resources team	In process	Hold weekly meetings and work on the "Microsoft Teams" platform
VNG-007	Delay in acquisition of material for chassis	4*2 = 8	Francisco Plaza	Transfer: Search for an alternate material dealer	In process	Try not to make the prices very different from what was agreed
VNG-008	Retraso en adquisicion de materiales para realizar control automático	3*3 = 9	José Paredes	Transfer: Sear for an alternate element dealer	In process	Try not to make the prices very different from what was agreed
VNG-009	Pipe cut failure	5*3 = 15	Mateo Andrade	Avoid: Cross check wor in the machining area	Active	In the event that the first metal prototype "Ilaio" suffers pipe cutting failures, in the following iterations it will work with qualified labor
VNG-010	Transmission mechanism problems	5*3 = 15	Francisco Plaza	Reduce: Research alternatives that don't affect the project	In process	Check the calculations made
VNG-011	direction elemnts problems	5*3 = 15	Mateo Andrade	Reduce: Calculate precisely the elements that are going to be used	In process	Check the calculations made
VNG-012	Problems with elements externally fabricated	5*2 = 10	José Paredes	Prepare: Save funds to buy spare parts	Active	Have a stock of spare parts for parts that are more likely to cause problems (eg chains)

Following the risk analysis, the higher potential risk and solutions are explained below:

VNG-001: DEPLETED BUDGET

The most important single aspect of our project for developing the first prototypes is budget. Therefore, depleting out Budget before being able to raise what is needed to keep with the project is within our higher risks. The solution proposed to this issue has two main components. The first stage is to assemble a team with the sole purpose of raising funds. The second is setting personal funds as an emergency in case our budget exhausts.

VNG-005: NOT FOLLOWING THE SCHEDULE

Due to the limited time and resources of the project, delays in the vehicle development respect to what was planned can affect all the main objectives. The plan we propose to diminish the risk of this scenario is to carefully plan for possible delays ahead of time. This will allow us to have a small margin of time to correct stuff before it starts going off.

VNG-011: ISSUES WITH DIRECTION COMPONENTS

Because of the complexity and the quantity of components and factors to consider computing the direction design, we decided to omit little aspects that we did not consider relevant for our design. The calculations are going to be performed using Fusion 360, hand calculations and MATLAB. A preliminary analysis is required to size dimensions of our vehicle to our design parameters, for example the minimum 8 meters turn radius.

Results, discussion, and conclusions

The vehicle's design is compared with the user requirements for the *Ilalo* prototype. These were shown in the first sections of this report. Due to the design intention for infinite life, the vehicle will be able to provide year-round single person transportations in an urban area. Because of the fabric and cargo space provided, the vehicle is also suitable for commuting, shopping, and recreations. The vehicle is designed to be easy to propel and operate. However, this needs to be tested in the future stages of the project. We managed to achieve the benchmark standard for ASME vehicle in this iteration regarding size and weight.

Following with the chassis design, a material with lower density can be considered for future iterations. The structure has the lowest percentage of the budget which will allow to allocate some monetary resources to design for a higher performance material such as Aluminum or alloyed steels. Reducing the overall width of the vehicle to less than 1200 [mm] should be considered as well. This would allow the vehicle to use the bike lanes in the Quito Metropolitan District.

Because the structural analysis of the chassis was done using FEA, a strong test plan is required to prove the design and guarantee minimum safety standards. ANSYS proved to be powerful enough for our necessities, but the node limitation present has been an issue when trying to develop a more accurate model. SimSolid is more computationally efficient than ANSYS, but it presents issues when importing complicated geometry. Overall, a combination of both software applications is a good tool to validate the FEA before physical tests.

For Computer Aided Design we used two different CAD tools. Autodesk Fusion 360 proved to be great for team projects because of its cloud storing capacity and collaboration capabilities. Furthermore, it is completely user-friendly and easy to iterate upon. However, for

more technical applications such as welding design and frame technical drawings, it is not so powerful. SolidWorks proved to be a better tool for this application. Overall, SolidWorks technical drawing module is more profound, powerful and detailed than Fusion 360's, and it is better for high-level applications. However, Fusion 360 is better for prototyping. The FEA module of both CAD tools is not reliable for most of the complex geometries of the vehicle. To use a specialized tool for the structural analysis is recommended.

Concluding, a design for a good year-round single person transportation alternative was presented. Although this prototype still requires much work for being commercially feasible, it is a good concept in a vehicle type that will play a major role in urban transportation in the future.

Future Work

Future work related to this design consists in the manufacturing and testing stage. Furthermore, it should focus in reducing the overall weight of future iterations. We are holding back to start the manufacturing stage due to the global pandemic, but it is expected to resume with manufacturing once the health issues are no longer a major risk. After manufacturing, the prototype test plan should be implemented to validate the design for performance and safety regulations.

The test stage will be of great interest for the project because it will give us insights of the actual loads the vehicle is subjected to. Therefore, this would help the future iterations in the design for reducing weight and improving the overall performance of the vehicle. Because ergonomics represents a grey area in our design engineering, the test stage will help us achieve a better understanding human comfort. This aspect of design will be implemented later in future iterations.

Once the test stage of this prototyping is finished, the team should go back to the drawing table to improve the overall structure design, enhance performance and add other key features that were not implemented in this design because of time and resource limitations. These future features might include the automation of some vehicle's components, the implementation of energy recovery mechanisms, E-bike modularity, weather protection mechanisms and street-legal night driving lights.

Additional engineering studies are part of the programmed future development of the design. A vibration analysis for the chassis, direction and drivetrain components will be a core aspect of future designs. This would help understand the long-term structural performance and resistance to fatigue, in order to extend the product life cycle.

References

- Archibald, M. (2016). Overview of Human-Powered Vehicles. In *Design of Human Powered Vehicles* (2016th ed.). ASME Press. https://doi.org/10.1115/1.861103_ch2
- Archibald, Mark. (2017). *Design of Vehicles*.
- Budynas, R. G., & Nisbett, J. K. (1394). *Mechanical Engineering Design*.
- Gaikwad, R. S. Finite Element Analysis of Bicycle Crank.
- Höchtel, F., Böhm, H., & Senner, V. (2010). Prediction of energy efficient pedal forces in cycling using musculoskeletal simulation models. *Procedia Engineering*, 2(2), 3211-3215.
- Hung, N. B., & Lim, O. (2020). A review of history, development, design and research of electric bicycles. *Applied Energy*, 260 (August 2019), 114323. <https://doi.org/10.1016/j.apenergy.2019.114323>
- Keiper, T. (2020). Electric Motor. <https://grabcad.com/library/electrically-powered-turbocharger-as-cooling-fan-1>
- Laaribi, I. (2019). Go kart car chassis. <https://grabcad.com/library/go-kart-car-chassis-1>
- Mahmood, k. (2015). HPV. <https://grabcad.com/library/hpv-2>
- Moog. (2018). How a steering wheel works. <https://www.moogparts.eu/blog/how-a-steering-system-works.html>
- Mustain, Z. (2019). Tricycle from MTB bike. <https://grabcad.com/library/tricycle-from-mtb-bike-1>

Roumega, D. (2017, January 10). Bluetooth Door Lock (Arduino). Retrieved from [https://create.arduino.cc/projecthub/BuildItDR/bluetooth-door-lock-arduino-bc2035?ref=search&ref_id=bluetooth servo&offset=1](https://create.arduino.cc/projecthub/BuildItDR/bluetooth-door-lock-arduino-bc2035?ref=search&ref_id=bluetooth%20servo&offset=1)

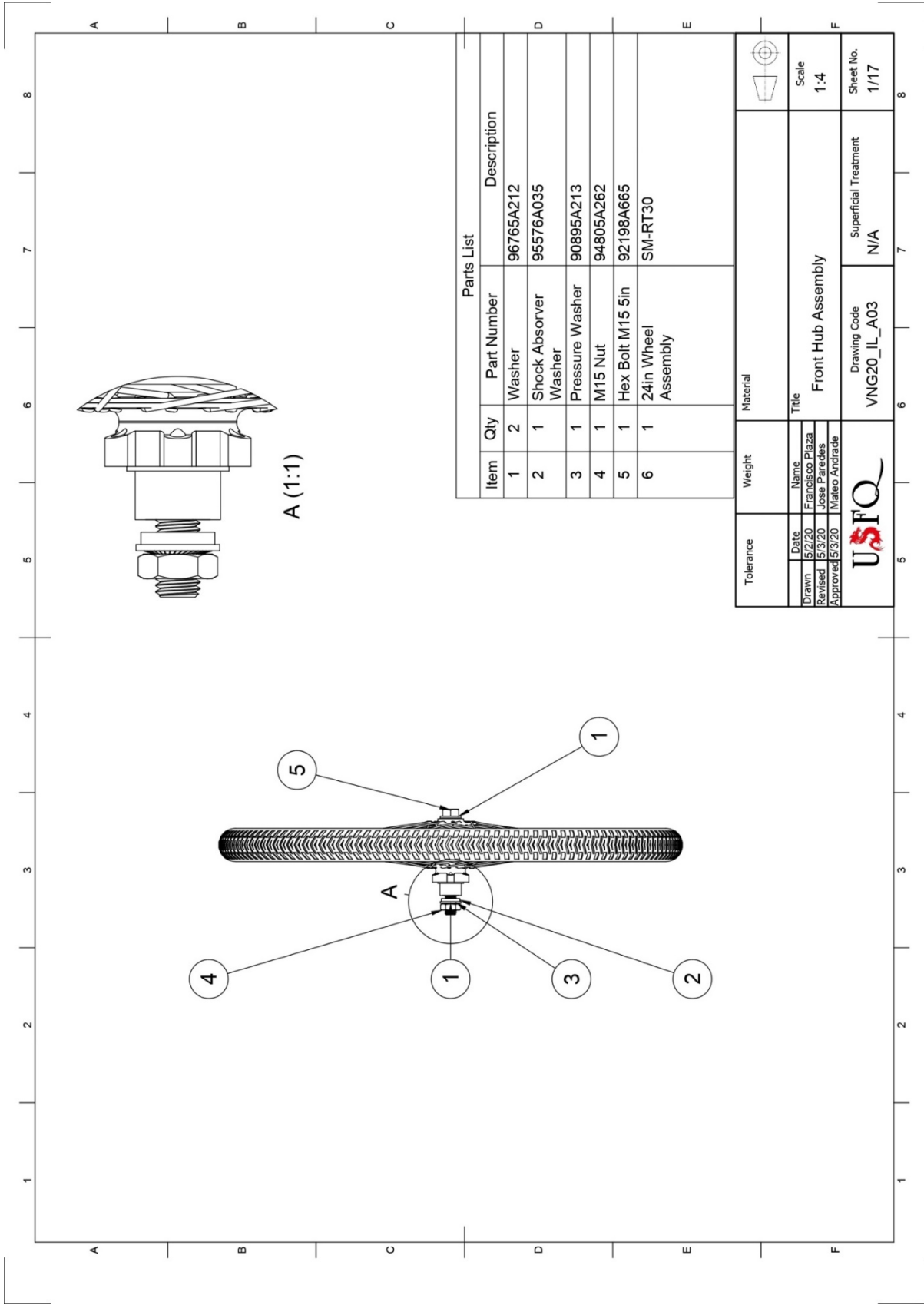
Tiku, S., Bhat, S., Tripathi, D. K., & Bharath, M. N. (2019). *Design Optimization of Bicycle Crank using Finite Element Analysis*. 5, 1–6.

APPENDIXES

Appendix A - Engineering drawings and detailed calculations

Drawing List

Name	Code	Sheet Number
Front Hub Assembly	VNG20_IL_A03	1
Bottom Bracket	VNG20_IL_CH01	2
Calliper Mount	VNG20_IL_CH02	3
Calliper Mount Support	VNG20_IL_CH03	4
Main Frame	VNG20_IL_CH04	5
Frontal Frame	VNG20_IL_CH05	6
Lower Frontal Frame	VNG20_IL_CH06	7
Tensor	VNG20_IL_CH07	8
Direction Bar	VNG20_IL_CH08	9
Cargo Space Support	VNG20_IL_CH09	10
Roll Bar	VNG20_IL_CH010	11
Left Fork Dropout	VNG20_IL_CH011	12
Right Fork Dropout	VNG20_IL_CH012	13
Seat Belt Support	VNG20_IL_CH013	14
Seat Support	VNG20_IL_CH014	15
Seat	VNG20_IL_CH015	16
Rear Tensor	VNG20_IL_CH016	17
Chasis Cut List	VNG20_IL_A04	1
Ackerman	VNG20_IL_DR01	1
TrackRod	VNG20_IL_DR02	2
Dropout	VNG20_IL_DR03	3
Lever	VNG20_IL_DR04	4
Lever Mount	VNG20_IL_DR05	5
Direction Assembly	VNG20_IL_A02	6
Ilalo Assembly	VNG20_IL_A01	1

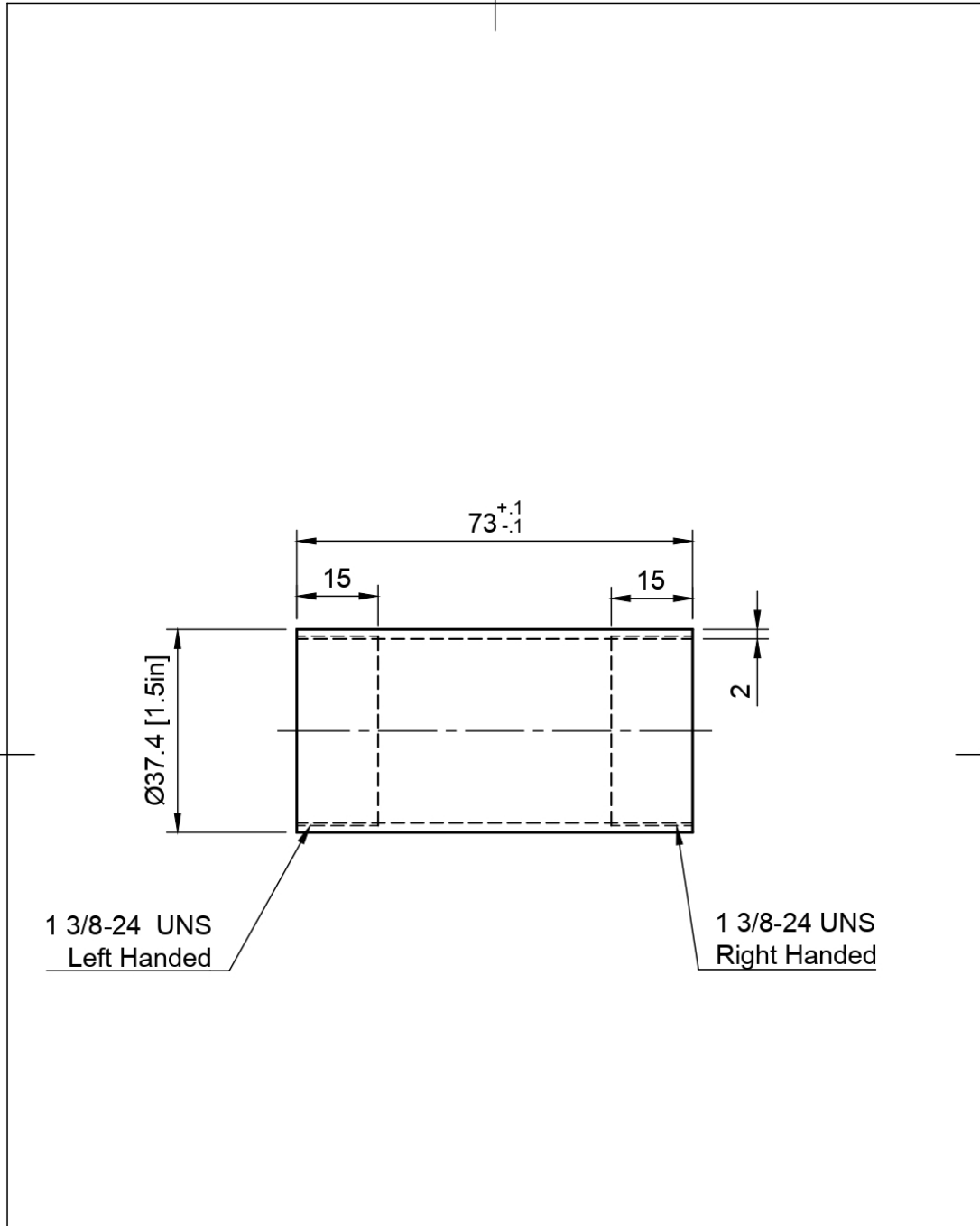


Parts List

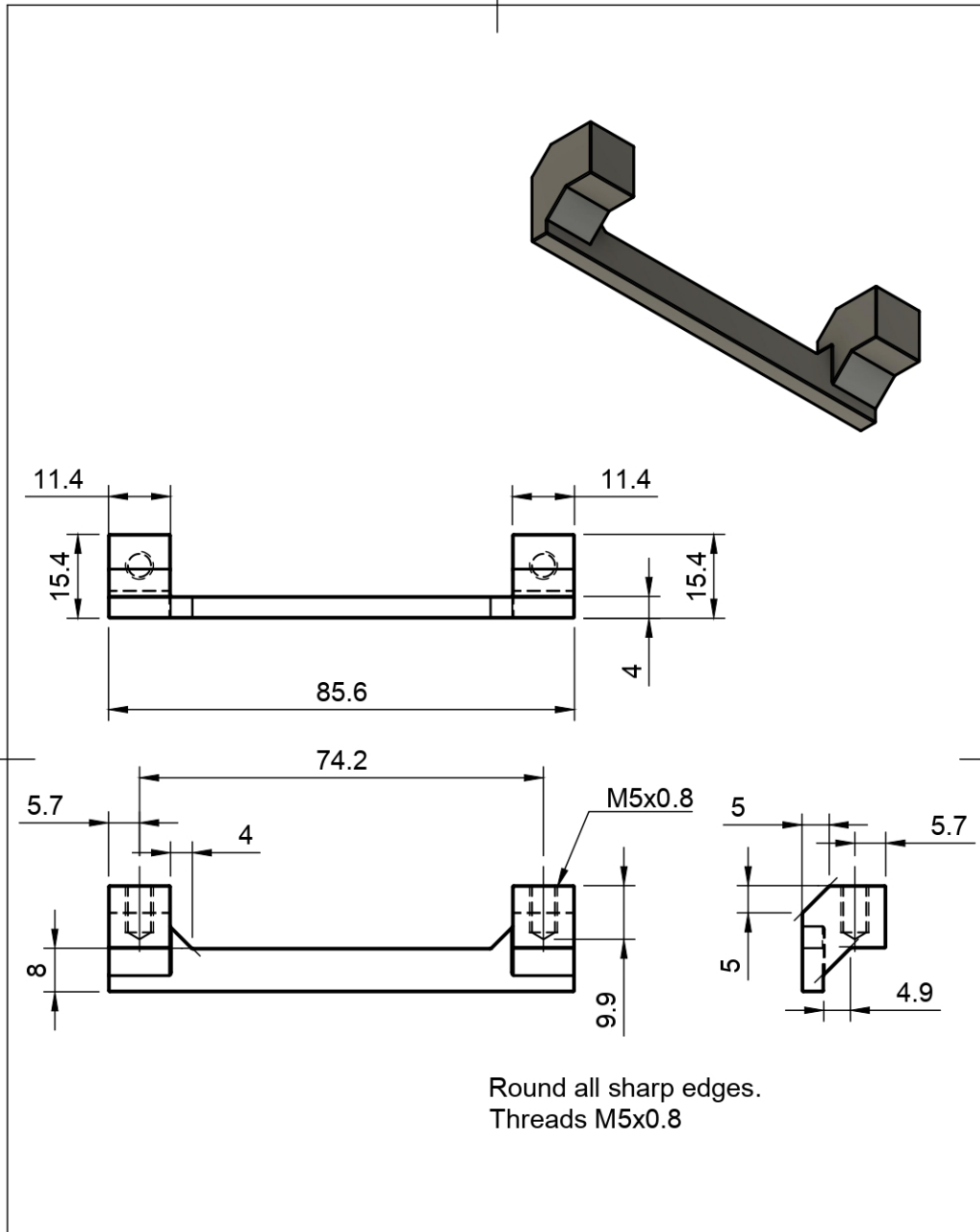
Item	Qty	Part Number	Description
1	2	96765A212	Washer
2	1	95576A035	Shock Absorber Washer
3	1	90895A213	Pressure Washer
4	1	94805A262	M15 Nut
5	1	92198A665	Hex Bolt M15 5in
6	1	SM-RT30	24in Wheel Assembly

Tolerance	Weight	Material								
<table border="1"> <tr> <td>Date</td> <td>Name</td> </tr> <tr> <td>5/2/20</td> <td>Francisco Plaza</td> </tr> <tr> <td>5/3/20</td> <td>Jose Paredes</td> </tr> <tr> <td>5/3/20</td> <td>Mateo Andrade</td> </tr> </table>	Date	Name	5/2/20	Francisco Plaza	5/3/20	Jose Paredes	5/3/20	Mateo Andrade		
Date	Name									
5/2/20	Francisco Plaza									
5/3/20	Jose Paredes									
5/3/20	Mateo Andrade									
Title										
Front Hub Assembly										
Drawing Code		Superficial Treatment								
VNG20_IL_A03		N/A								
Scale		Sheet No.								
1:4		1/17								

Chassis Drawings

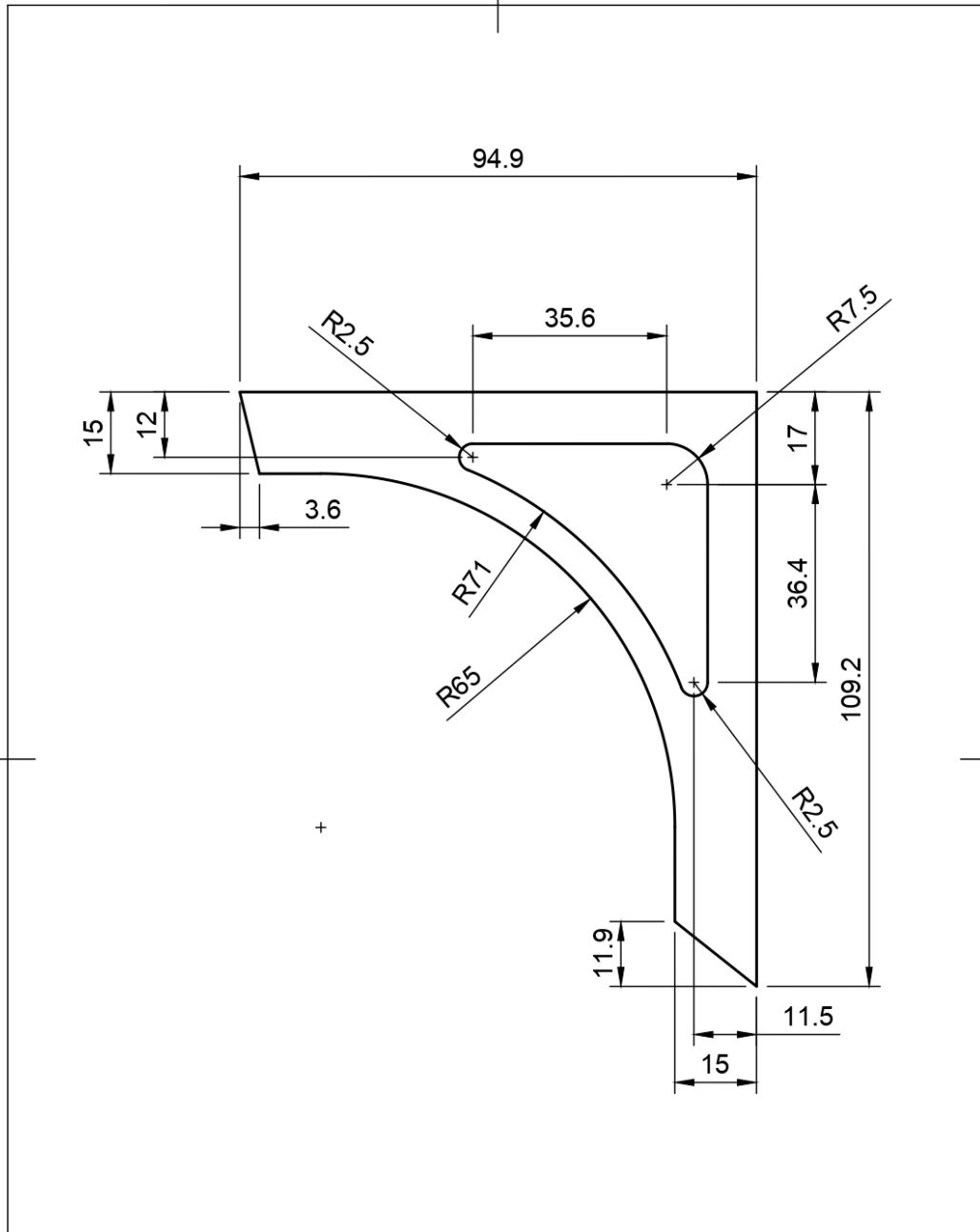


Tolerance ± 0.1		Weight 112.4 g		Material ASTM A500, Round Tube, 1.5 in D, 2mm THK			
Date		Name		Title Bottom Bracket		Scale 1:1	
Drawn	04/30/20	F. Plaza					
Revised	5/2/20	Jose Paredes					
Approved	5/3/20	Mateo Andrade					
				Drawing Code VNG20_IL_CH01		Superficial Treatment Non Corrosive Paint	
						Sheet No. 2/17	

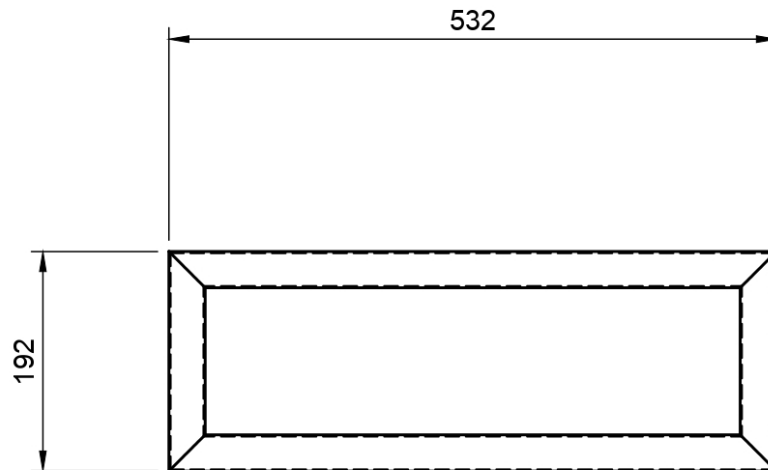


Round all sharp edges.
Threads M5x0.8

Tolerance ± 0.1		Weight 51.8 g		Material Acero ISO 1018			
Date		Name		Title Calliper Mount		Scale 1:1	
Drawn	5/2/20	Francisco Plaza					
Revised	5/3/20	Jose Paredes					
Approved	5/3/20	Mateo Andrade					
				Drawing Code VNG20_IL_CH02		Superficial Treatment Non Corrosive Paint	
						Sheet No. 3/17	

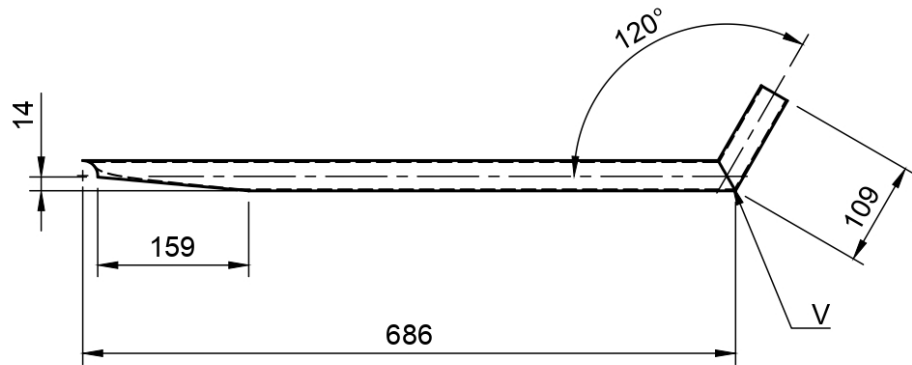


Tolerance ± 0.1		Weight 83.6 g		Material ASTM A500, Platine 4mm THK			
	Date	Name		Title Calliper Mount Support		Scale 1:1	
Drawn	5/1/20	Francisco Plaza					
Revised	5/3/20	Jose Paredes					
Approved	5/3/20	Mateo Andrade					
				Drawing Code VNG20_IL_CH03		Superficial Treatment Non Corrosive Paint	
						Sheet No. 4/17	

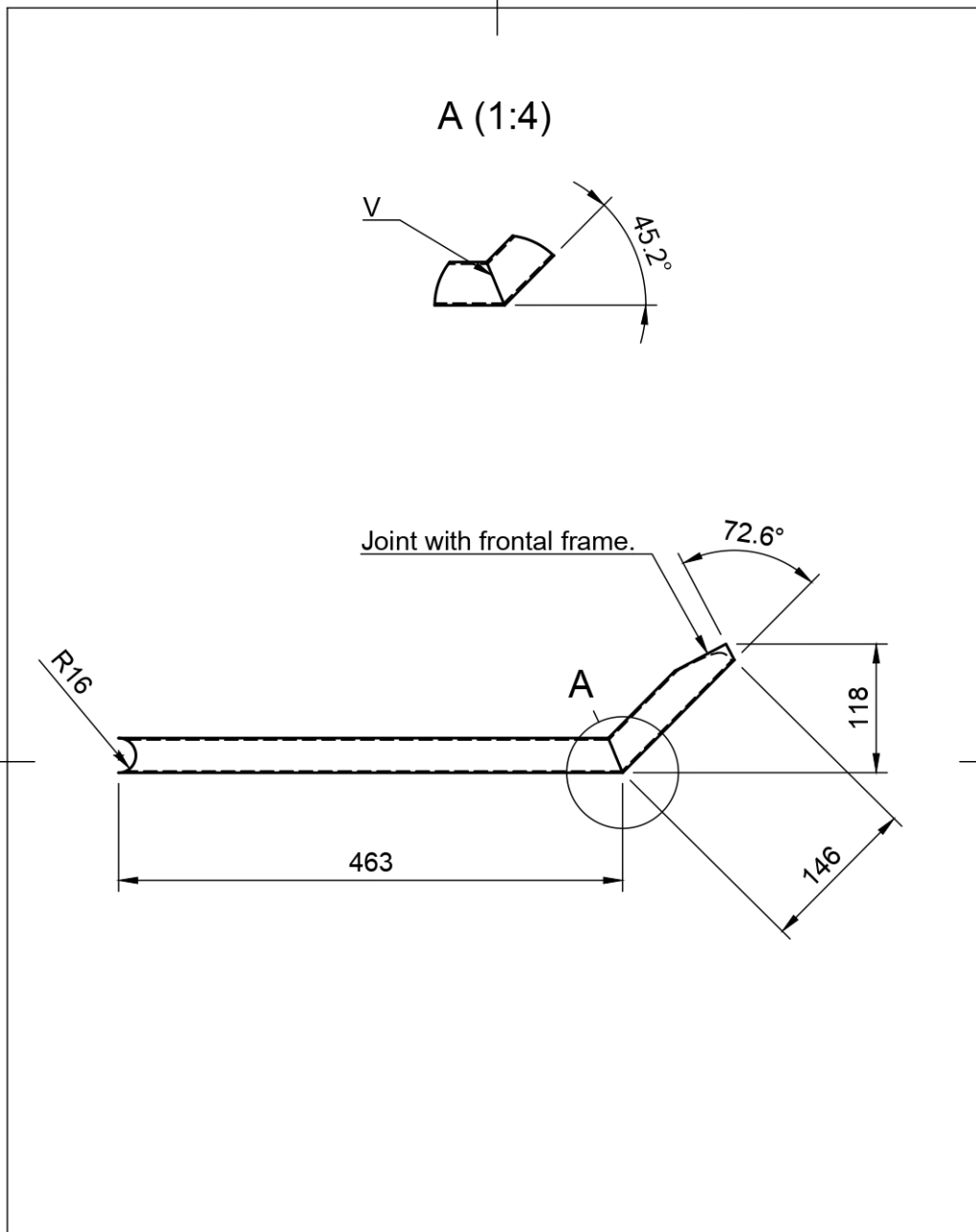


Notes:
All joints are welded
(V) at 90°

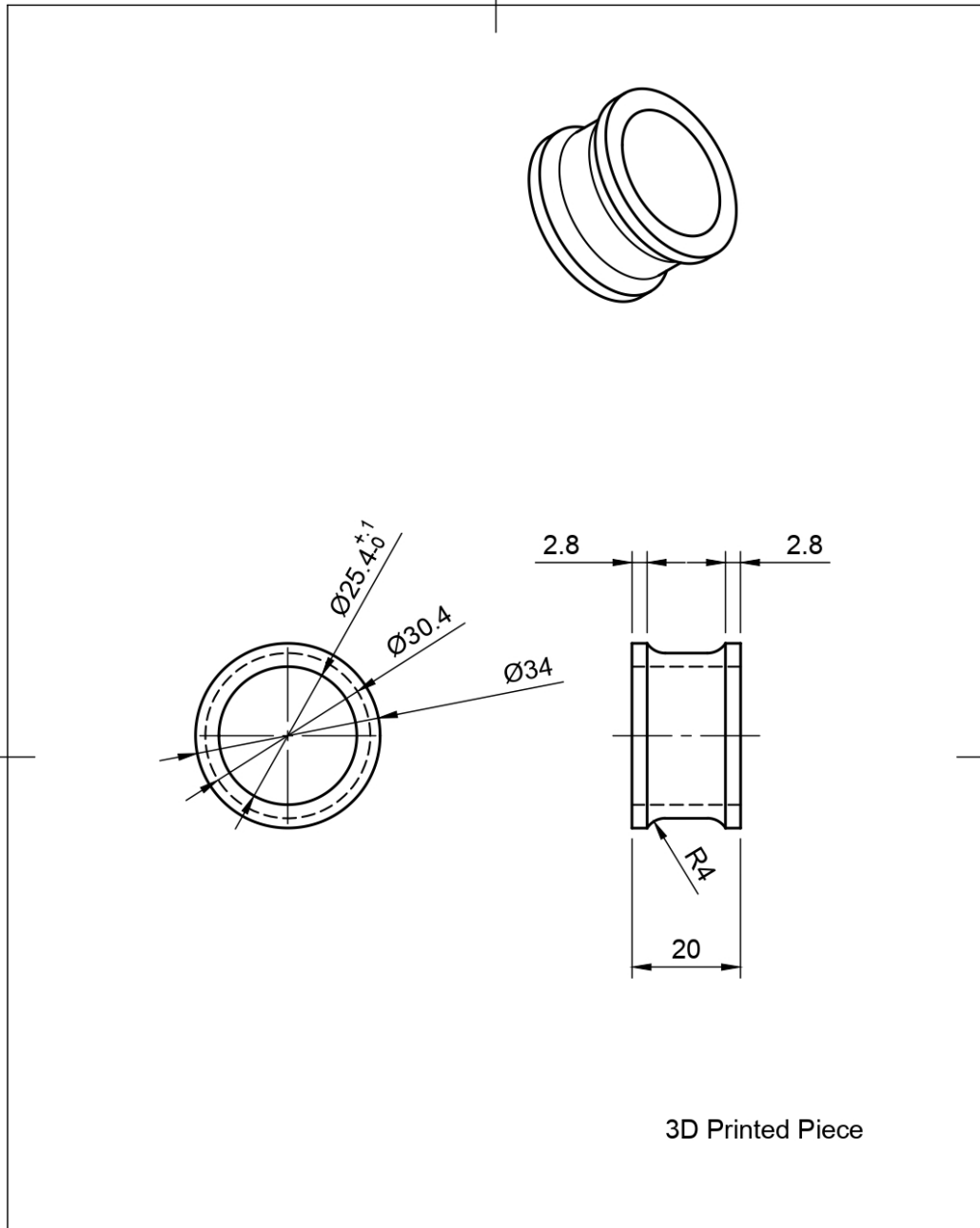
Tolerance ± 0.1		Weight 1481g	Material ASTM A500, Round Tube, 1.25 in D, 1.5mm THK	
	Date	Name	Title Main Frame	Scale 1:5
Drawn	5/2/20	Francisco Plaza		
Revised	5/3/20	Jose Paredes		
Approved	5/3/20	Mateo Andrade		
		Drawing Code VNG20_IL_CH04	Superficial Treatment Non Corrosive Paint	Sheet No. 5/17



Tolerance ± 0.1		Weight 800.7g		Material ASTM A500, Round Tube, 1.25 in D, 1.5mm THK			
	Date	Name		Title Frontal Frame		Scale 1:6	
Drawn	5/2/20	Francisco Plaza					
Revised	5/3/20	Jose Paredes					
Approved	5/3/20	Mateo Andrade				Sheet No. 6/17	
				Drawing Code VNG20_IL_CH05		Superficial Treatment Non Corrosive Paint	

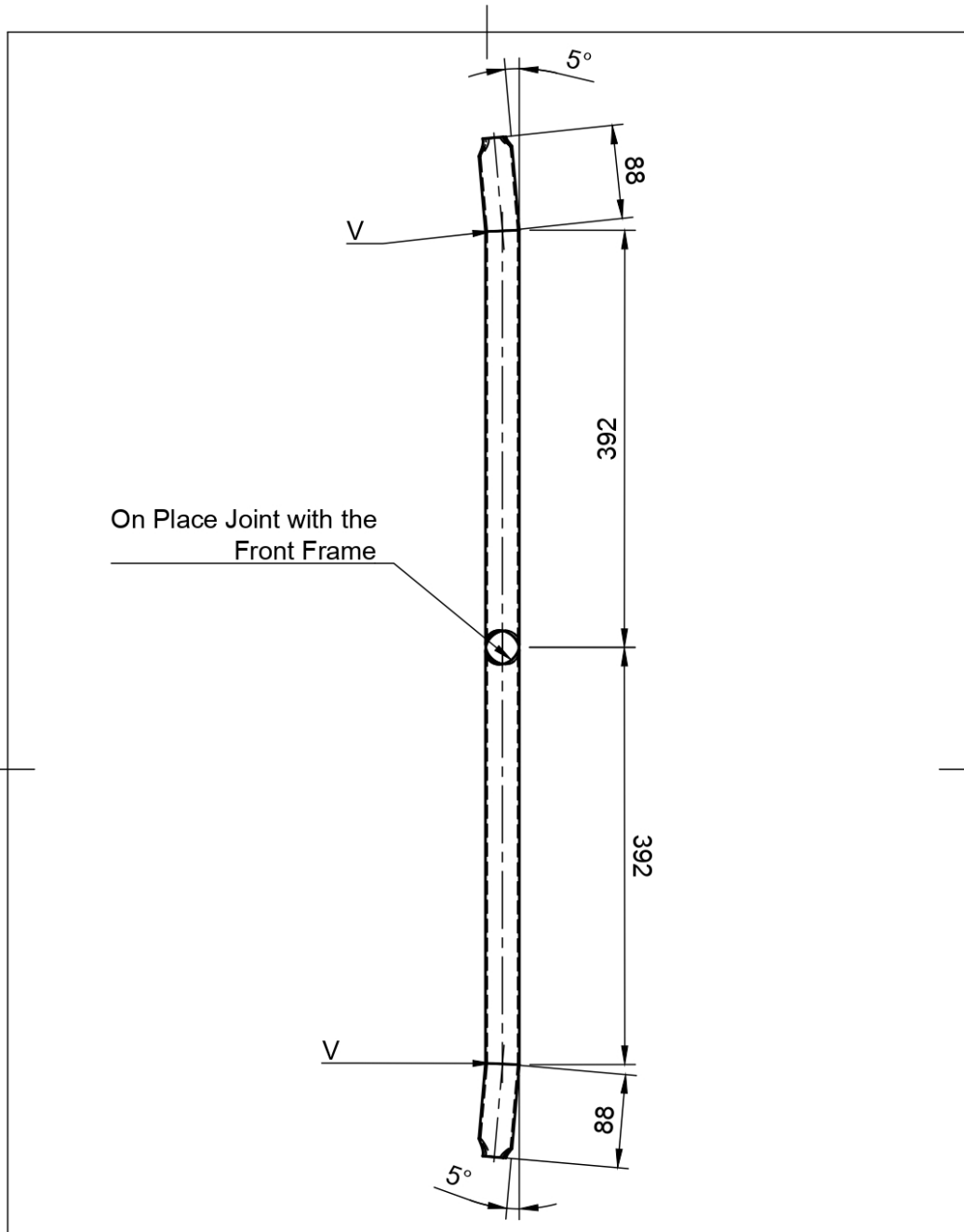


Tolerance ± 0.1		Weight 639.4 g	Material ASTM A500, Round Tube, 1.25 in D, 1.5mm THK	
Drawn	Date	Name	Title Lower Frontal Frame	Scale 1:5
Revised	5/2/20	Francisco Plaza		
Approved	5/3/20	Jose Paredes		
			Drawing Code VNG20_IL_CH06	Superficial Treatment Non Corrosive Paint
				Sheet No. 7/17

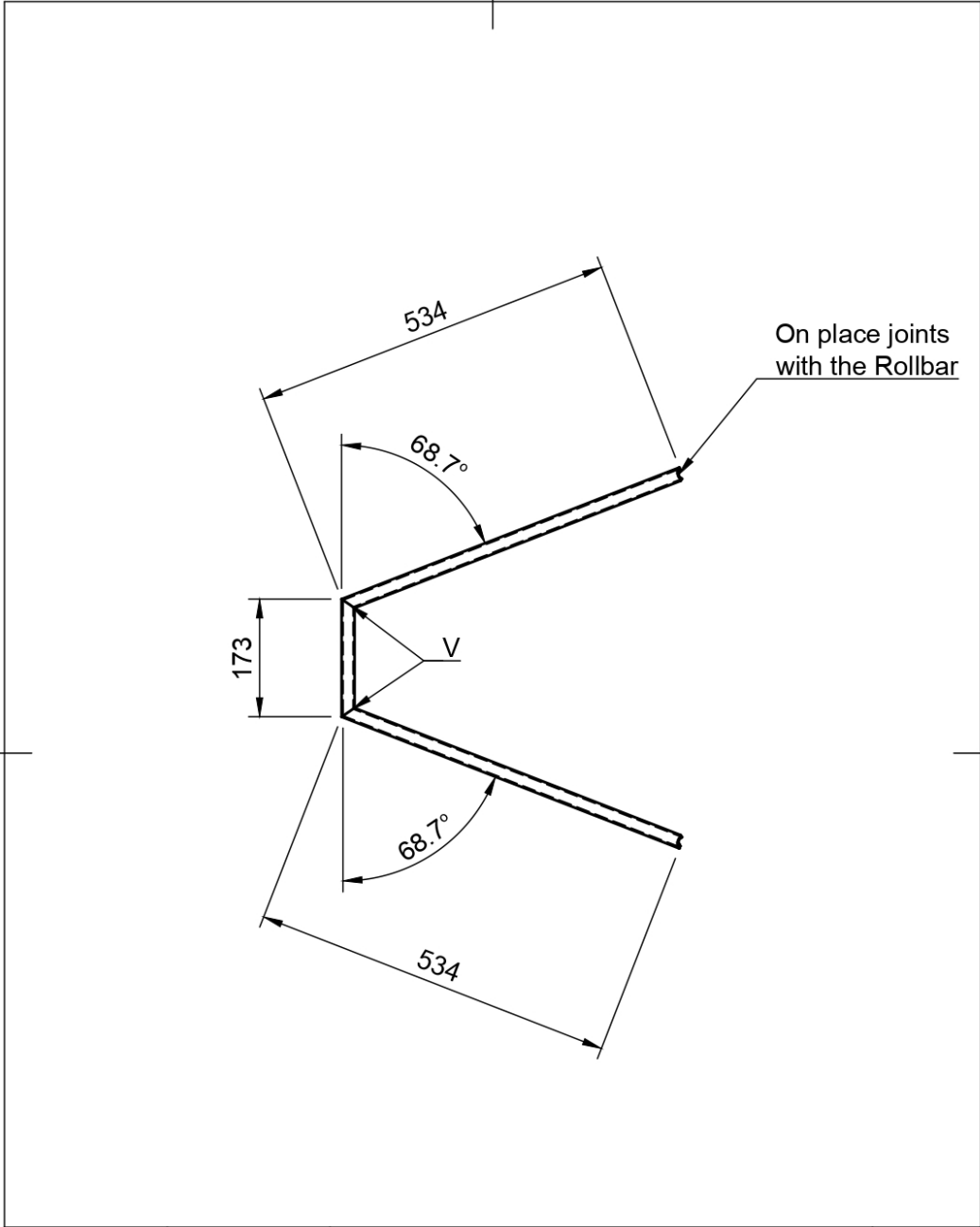


3D Printed Piece

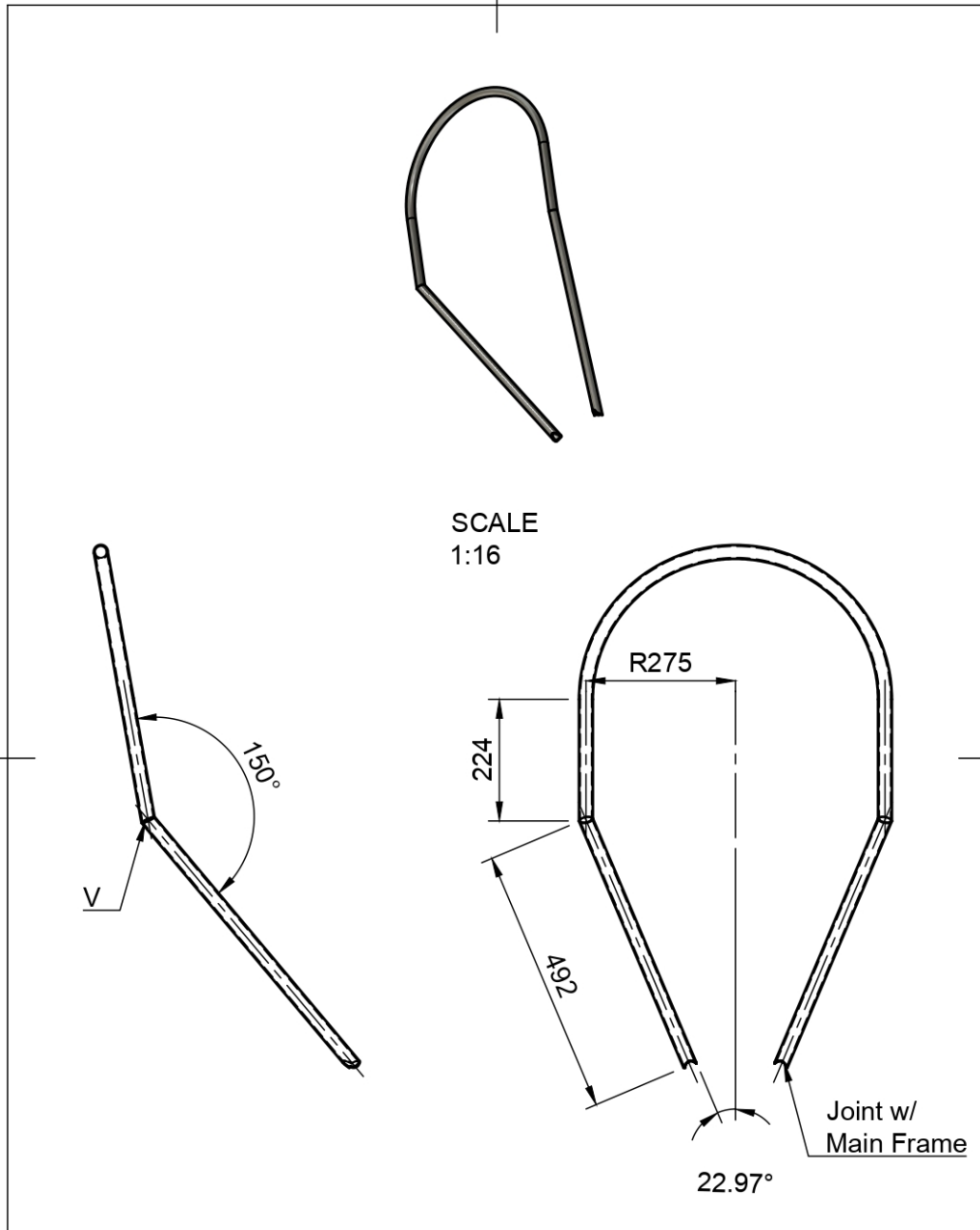
Tolerance ± 0.1		Weight 6.5 g		Material Nylon			
	Date	Name		Title Tensor		Scale 1:1	
Drawn	5/2/20	Francisco Plaza					
Revised	5/2/20	Jose Paredes					
Approved	5/3/20	Mateo Andrade					
				Drawing Code VNG20_IL_CH07		Superficial Treatment N/A	
						Sheet No. 8/17	



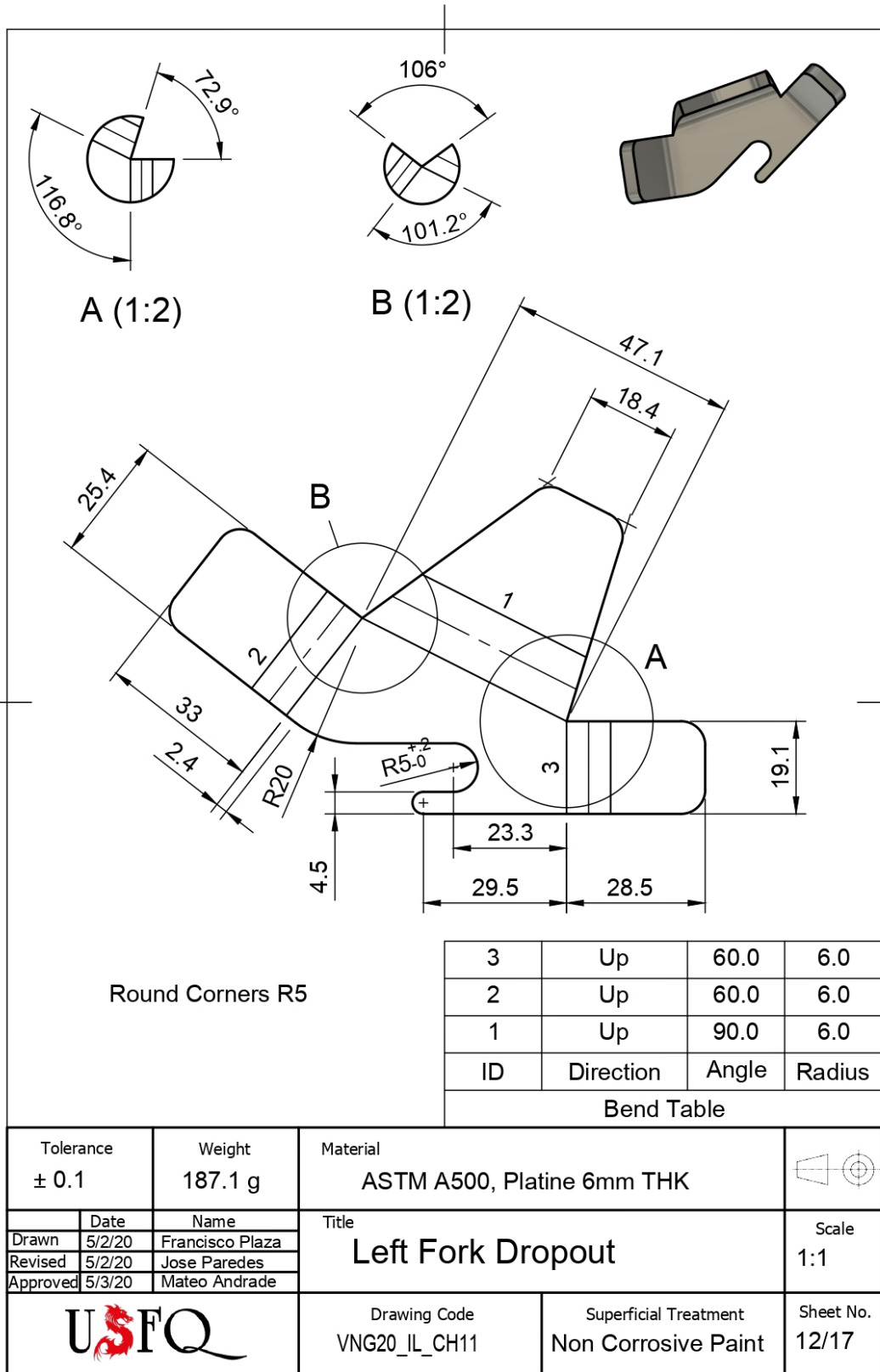
Tolerance ± 0.1		Weight 1036.3 g		Material ASTM A500, Round Tube, 1.25 in D, 1.5mm THK			
	Date	Name		Title		Scale	
Drawn	5/2/20	Francisco Plaza		Direction Bar		1:5	
Revised	5/3/20	Jose Paredes					
Approved	5/3/20	Mateo Andrade					
				Drawing Code VNG20_IL_CH08		Superficial Treatment Non Corrosive Paint	
						Sheet No. 9/17	

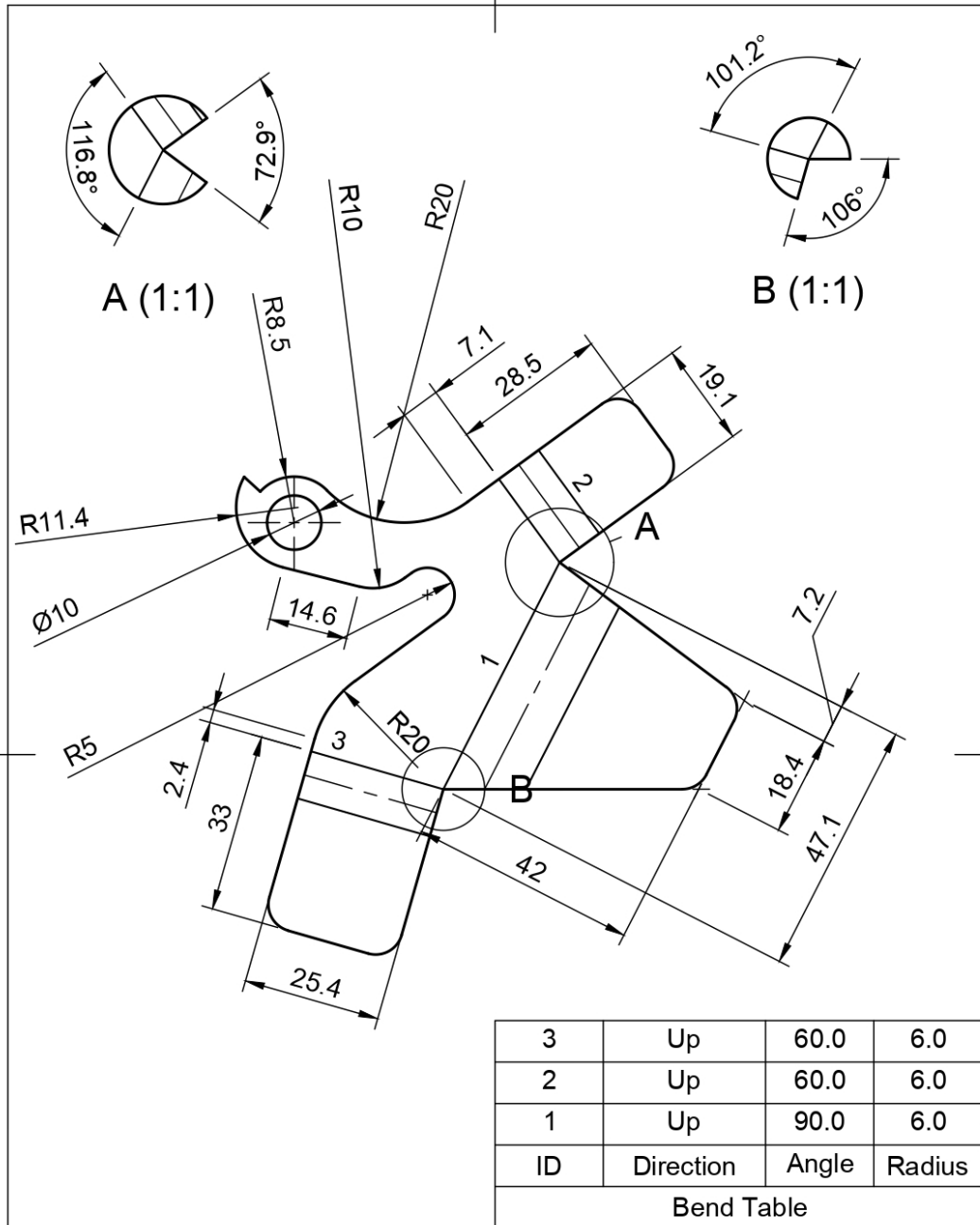


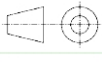
Tolerance ± 0.1		Weight 1018 g	Material ASTM A500, Round Tube, 0.75 in D, 2mm THK	
	Date	Name	Title Cargo Space Support	Scale 1:8
Drawn	5/2/20	Francisco Plaza		
Revised	5/3/20	Jose Paredes		
Approved	5/3/20	Mateo Andrade		
		Drawing Code VNG20_IL_CH09	Superficial Treatment Non Corrosive Paint	Sheet No. 10/17

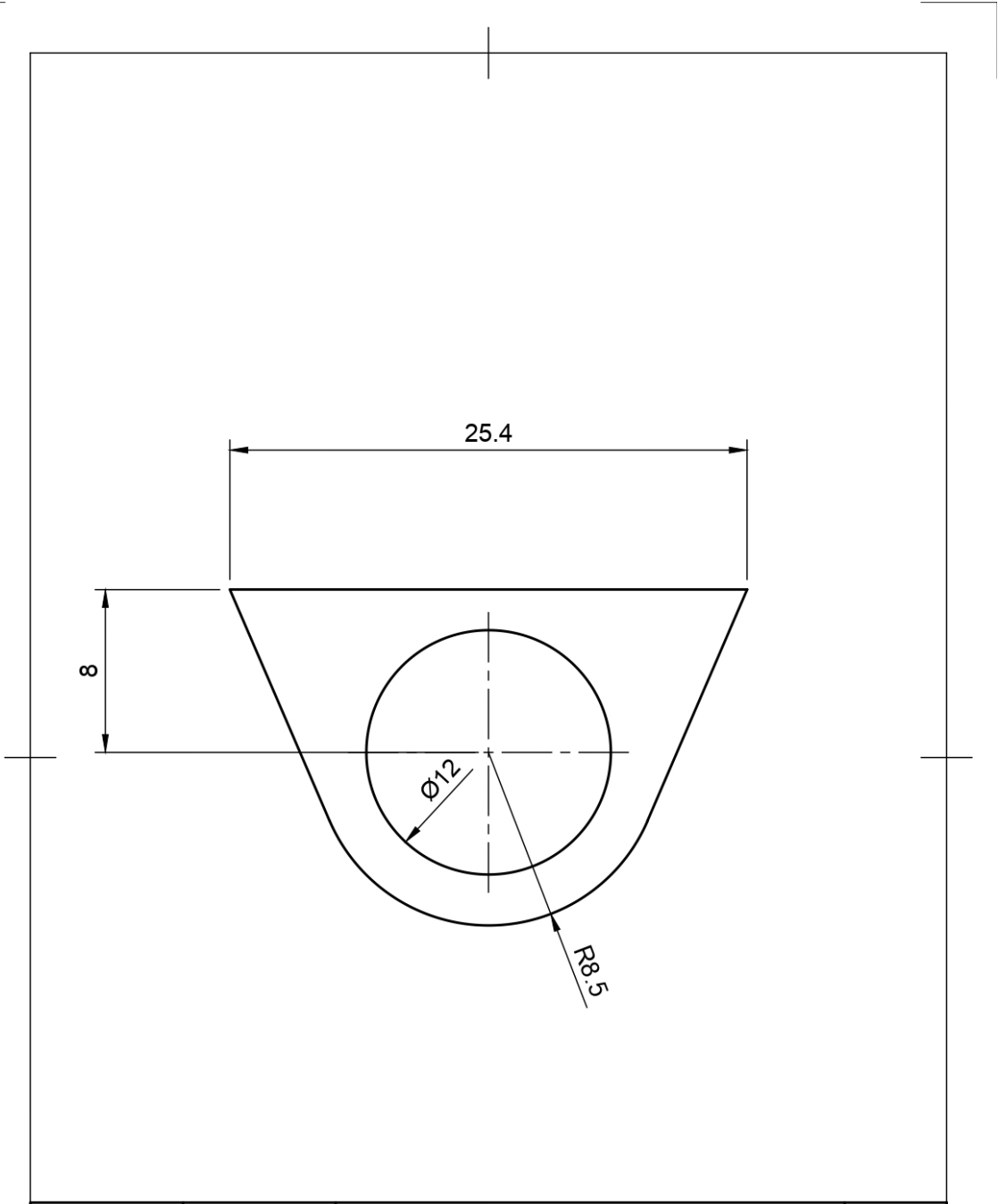


Tolerance ± 0.1		Weight 2943.8 g		Material ASTM A500, Round Tube, 1in D, 2mm THK			
Date		Name		Title		Scale	
Drawn	5/2/20	Francisco Plaza		Roll Bar		1:10	
Revised	5/3/20	Jose Paredes					
Approved	5/3/20	Mateo Andrade					
				Drawing Code VNG20_IL_CH10		Superficial Treatment Non Corrosive Paint	
						Sheet No. 11/17	

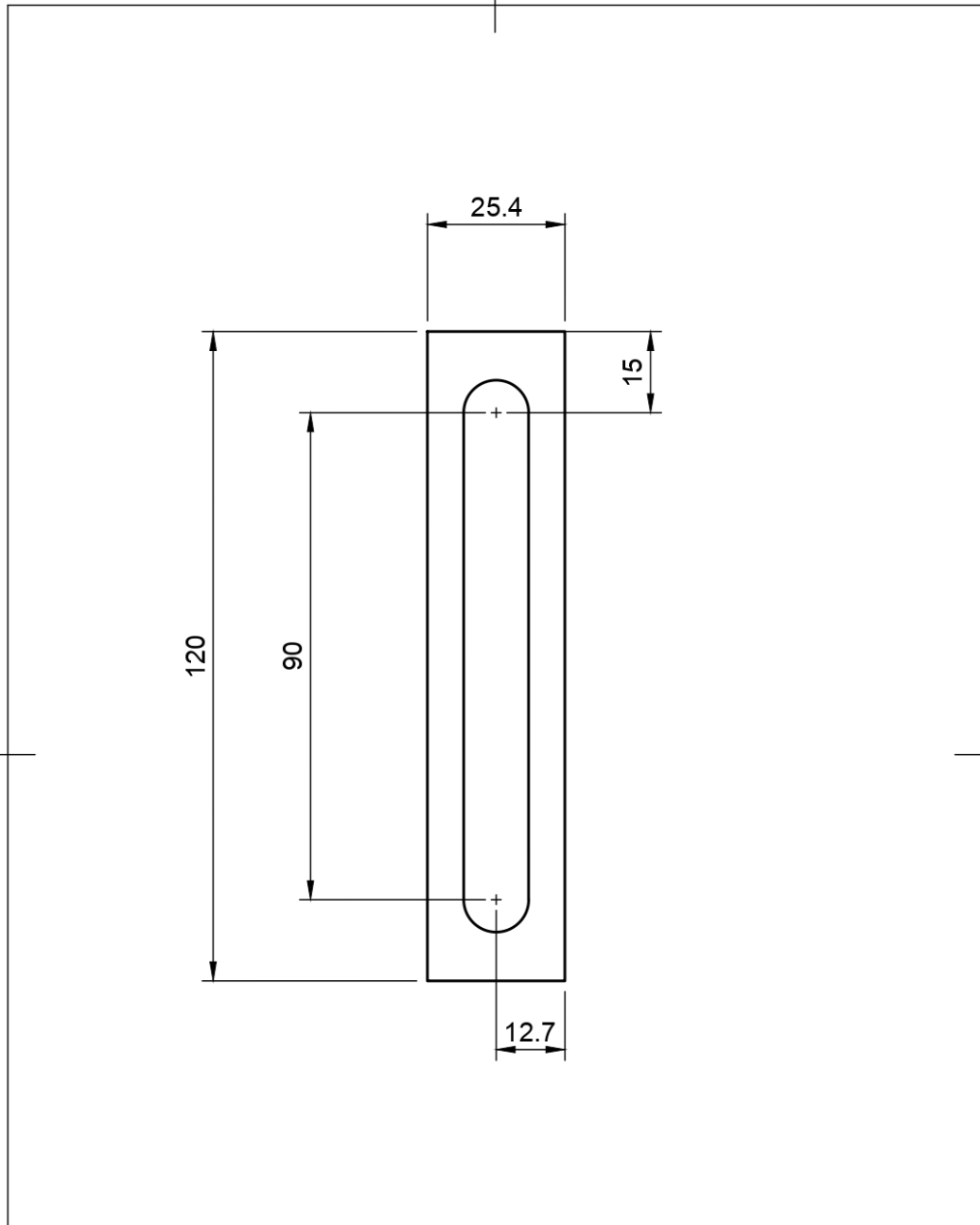




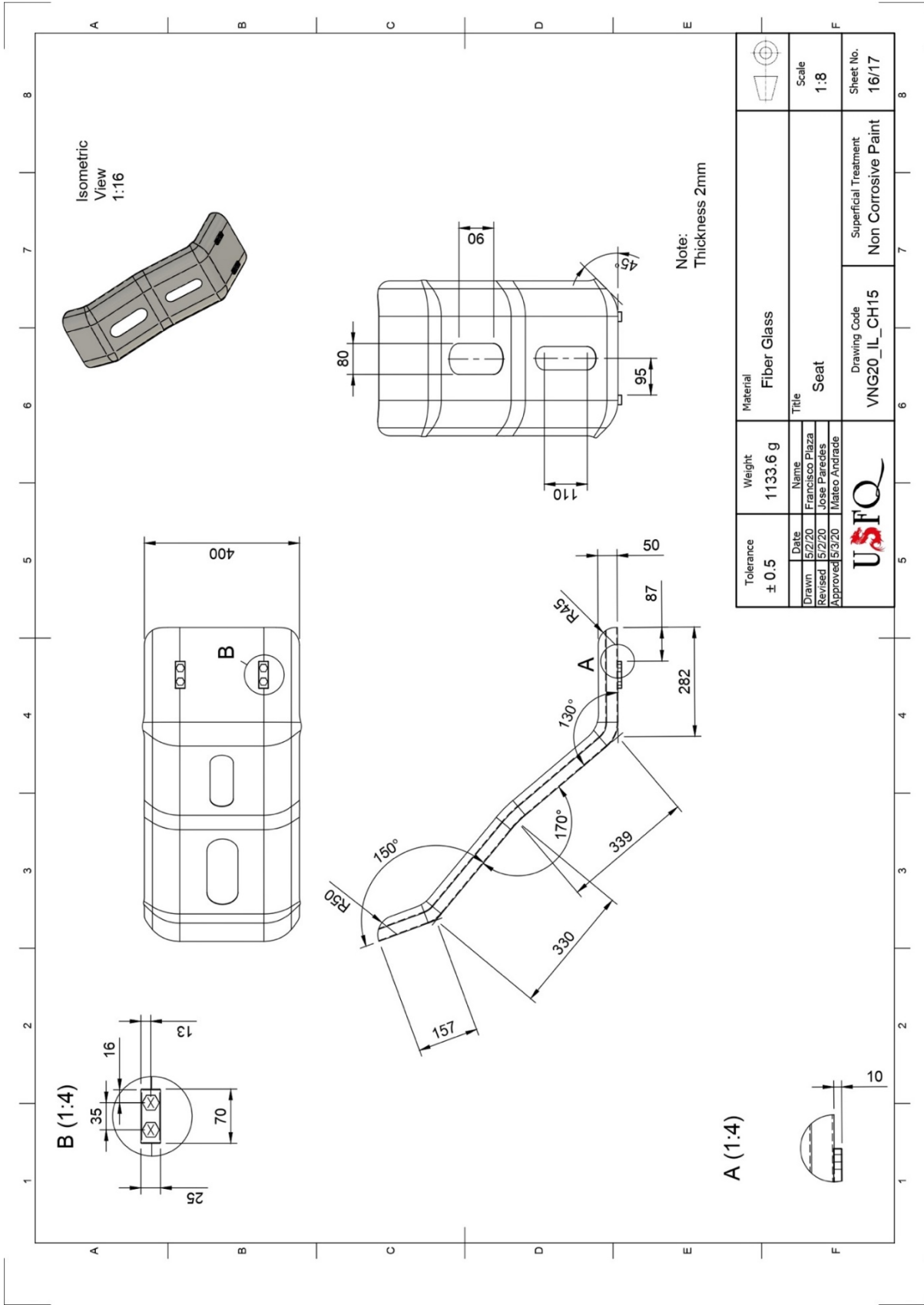
Tolerance ± 0.1		Weight 201.3 g		Material ASTM A500, Platine 6mm THK			
Date 5/2/20		Name Francisco Plaza		Title Right Fork Dropout			
Drawn		Date		Name		Title	
Revised		5/2/20		Jose Paredes		Right Fork Dropout	
Approved		5/3/20		Mateo Andrade		Right Fork Dropout	
				Drawing Code VNG20_IL_CH12		Superficial Treatment Non Corrosive Paint	
						Sheet No. 13/17	



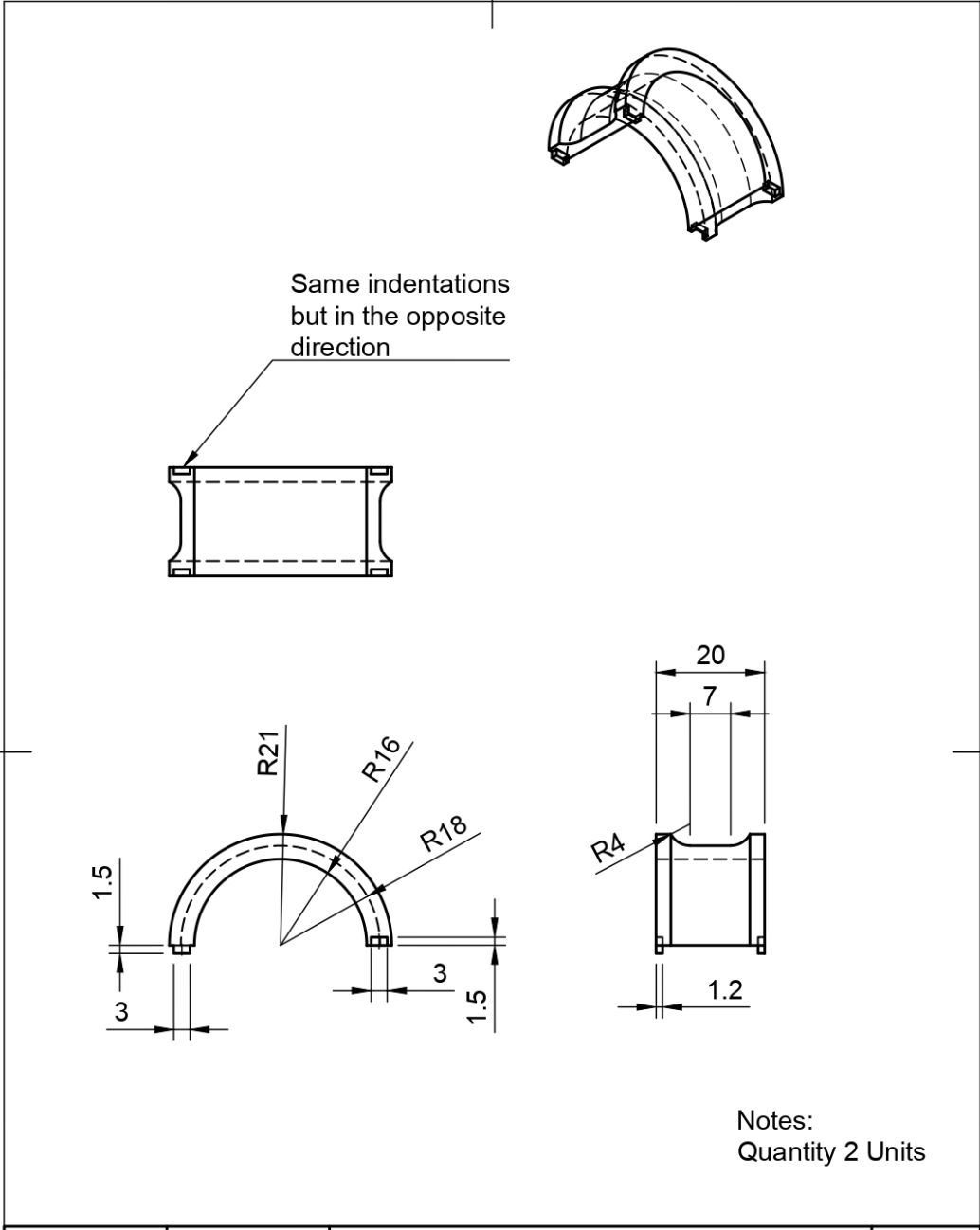
Tolerance ± 0.1		Weight 5.6 g		Material ASTM A500, Platine 4mm THK					
	Date	Name		Title Seat Belt Support		Scale 4:1			
Drawn	5/2/20	Francisco Plaza							
Revised	5/2/20	Jose Paredes							
Approved	5/3/20	Mateo Andrade							
				Drawing Code VNG20_IL_CH13		Superficial Treatment Non Corrosive Paint		Sheet No. 14/17	

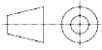


Tolerance ± 0.1		Weight 29.2 g		Material ASTM A500, Platine 2mm THK					
	Date	Name		Title Seat Support		Scale 1:1			
Drawn	5/2/20	Francisco Plaza							
Revised	5/2/20	Jose Paredes							
Approved	5/3/20	Mateo Andrade							
				Drawing Code VNG20_IL_CHS14		Superficial Treatment Non Corrosive Paint		Sheet No. 15/17	

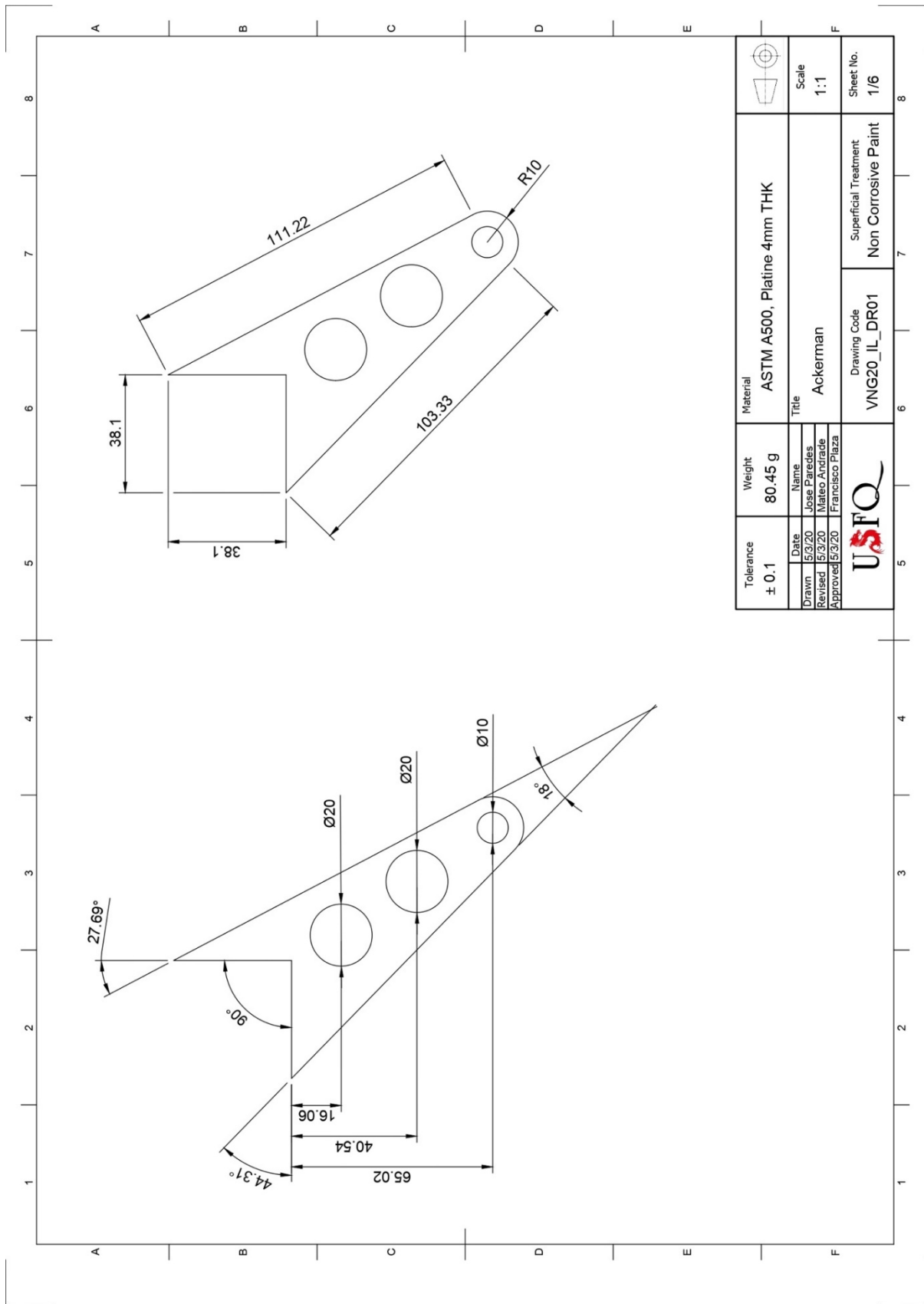


Tolerance ± 0.5	Weight 1133.6 g	Material Fiber Glass	Title		Scale 1:8
			Seat		
Drawn 5/2/20	Name Francisco Plaza	Drawing Code VNG20_IL_CH15	Superficial Treatment Non Corrosive Paint	Sheet No. 16/17	8
Revised 5/2/20	Name Jose Paredes				
Approved 5/3/20	Name Mateo Andrade				
USFO					

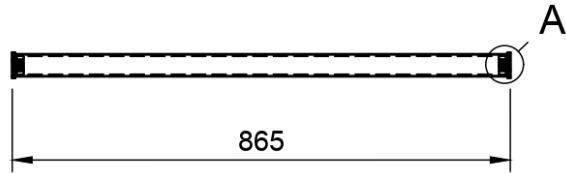


Tolerance ± 0.1		Weight 4.1 g		Material Nylon					
Date		Name		Title				Scale	
Drawn	5/2/20	Francisco Plaza		Rear Tensor		1:1			
Revised	5/3/20	Jose Paredes							
Approved	5/3/20	Mateo Andrade							
				Drawing Code VNG20_IL_CH16		Superficial Treatment N/A		Sheet No. 17/17	

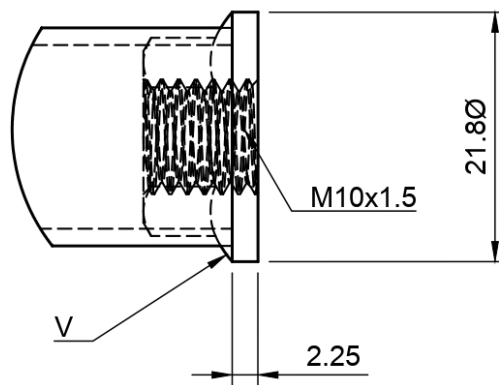
Direction System Drawings



Tolerance ± 0.1	Weight 80.45 g	Material ASTM A500, Platine 4mm THK		Scale 1:1	Sheet No. 1/6
		Title Ackerman			
Drawn 5/3/20 Jose Pareides	Date 5/3/20	Drawing Code VNG20_IL_DR01		Superficial Treatment Non Corrosive Paint	
Revised 5/3/20 Mateo Andrade	Name Jose Pareides	Drawing Code VNG20_IL_DR01		Superficial Treatment Non Corrosive Paint	
Approved 5/3/20	Name Mateo Andrade	Drawing Code VNG20_IL_DR01		Superficial Treatment Non Corrosive Paint	
	Name Francisco Plaza	Drawing Code VNG20_IL_DR01		Superficial Treatment Non Corrosive Paint	

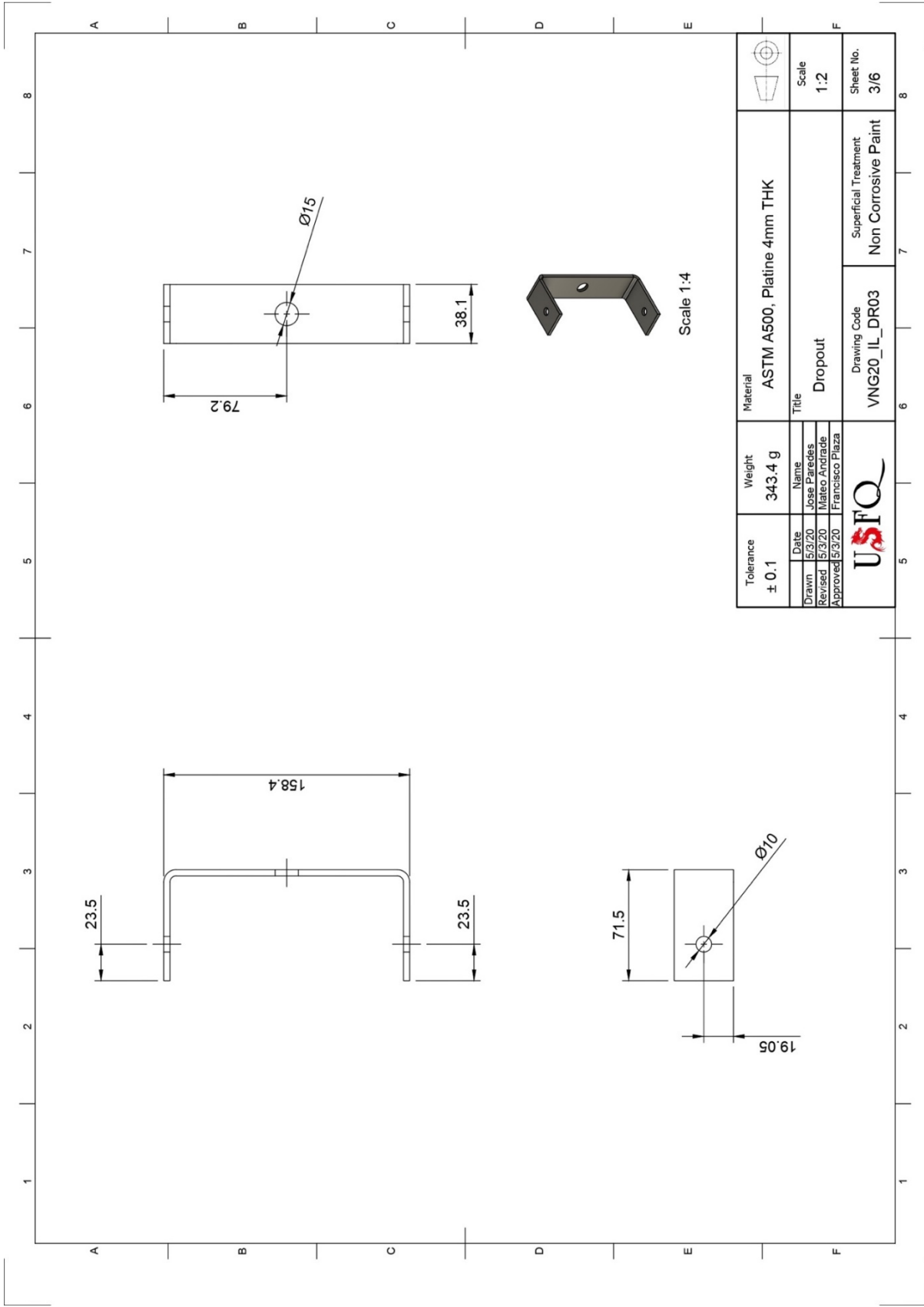


A (2:1)

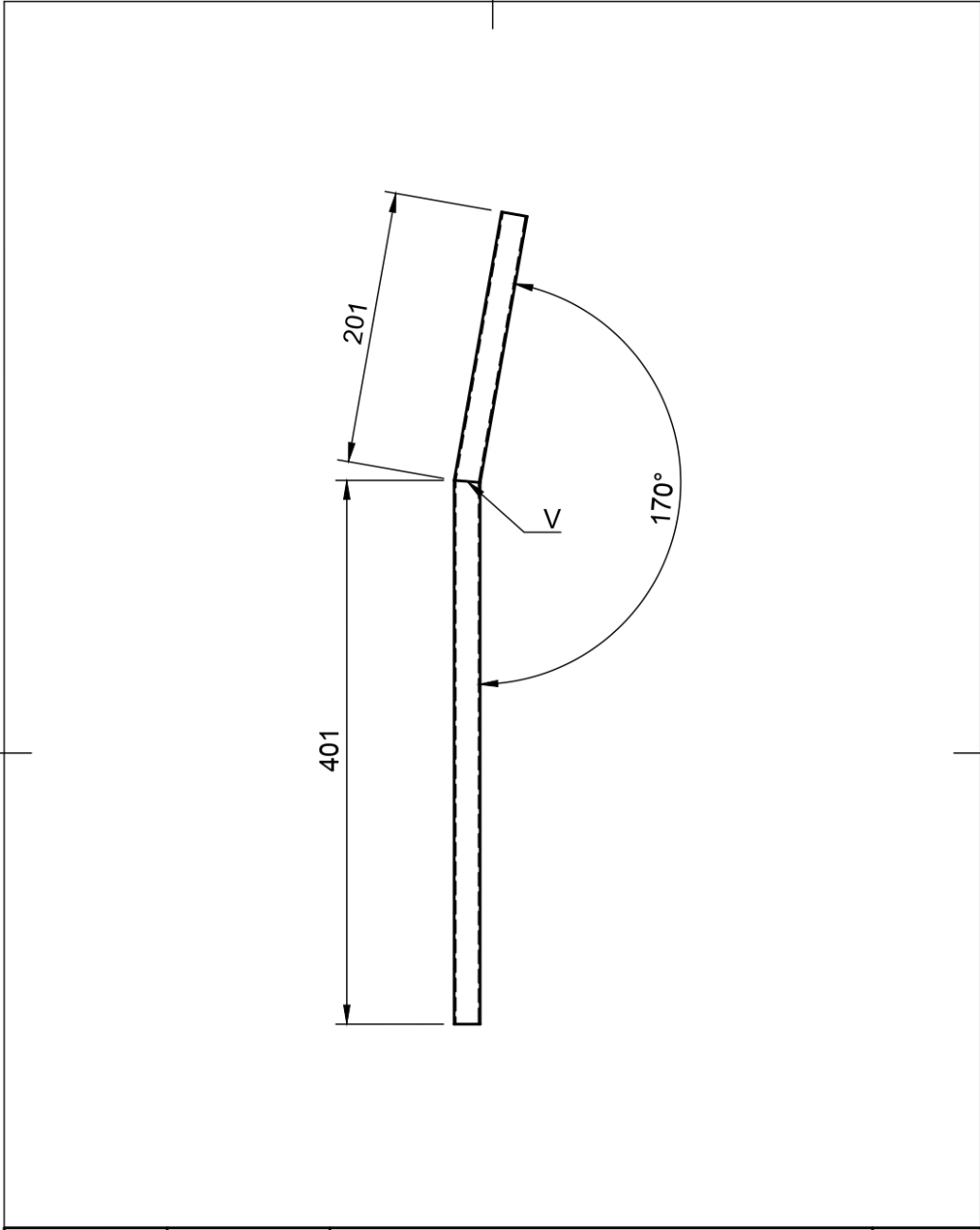


Note:
Both ends of
the rod use the
information
from the Detail
View A

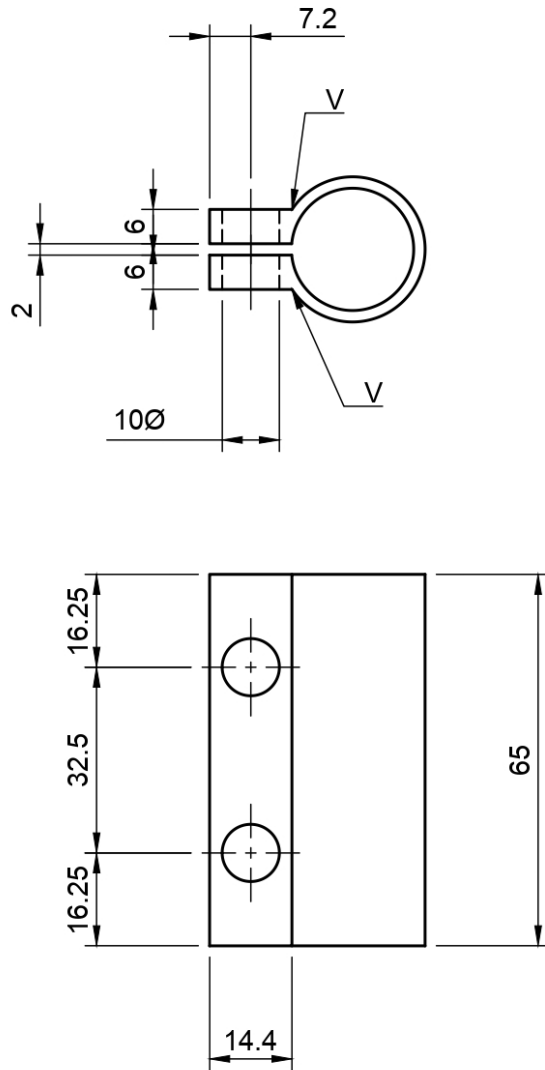
Tolerance ± 0.1		Weight 310.4 g		Material ASTM A500, Round Tube, 0.75 in D, 2mm THK			
		Date		Name		Title	
Drawn		5/3/20		Jose Paredes		TrackRod	
Revised		5/3/20		Mateo Andrade			
Approved		5/3/20		Francisco Plaza			
				Drawing Code VNG20_IL_DR02		Superficial Treatment Non Corrosive Paint	
						Scale 1:5	
						Sheet No. 2/6	



Tolerance ± 0.1	Weight 343.4 g	Material ASTM A500, Platine 4mm THK		Scale 1:2
		Title Dropout		
Drawn 5/3/20 Jose Paredes	Date 5/3/20	Drawing Code VNG20_IL_DR03		Sheet No. 3/6
Revised 5/3/20 Mateo Andrade	Date 5/3/20	Superficial Treatment Non Corrosive Paint		
Approved 5/3/20 Francisco Plaza				



Tolerance ± 0.1		Weight 267.1 g		Material ASTM A500, Round Tube, 0.75 in D, 2mm THK			
		Date		Name		Title	
Drawn		5/3/20		Jose Paredes		Lever	
Revised		5/3/20		Mateo Andrade			
Approved		5/3/20		Francisco Plaza			
		Drawing Code VNG20_IL_DR04		Superficial Treatment Non Corrosive Paint		Scale 1:4	
						Sheet No. 4/6	



Tolerance ± 0.1		Weight 138.31 g	Material ASTM A500, Round Tube, 1 in D, 6mm THK	
	Date	Name	Title Lever Mount	Scale 1:1
Drawn	5/3/20	Jose Paredes		
Revised	5/3/20	Mateo Andrade		
Approved	5/3/20	Francisco Plaza		
		Drawing Code VNG20_IL_DR05	Superficial Treatment Non Corrosive Paint	Sheet No. 5/6

Engineering Analysis

Crank FEA

This section deals with the study of the critical loading cases of the crank used in the transmission system. Since it is one of the parts that will be a constant subject of abuse and is the key area where the power goes into the vehicle, an in-depth analysis of the behavior of the crank was considered necessary. The objective of the study is to evaluate the stress distribution of the crank during an average rotation. This is to identify the angle at which it will receive the most impact. This will be considered the critical position for the crank, which will then be used in a critical load case to analyze the stress behavior of the crank at its maximum possible abuse conditions and ensure the safety of the design. The part used, according to our design specifications, is the Shimano Alivio FC-M4050, which is made from aluminum. The figure 26 shows the CAD model used in Autodesk Fusion 360 to perform the finite element analysis.



Figure 26 Shimano Alivio FC-M4050

Schematic, assumptions, and data

The following diagram (figure 27) shows the basic decomposition of the force applied to the crank during pedaling into the radial and tangential components. The layout is in two dimensions to simplify the dynamic analysis, which can be done on account of the pedaling mostly acting on two directions. The changes in the magnitude and direction of the pedaling force during the rotation of the crank will be reflected on variations in the magnitudes and proportions of these component forces.

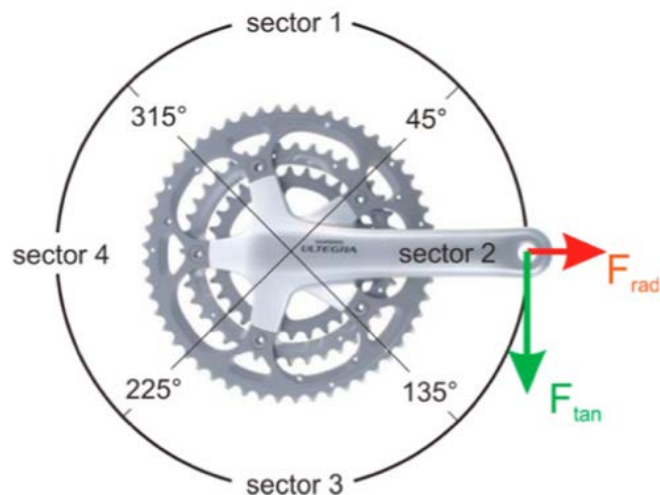


Figure 27 Decomposition of force in the rotation (Höchtl, 2010)

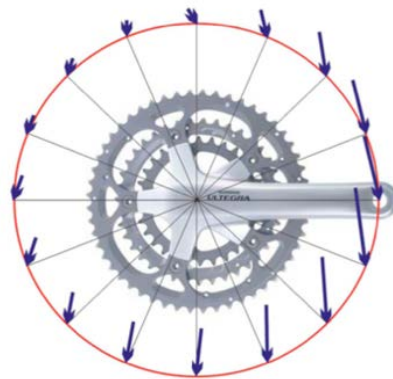


Figure 28 Distribution of pedaling force along the rotation (Höchtl, 2010)

Figure 28 shows how the general force vector changes in magnitude and direction along the pedaling cycle. This study uses data from Höchtl's dedicated study to the pedaling force distribution during a normal cycle (pedaling force of 500 N, which is average recreational pedaling), extracted from their results, which provide information for the tangential and radial components during the whole rotation. Figure 29 presents a graph regarding details on this information, where it is particularly noteworthy that the forces do not show a symmetrical pedaling pattern, which limits the possible simplifications (this graph was created with the data extracted from Höchtl's study). Therefore, to find out in what part of the rotation do the combination of these forces translate to the bigger stress load on the crank, a finite elements simulation was made for every 15 degrees of rotation. Out of these 25 simulations, the one with the highest Von Mises stress was the critical pedaling position. The ratio between both

force components on this angle can be used to maintain the same vectoral direction of the pedaling force, with any desired magnitude, while still keeping the critical effect on the crank in relation to other parts of the rotation. Therefore, a critical pedaling force of 1400 [N] was applied using this ratio to separate into the corresponding tangential and radial components without losing the proportion of the vector, to evaluate the most critical scenario for the crank. This force was cited in Archibald's book as the maximum pedaling output that an elite athlete can provide, representing the highest level of abuse that the crank would face. (Archibald, 2016)

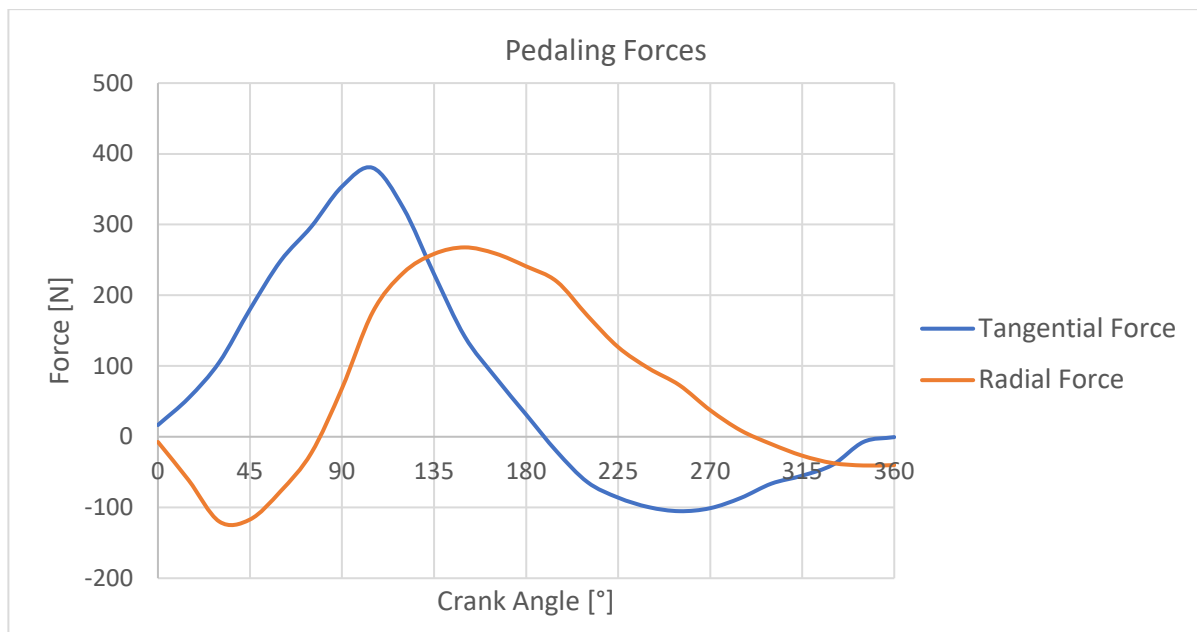


Figure 29 Adaption of the tangential and radial force along the rotation (Höchtel, 2010)

Loading Cases and Boundary Conditions

The tangential and radial components of the pedaling force were used in two kinds of load cases, both of which have been extensively used of previous studies in order to evaluate the most critical result possible. In one case, denominated *Direct*, the forces are applied directly into the internal surface of the hole in the crank where the pedal would be inserted. The second case, denominated *Pedal*, has remote forces with a 5 [cm] elevation (the point in space where the centroid of the pedal would be located) applied to the same surface as the previous case. This offset has the purpose of emulating the torque that the pedal would produce on the crank during the pedaling, leading to a more accurate simulation. Both load cases are used because the research done on the subject proves that they both have their degrees of credibility in

accordance to the involved biomechanics. By comparing the results of both cases, the results of the critical pedaling position can be corroborated. Both cases use the same boundary condition: a fixed support in all directions located in the interior face of the hole that joins the crank with the rest of the transmission. Figure 30 shows how the force in the *Pedal* load case was applied from different points of view. (Tiku, 2019)

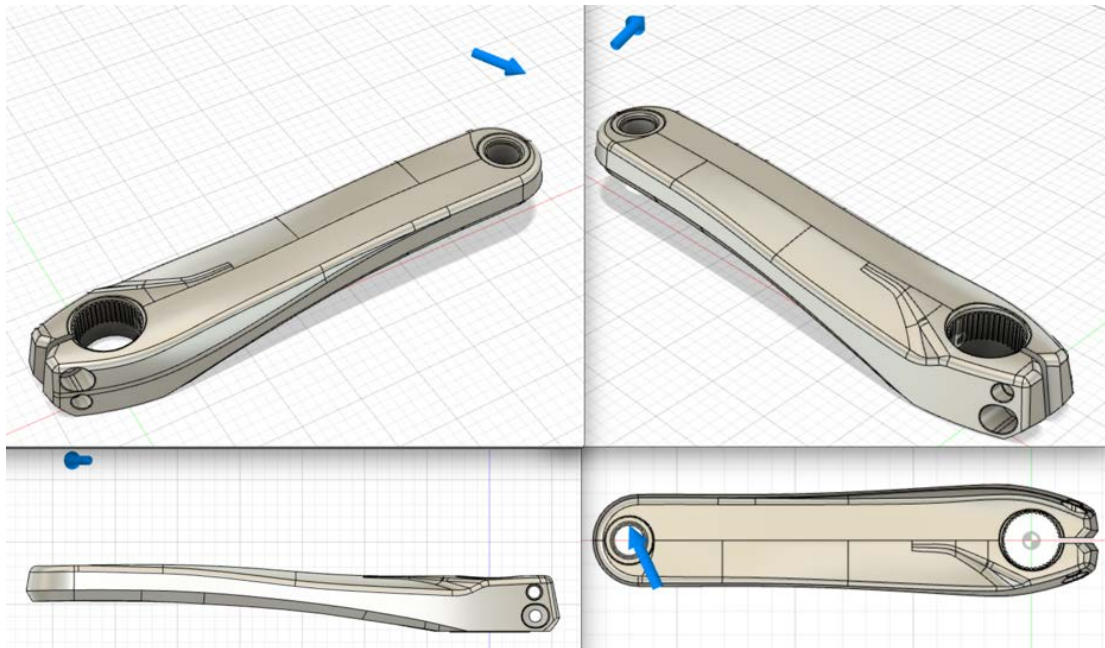


Figure 30 Pedaling force application

Mesh

The mesh was generated automatically by Fusion 360's software from the CAD's geometry. The elements used were tetrahedral with a parabolic order generation that efficiently adapts to the complex geometry of the crank. To ensure the meshing convergence, four levels of element sizes were tested. The software uses a percentage system to identify the average size of elements in the mesh, based on the size of the smallest surfaces on the CAD, in which the smaller the percentage, the finer the mesh. The tested meshes were on the order of 7% (33705 elements), 5% (38464 elements), 3% (42374 elements) and 1% (141838 elements). The change in the Von Mises stress result in the critical point was used as the comparison point to determine the validity of the mesh convergence. Adaptive Mesh Refinement, a software tool that helps ensure that the mesh does converge, was always used. The results showed that in all cases, the values had a small variation within their order of magnitude (decimals of megapascals), which means that the mesh was valid for the study. Only the 7% mesh had a

slightly higher variation (1.7 [MPa]) in relation to the rest, so for the remainder of the study, a 5% mesh was used. This size represents a good balance between performance and validity of results. The following figures show the different levels of mesh tested for convergence.

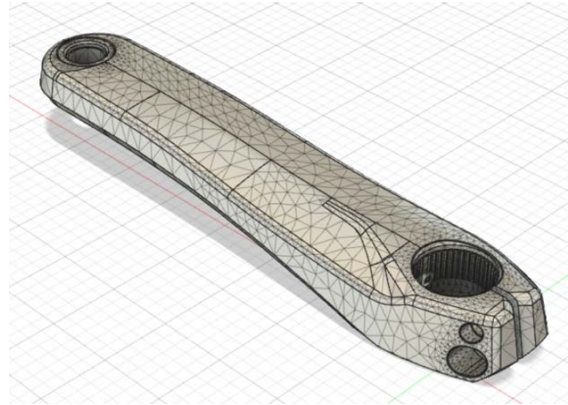


Figure 31 7% proportional mesh

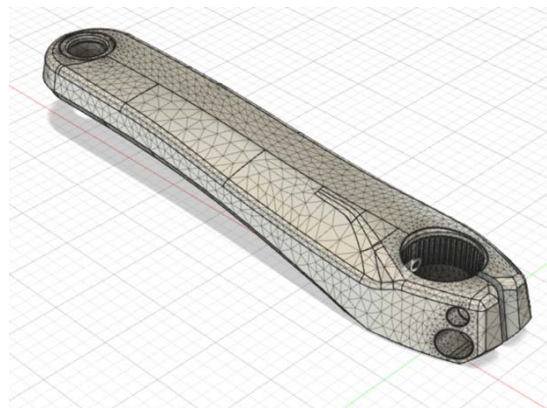


Figure 32 5% proportional mesh

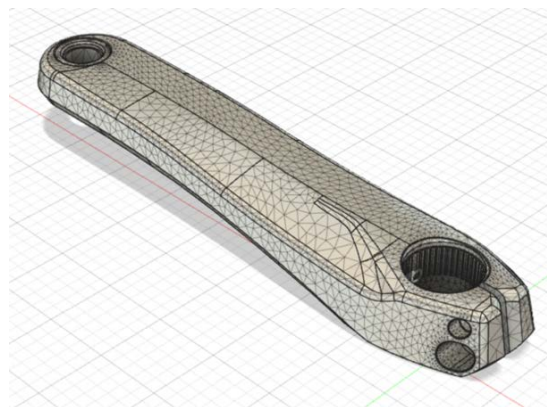


Figure 33 3% proportional mesh

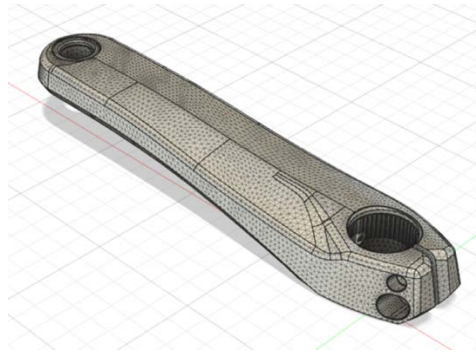


Figure 34 1% proportional mesh

Results

As described previously, 25 studies with two load cases were made to analyze the behavior of the crank during the rotation cycle. The following results show the maximum Von Mises stress for each of the 25 positions, for both case studies. Figure 35 shows these results in a polar graph to appreciate visually how the maximum stress varies during the 360 degrees of rotation. The vertical axis stands for the maximum Von Mises stress obtained [MPa], with the outer values representing a higher stress. This graph is particularly useful to understand the asymmetrical behavior of the crank during pedaling, and to easily find the critical angles of pedaling.

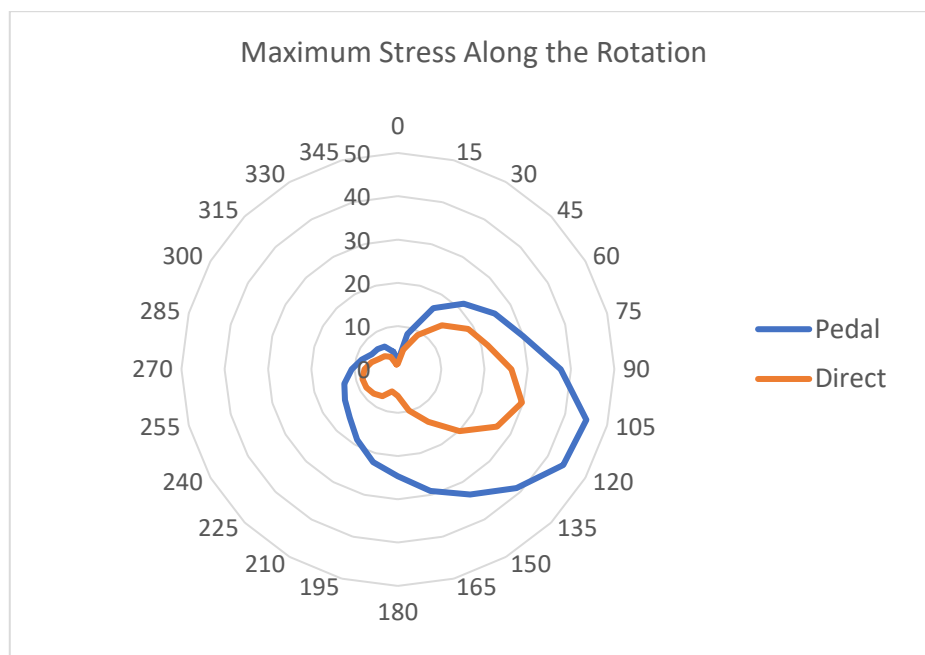
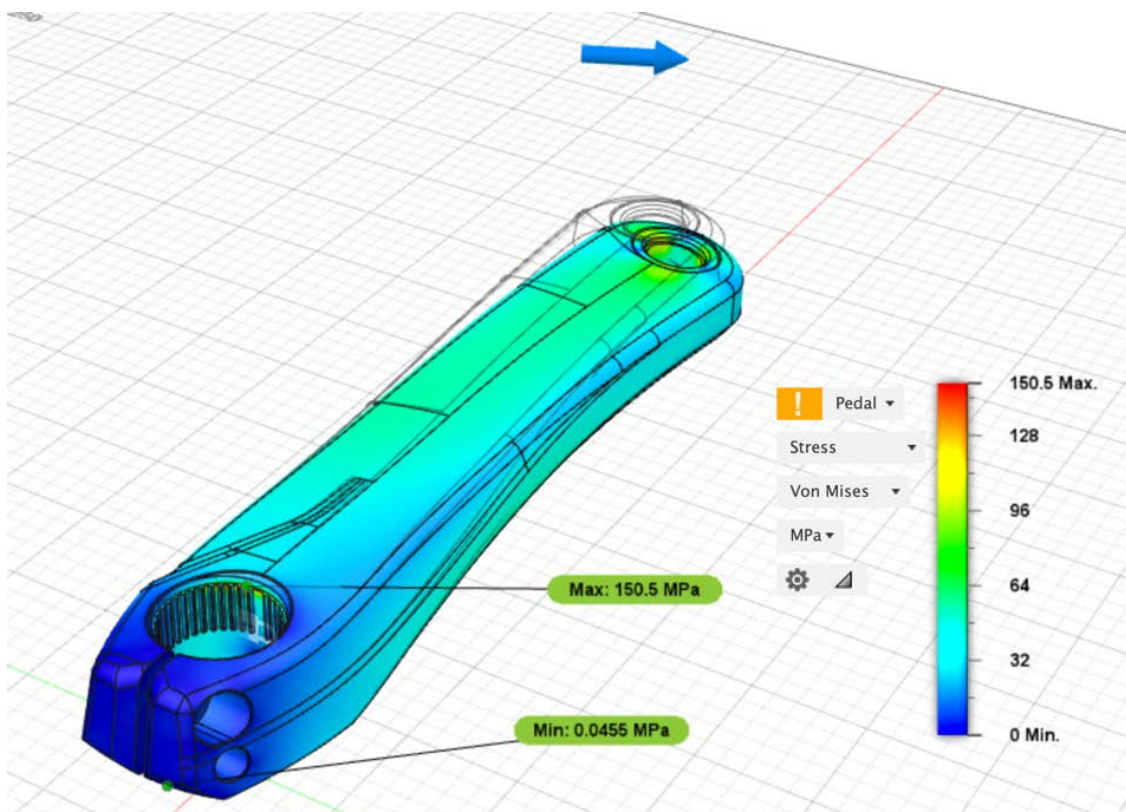


Figure 35 Maximum stress polar graph.

The maximum stress is located in the rotation angle of 105°, and the graph shows an asymmetrical distribution of stress along the rotation.

Clearly, the results show that the crank undergoes a maximum stress when its rotation is at 105 degrees. Therefore, using the logic described previously, the critical load of 1400 [N] was applied using the force component conditions and proportions corresponding to the 105 degrees of rotation for a critical study, using the Pedal load case, since it yielded the highest stress results. This simulation is shown in figure 36, which exposes the stress distribution in the crank, where the maximum Von Mises stress was of 150.5 [MPa]. Considering that aluminum has a yield strength of 275 [MPa], it can be said that the crank has a safety factor of 1.8 on its most critical scenario. Therefore, the design is appropriate for our product since it barely fits into our proposed minimum safety factor. It is relevant to consider that this safety factor will only be active when an elite athlete works under maximum capabilities, and only during that specific moment in the pedaling rotation. This means that under normal conditions, the crank will never reach such a high stress and will never fail, and even under high elite performance, during most of the rotation the crank will not receive enough abuse to match these results (since our previous results prove that the stress distribution is asymmetrical).



*Figure 36 Von Mises stress distribution on a critical scenario.
The maximum stress was 150.5 [MPa] with a safety factor of 1.8*

The maximum stress concentrator is in the internal area of the fixed face, in contact with the stripped geometry used to attach the rest of the transmission components. Due to the presented geometry, the fact that the stress concentrator was located here was expected. A close up of this stress concentrator is seen in figure 37.

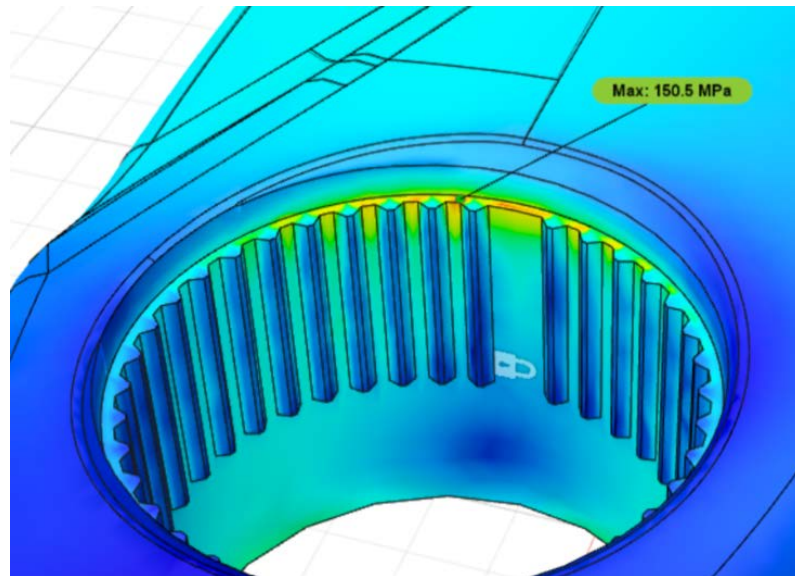


*Figure 37 Stress concentrator in a critical scenario.
The stress concentrator is located in the stripped geometry*

It is also of interest to appreciate the amount of deformation that the crank would suffer during the critical scenario. According to the results shown in figure 38, the maximum general displacement would be of 0.76 [mm]. This means that the deformation on the crank would be so small that the human eye would not be able to appreciate it, resulting in no possible changes or effects that could affect the pedaling performance or safety. The figure enhances the displacement just for graphical purposes and is not to scale, and the expected effect of the pedaling torque can be seen slightly twisting the crank. Again, this is only for graphical purposes, since if the actual displacement was shown, the change would not be noticeable.

It is also of interest to appreciate the amount of deformation that the crank would suffer during the critical scenario. According to the results shown in figure 38, the maximum general displacement would be of 0.76 [mm]. This means that the deformation on the crank would be so small that the human eye would not be able to appreciate it, resulting in no possible changes or effects that could affect the pedaling performance or safety. The figure enhances the displacement just for graphical purposes and is not to scale, and the expected

effect of the pedaling torque can be seen slightly twisting the crank. Again, this is only for graphical purposes, since if the actual displacement was shown, the change would not be noticeable.

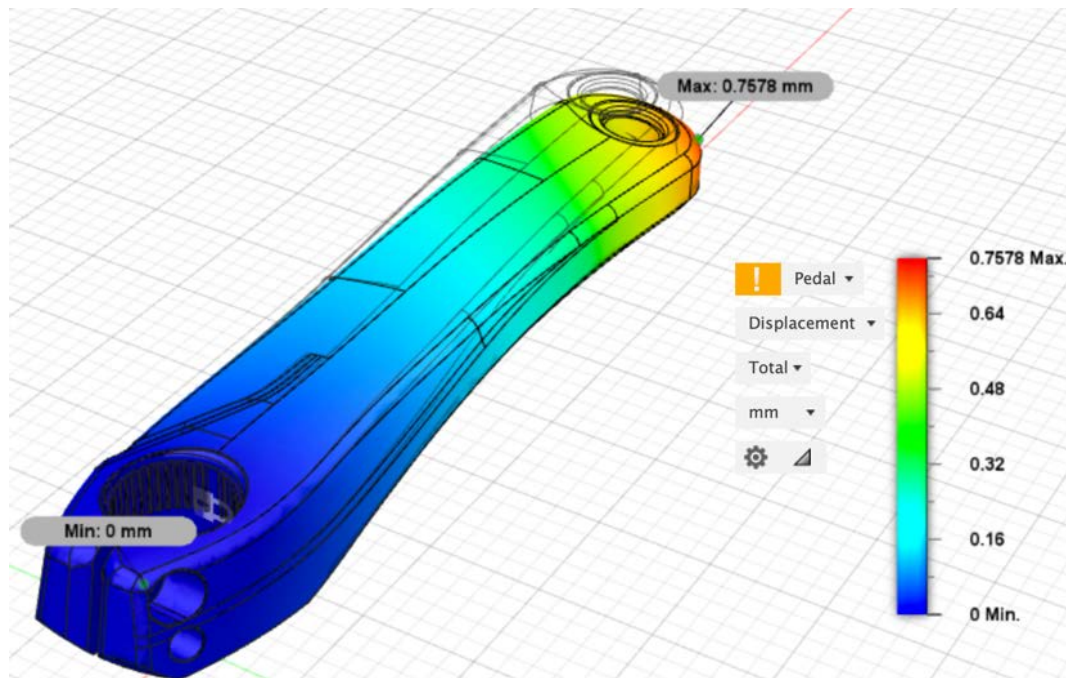


*Figure 38 Displacement distribution on a critical scenario.
Maximum general displacement of 0.76 [mm] on critical scenario.*

Chassis Analysis

Loading Cases

The objective of this section is to explore all the different loading conditions relevant to the performance of this Human Powered Vehicle. Without understanding all the different loading cases at which the vehicle can perform, a proper chassis design cannot be developed. This scenario includes the static loads at different grade conditions, maximum acceleration, maximum braking, turning and Low Speed crash simulations. Once these are fully understood theoretically, the vehicle may be designed. However, a proper experiment should be performed with the first prototype to validate and improve the design.

Problem Definition

The full vehicle weight, including all its structural and dynamic components, is expected to be 25 kg. The minimum turning radius is assumed to be 3 meters. The vehicle should make a complete stop from 25 km/h within no more than 6 meters. The driver weight is assumed to be 75 kg. The vehicle will go uphill and downhill in slopes of 15%.

Assumptions

The assumptions were based on an exhaustive literature review of design reports of universities that had participated in previous HPVC contests and (M. Archibald, 2016), a Human Powered Vehicle design book.

- Vehicle Mass (m) = 25 [kg]
- Wheelbase (L) = 1.2 [m]
- Center of Mass position
 - $b = 0.45$ [m]
 - $h = 0.50$ [m]
- Grades from -15% to 15%
- Rolling Resistance Coefficient = 0.005
- Power Input = 200 [W] (M. Archibald, 2016)
- Target Cruise Speed = 30 [km/h] at level
- Drive wheel diameter = 0.6604 [m]
- Turning radius = 3 [m]
- Aerodynamic Cross-Sectional Area = 1.08 [m²]
- Aerodynamic Drag Coefficient = 0.5
- Braking Velocity = 7 [m/s]

- Braking distance = 6 [m]
- Static Friction Coefficient = 0.75
- Drive Wheel Coefficient = 0.9
- Perfect Welding in joints

Static Load & Vertical Drop

This scenario helps understanding the most basic condition of the chassis design which is sustaining the driver's weight and his own. This study is performed for grades ranging from -15% to 15%. This is important because it helps understand how the center of mass placement affects the weight distribution of the vehicle for the rear and front wheels.

$$W_R = W * \frac{((L - b) * \cos \theta + h * \sin \theta)}{L}$$

$$W_F = W * \frac{(b * \cos \theta - h * \sin \theta)}{L}$$

The weight distribution for the different grades for the rear and front axis is shown in figure 25. This solution was computed in MATLAB using the code presented in the annexes.

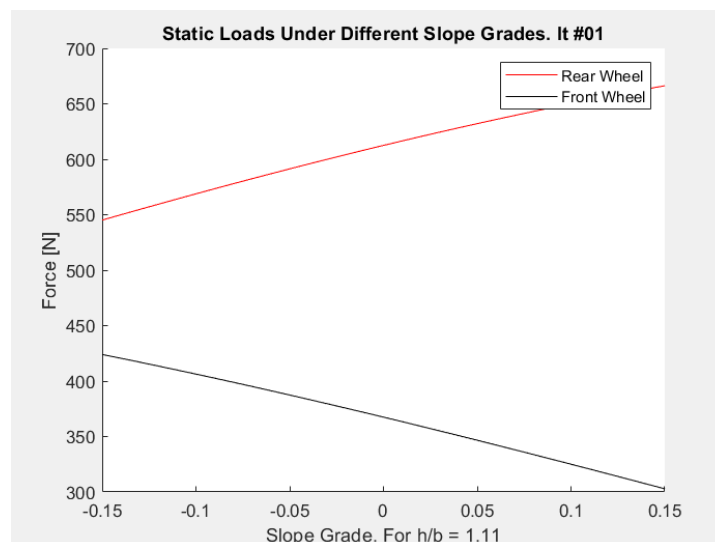


Figure 39 Static Loads Under Different Slope Grades. Shows the effect of the slope in the vehicle rear and front wheel loading.

As it is shown in figure 40, the maximum static rear load happens at the maximum slope over 650 [N], and the maximum front load happens at the minimum slope around 425 [N]. Therefore, the critical component for this scenario is the rear axis.

The vertical drop scenario will be performed in the FEA software to simulated fatigue and vibrations wear-out on the chassis without knowing the actual loads. This study is performed only for a complete vertical drop out assuming an acceleration of 3 G's.

Constant Speed

The constant speed scenario is performed to understand the effect of the Human Powered Vehicle design on the power inputs requirements. This includes effects on surface friction, rolling resistance, and aerodynamic drag. The computation of this scenario is shown below for different grades. Figure 40 shows the input requirement for different grades to maintain a constant speed of 30 [km/h].

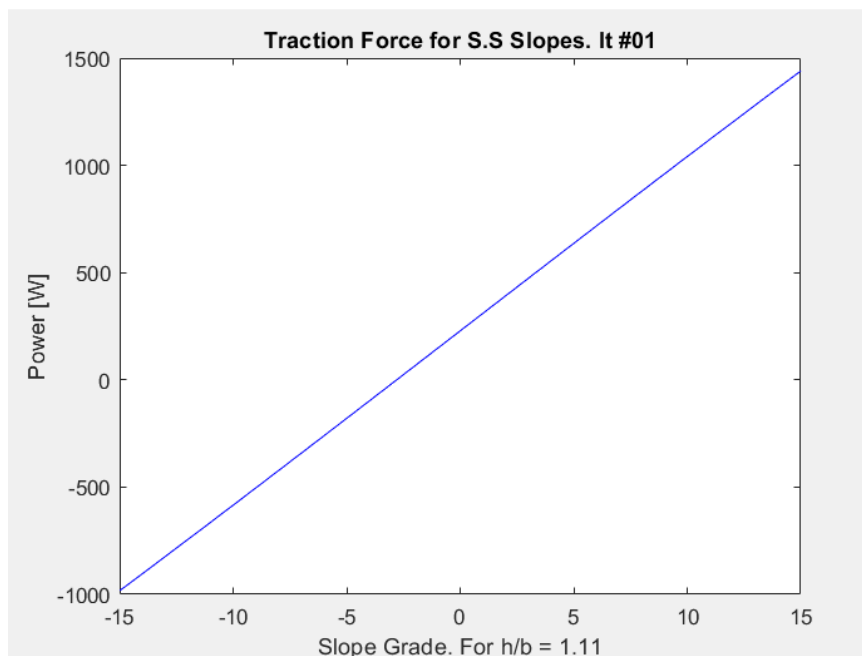


Figure 40 Traction Force Steady State Slopes.

The power input required to sustain a 30 [km/h] constant speed for different grade. This speed can only be sustained by a human for grades up to 5%.

This study shows that keeping steady state velocity of 30 [km/h] with human power input is impossible for grades bigger than 5%. According to (M. Archibald, 2016), the maximum human power input for an athlete is around 400 [W]. However, for small slopes and level conditions the power input require fall within the possible range. Therefore, the vehicle will be able to operate at 30 [km/h] under human power. Once the design stage is finished, the assumptions should be revised to verify the vehicle performance and iterate.

Maximum Acceleration

The maximum acceleration scenario is important to understand the maximum traction force the vehicle might experience in the case of extreme torque from the user. This depends on the ground conditions, geometry and physical characteristics of the vehicle, and user power input.

$$a_{ax} = \frac{1}{m\tau} * \left(\frac{P'}{V} - \left(F_{aero} + F_{RR} + mgG \right) \right)$$

$$F_{ax,max} = \mu * W_{DW}$$

Figure 41 illustrates how these two functions interact. At first, the ground characteristics determine the maximum traction force. Then, the human input determines the actual power input assuming perfect power transmission. The maximum possible force for this condition is 735 [N].

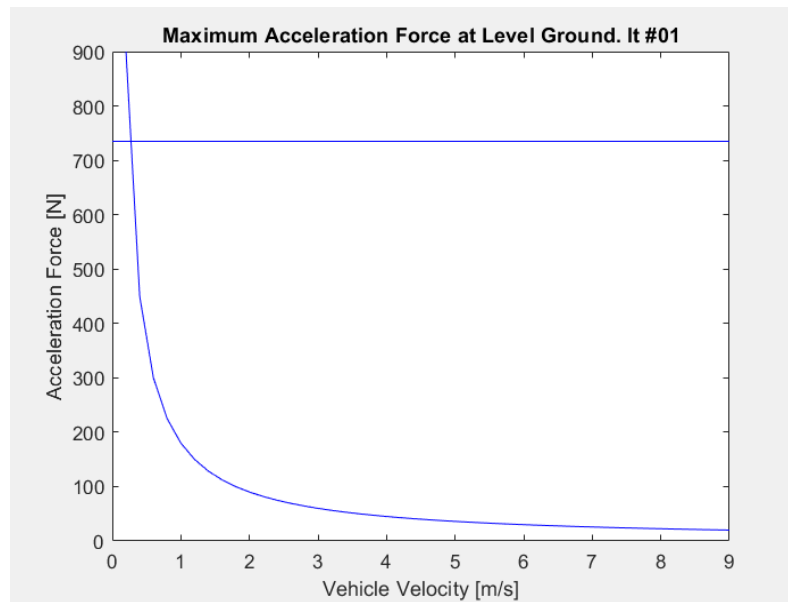


Figure 41 Max Acceleration Force Study.

Maximum acceleration force feasible at level ground is below 750 [N].

Moreover, figure 41 shows the effect of the maximum power input in the maximum vehicle acceleration near to 1 G. This is important when designing the vehicle chassis to verify that the structure will be able to support the longitudinal loads of the chain and transmission gears. The acceleration use for the chassis study will be $7.5 \text{ [m/s}^2\text{]}$.

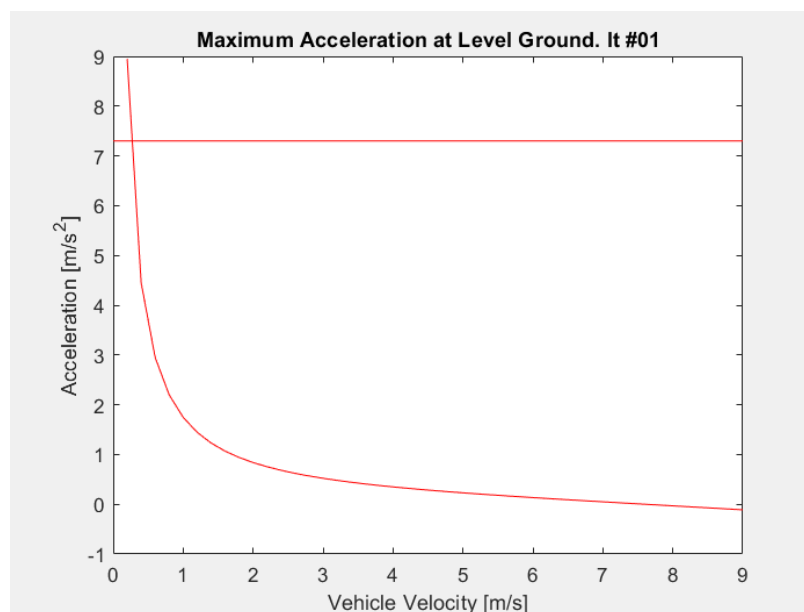


Figure 42 Max Vehicle Acceleration Study.

Maximum acceleration is $7.5 \text{ [m/s}^2\text{]}$

Maximum braking

The maximum braking study, as the maximum acceleration study, is important to understand the maximum load applied longitudinally to the vehicle. The maximum braking force and braking acceleration is computed. This will be useful when designing for the wheel hubs and chassis supports.

$$A_{x,max} = - \frac{L - b}{h}$$

$$A_{x,max} = -\mu$$

The computation performed by MATLAB suggest a maximum acceleration force for pitch over of 1.5 Gs and for sliding of 0.75 Gs. Therefore, the study for braking will be using a deceleration of 0.75 Gs.

Turning

The turning scenario is crucial for the chassis design. It requires the chassis to be stiff enough so proper turning radius can be achieved at a given speed. This load case is also important because it is the only one at which axial loads are consider for the chassis design due to centripetal acceleration. Using (M. Archibald, 2016), the following equations were derived to compute the centripetal force and turning forces in the front and rear wheel.

$$F_{yF} = W_f * \left(\frac{V^2}{gR} \right)$$

$$F_{yR} = W_r * \left(\frac{V^2}{gR} \right)$$

The study was performed for different turning velocities to understand the ranges at which turning was possible. A velocity of 5 [m/s] was selected. Figure 29 & 30 shows the

computations results given an average rear wheel turning reaction force of 500 [N] and a front wheel turning reaction force of 450 [N].

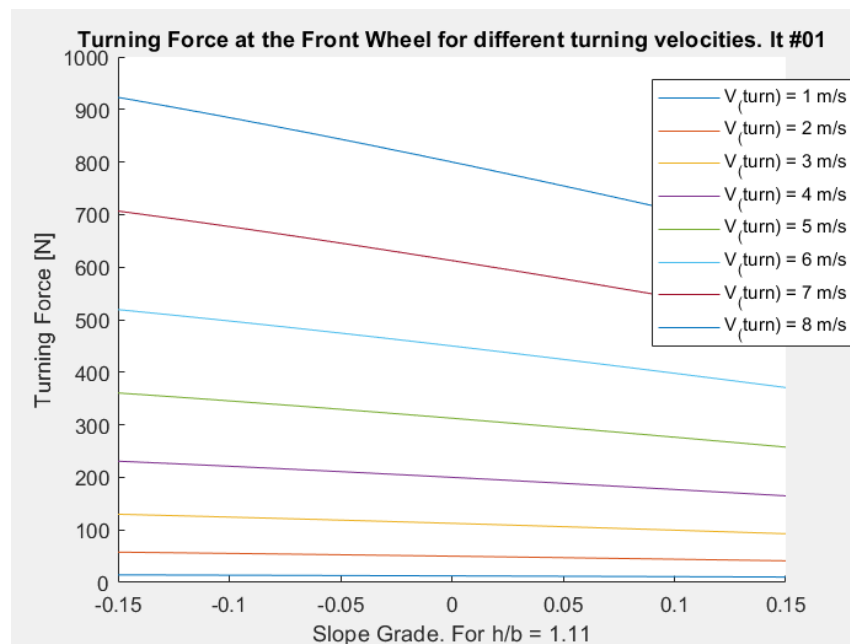


*Figure 43 Front Wheel Turning Reaction Force.
Average front wheel turning reaction force is 450 [N]*

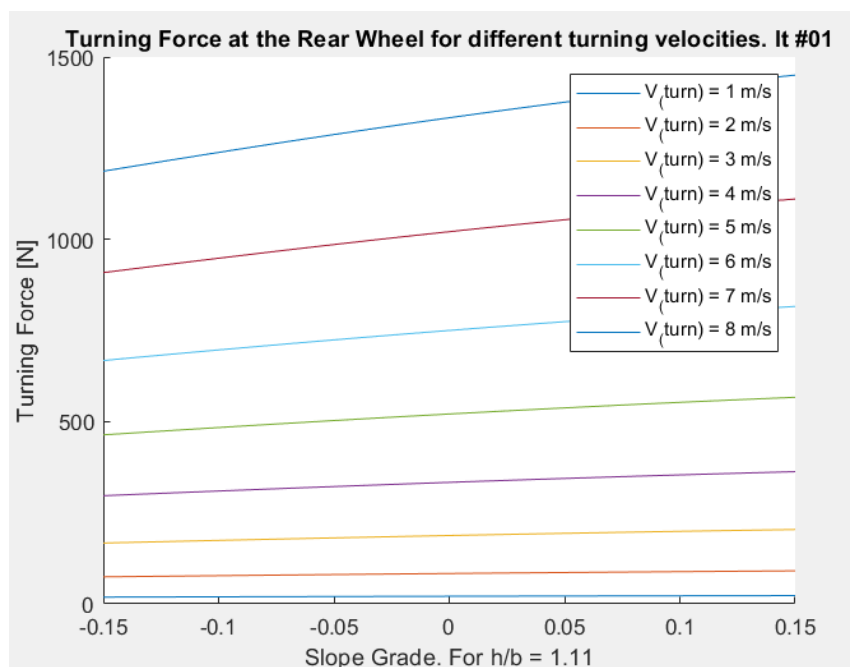


*Figure 44 Rear Wheel Turning Reaction Force.
Average rear wheel turning reaction force is 500 [N]*

Finally, the centripetal force for turning at level ground was computed to understand the final load to add to this load scenario. Figure 45 shows this result.

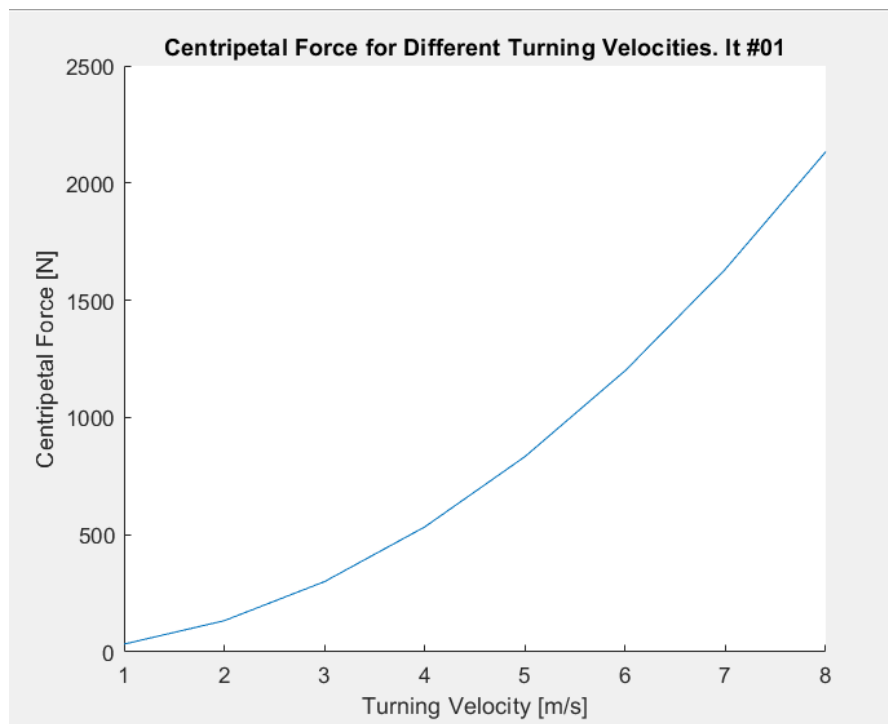


Figure 45 Centripetal Force for Different Turning Velocities. Maximum turning velocity around 5 [m/s].

With the loads computed in this section, the load cases simulations are prepared to analyze the design concept for the chassis. Moreover, other load cases were added to the FEA simulations related to low speed front crushes and vibrations wear out of the vehicles frame. The fully developed chassis design process is presented in the next section.

Chassis Design

The design of the chassis was guided using chapter 13 of (M. Archibald, 2016) on frame analysis. The design methodology consists of defining the mechanical properties of the material to be used and the failure criteria. Then, using a Finite Element Analysis Package the chassis concept is analyzed. The design objective is to achieve a minimum safety factor of 1.5

for regular load scenarios. With the FEA results, the chassis design will be revised and iterated until design objectives are achieved for all the different load scenarios.

Mechanical Properties and Failure Criteria

The material selected for the chassis was steel AISI 1018. It was found that the most similar steel to AISI 1018 available in the Ecuadorian market in round profiles is steel ASTM A500. Its mechanical properties are ultimate strength (S_{ut}) 354 [MPa] and yield strength (S_y) 250 [MPa]. Two failure criteria were selected for the chassis design.

For static failure, the minimum deformation energy criterion was selected:

$$\eta = \frac{S_y}{\sigma_{VM}}$$

For fatigue analysis the criteria selected was the modified Goodman:

$$\frac{\sigma_a}{S_e} + \frac{\sigma_m}{S_{ut}} = \frac{1}{n}$$

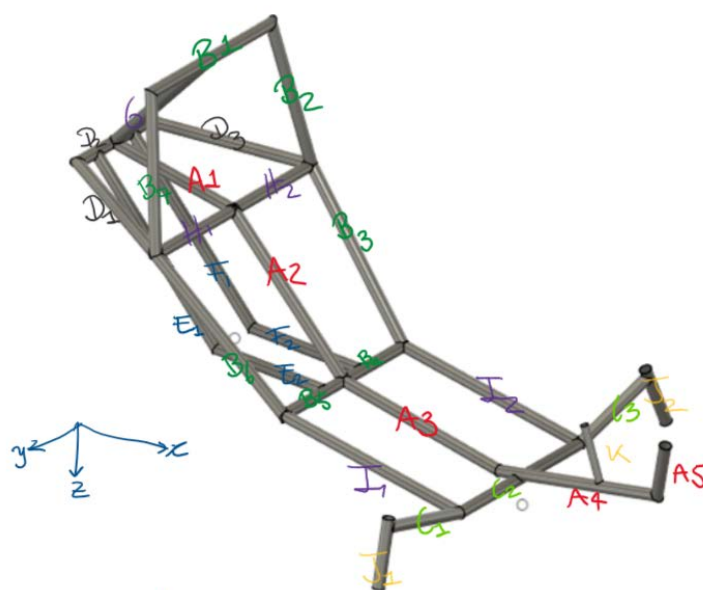
Where, (S_e) is the materials endurance limit. The constant values were computed using (Budynas & Nisbett, 1394).

$$S_e = K_a * K_b * K_c * K_d * K_e * K_f * 0.5 * S_{ut}$$

A MATLAB script was generated to facilitate quick iteration. The S_e of the material for $\frac{3}{4}$ [in] tubes of 1.5 [mm] thickness is 170 [MPa].

Chassis Concept

The challenge when developing the chassis is designing for manufacturing. The CAD workflow was to select a profile available in Ecuador and design for its joints, so workshop drawings are easy to prepare. Figure 33 shows the different subassemblies designed for manufacturing of the HPV chassis. The FEA will aid selecting the correct profiles to avoid oversizing of the frame and reduce the overall vehicle weight.



1. Drop test: This is the go/no-go for chassis design. It is designed to test fatigue endurance of unknown loads in the vehicle. It takes in consideration vehicle, driver and cargo weight. Also, it is set up for 3 G's downward acceleration to simulate the drop. Proper constraints need to be set up.
2. Frontal Crash: Taken from (Archibald, 2016) a load of 2000 N frontal through the x-axis was studied.
3. Frontal crash wheel: Same as the previous case but the frontal x-axis force is applied on a single wheel.
4. Maximum Acceleration: Maximum load in the chassis due to riders' input and ground interaction. Maximum torque input by pedaling is 1400N and maximum tension in the chain is 2.5kN.
5. Maximum braking: Maximum braking force applied to both front wheels of 7.5ms⁻².
6. Maximum turning: Maximum centripetal acceleration case of 0.75Gs.
7. Roll Bar vertical: A roll-over study set-up by ASME HPVC 2020 contest rules.
8. Roll Bar Horizontal: A roll-over study set-up by ASME HPVC 2020 contest rules.
9. Back Crash: Study like the frontal crash scenario but to simulate a rear impact.

The software selected to perform this study was ANSYS due to simplicity and node availability in the student's version. Other packages such as Abaqus only allow a thousand nodes in the students' version while ANSYS allow for 32 000 nodes in the student's version. The same mesh that uses beam elements was used for all the load cases shown below. To account for errors in the roll bar bend tube for the Roll Bar load cases a pipe assumption in Ansys was used to account for cross sectional area deformation.

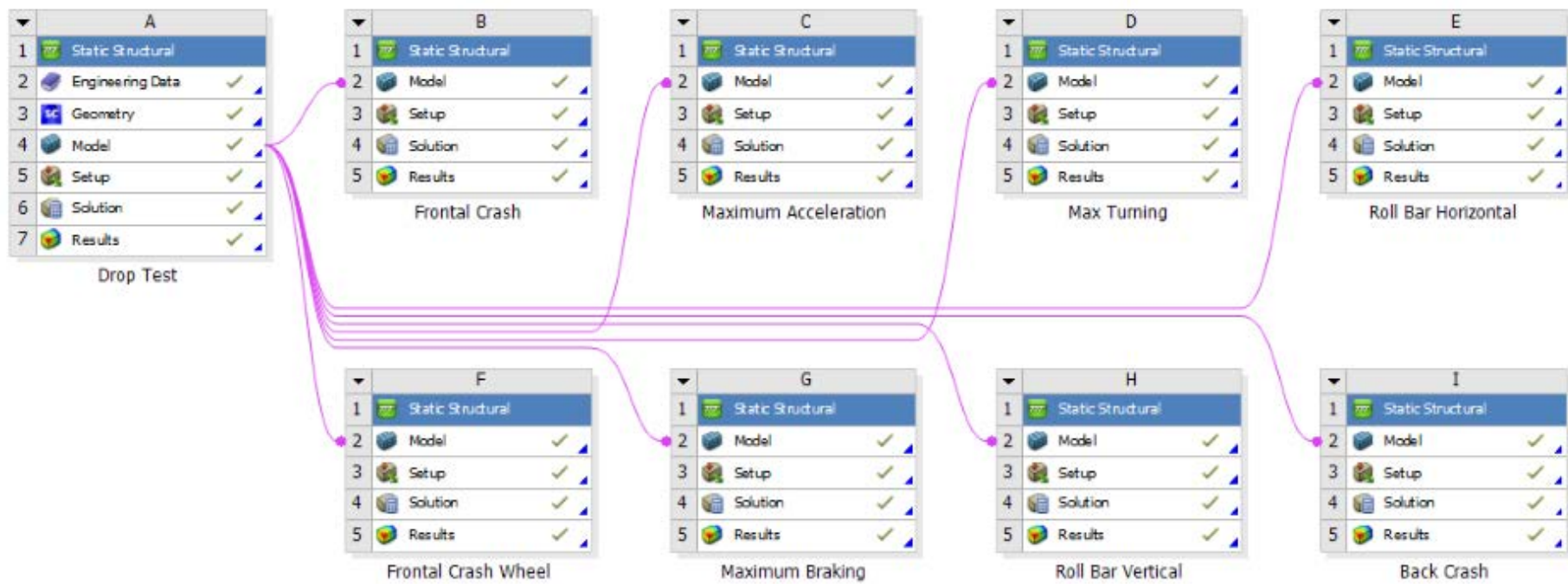


Figure 47 FEA Set-up.

9 Different load cases were analyzed for testing the chassis concept.

Table 5 Preliminary FEA Results.

Two critical load scenarios were found: Max Acceleration and Back Crash.

Simulation	Critical Components			
	Component	Maximum Stress [Mpa]	Strain Energy [J]	Safety Factor
Drop Test	Horizontal Frame	50	0.022	3.4
Frontal Crash	Front Tensor Joint	150	0.18	1.9
Frontal Crash Wheel	Horizontal Bar Joint	150	0.15	1.9
Max Acceleration	Front Tensor Joint	155	0.176	1.1
Max Front Braking	Front Hub Joint	95.5	0.112	1.8
Max Turning	Horizontal Bar Joint	17.3	0.002	9.8
Roll Bar Vertical	Roll Bar	20.2	0.024	8.4
Roll Bar Horizontal	Roll Bar Joint	69.7	0.04	2.4
Back Crash	Roll Bar Joint	113.9	0.15	1.5

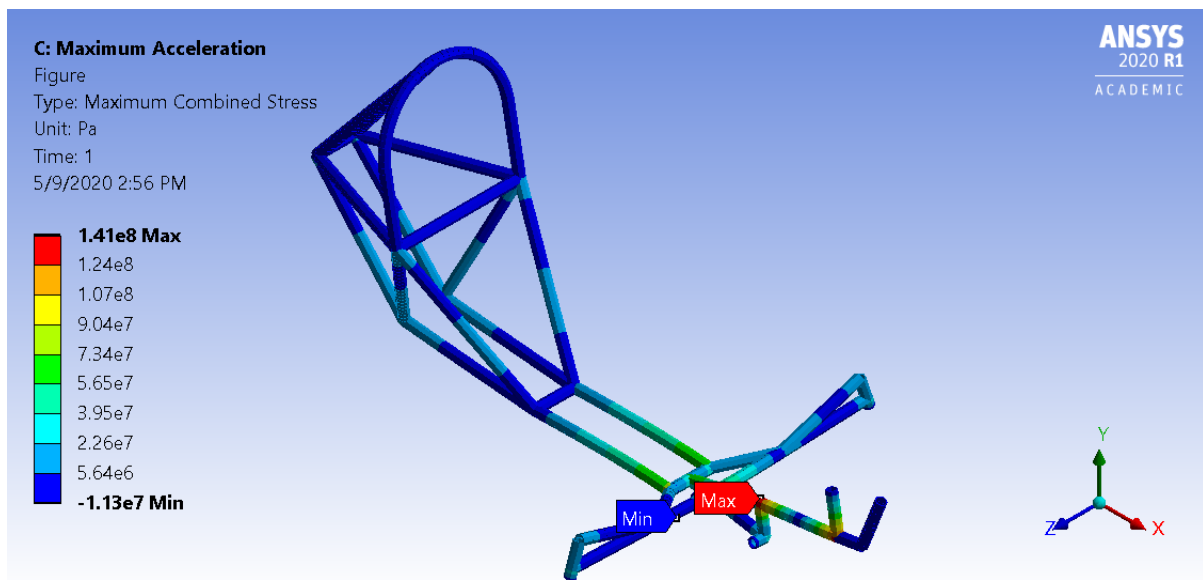
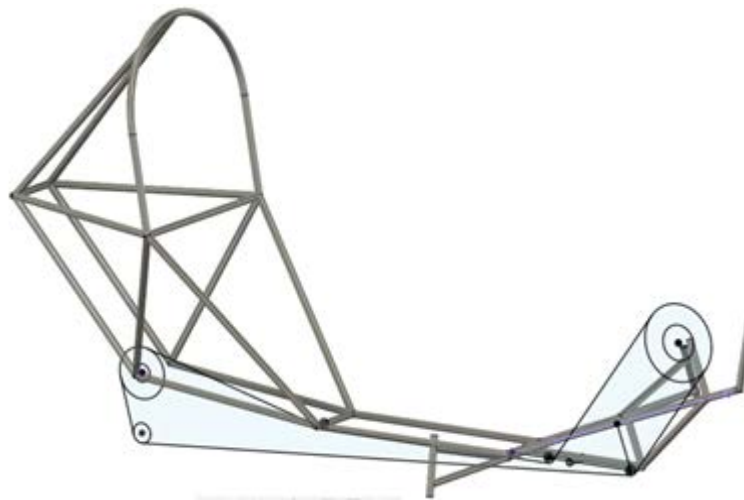


Figure 48 FEA Critical Scenario Display.

Critical component is the joint between the tensors support and the frontal frame of the vehicle.

The FEA yield 2 load cases with a minimum factor of safety below the target value. This critical scenario were the back crash and the maximum acceleration case. Strain energy computations show the stiffness of the model and are consider appropriate for the simulation. It was decided to consider this in the detail design stage of the project. The solution proposed

will be to reinforce these joints with a specialized component. Overall, the chassis concept was approved to enter the detail design stage.



*Figure 49 Final Chassis Design Concept.
This picture shows the chain pad and main features of the concept.*

Within the next steps are the detail FEA study and the weld design for critical components.

Detailed Design

The following section explores the process of using the chassis concept as a base for the detail design stage. This will consider the development of the required parts that will allow the chassis to mount the required transmission components manufactured by Shimano and the respective safety requirements such as seat and seatbelt. The following table shows the required external components for the proper functionality of the vehicle.

Table 6 Ilalo External Components Selection

ILALO EXTERNAL COMPONENTS			
# Part	Part Code	Quantity	Description
Transmission			
1	SM-BB52	1	Threaded 68/73mm Bottom Bracket
2	FC-M4050	1	170mm Crankset for BB52 9 x 3
3	SM-RT30	2	160mm Disk Brake
4	BR-M4050	3	Hidraulic break calliper
5	HB-MT400	2	E-Thru Axle Front Hub
6	-	2	24in Wheel Assembly
7	FD-M980-E	1	Mount E Type with BB plate. Compatible for 3x9 speeds
8	RD-M4000	1	Rear Wheel derailleur
9	SM-RT30	1	180mm brake disk
10	FH-M3050	1	Quick Release Free Hub Rear wheel O.L.D 135mm
11	CS-HG400-9	1	9 plate Cassetes
12	CN-HG54	1	Any chain compatible w/ the system
13	-	1	27.5 in Wheel Assembly
14	ST-M4050-R & L	1	Shift/Brake Lever Right and left
Chassis			
15	91290A601	8	M12 bolts from MacMaster
16	-	1	FIA 4-points Seat Belts
17	96505A118	8	Washers for M12 bolt
18	90593A009	8	M12 hexagonal nuts
19	-	1	Cargo Space Fabric
20	-	2	225mm Rubber 2mm THK

Each of the components required have different standard mounts depending on the manufacturer. Therefore, the best components that will fit our application and manufacturing abilities were selected. Then, the mounts were designed.

The bottom bracket in a bicycle is the component responsible of the free rotation of the crankset. There are different standards to mount bottom brackets. The principal ones are press fit and threaded shells. The threaded shell bottom bracket standard was selected due to its easiness of manufacturing. This consist of either a 68/73mm long shell with 1.37in x 24TPI left-handed thread in the drive size and right-handed in the non-drive side. The crankset was selected to fit in the bottom bracket type selected. This information can easily be found in Shimano's product web page.



*Figure 50 Bottom Bracket Mount.
The drive side thread is shown (1.37in x 24TPI left-handed)*

A hydraulic brake system was selected over the regular braking system to achieve a better year-round performance. In the initial research, it was found that cable disk brakes performance reduces with riding time due to riders' fatigue. Hydraulic brakes solve this issue. The disk size is available in 3 dimensions: 160, 180 and 200mm diameters. For the front wheels, a 160 mm disk was selected due to the smaller size of the front wheel. For the rear wheel, a 180mm disk was selected because of geometry interference and to increase braking power. Moreover, there are different types of mount for disk brakes. The post mount standard was chosen because it is easily available in the market. A 27.5in rear wheel was selected to increase the vehicle maximum speed without selecting a more expensive set of cassettes. 24in wheels were selected for the front to increase the vehicle's maneuverability.



Figure 51 Rear Wheel Caliper Mount

The shortest available front hubs were selected to reduce torque generated by the reaction force of the ground with the wheel in the hub. Also, it needs to have a center locked mechanism for the disk brake. The rear free hub was selected for a quick release technology. This will make easier vehicles maintenance. The rear wheel hub has an O.L.D (Over locknut Dimension) standard for mountain bikes of 135mm. The fork dropout needs to be at least 5mm thick for its proper mount with a dropout diameter of 10mm.

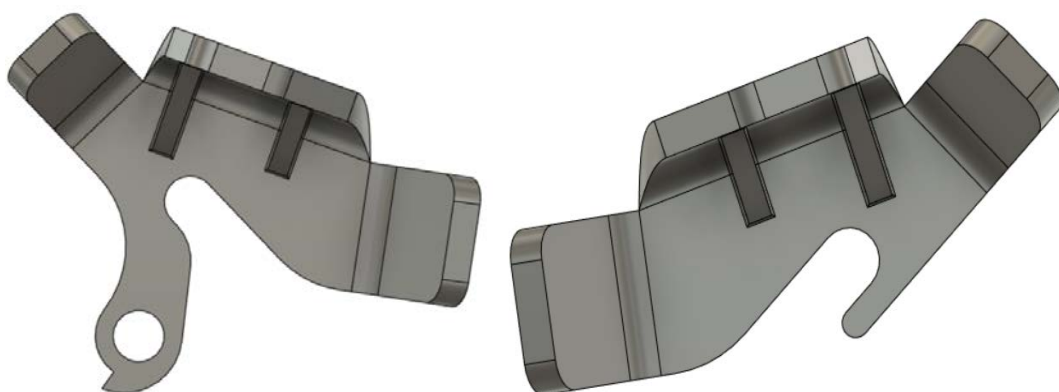


Figure 52 Rear Wheel Right & Left Dropouts

The rear wheel derailleur was designed for the Shimano Direct Link technology by reverse engineering a mountain bike available. The front derailleur was selected to use Shimano

E2 Direct Mount with a bottom bracket mount. This significantly simplified the bottom bracket mount design.

The seat was designed by reverse engineering other recumbent bike seats available in the market. This is designed to be manufactured using glass fiber due to its low density. Rubber paths under the seat are used to reduce the vibrations transmitted from the chassis to the rider. Moreover, the seat mounts were placed by using the FIA suggested mount positions for a 4-points seat belt.

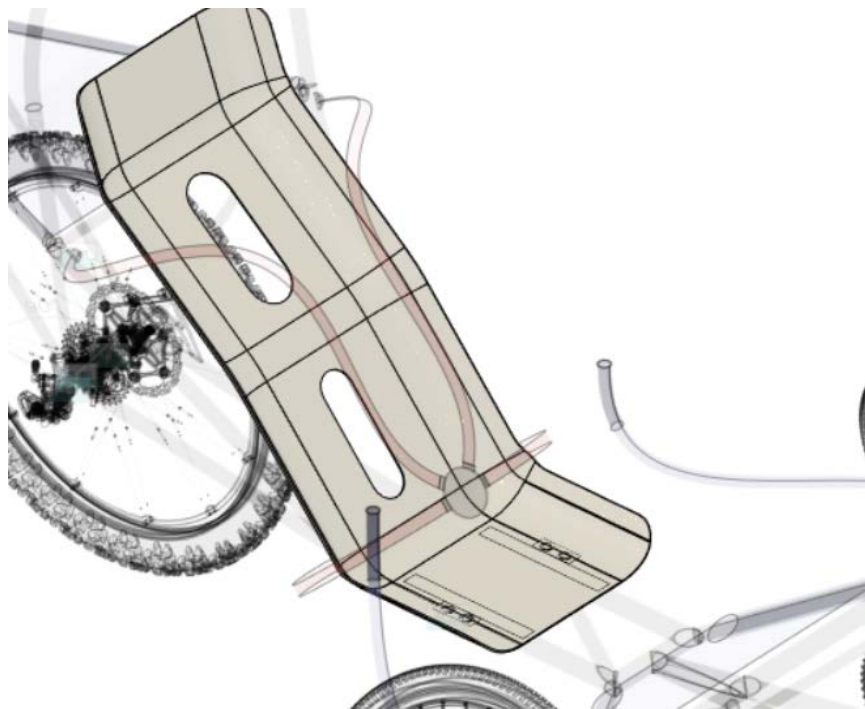


Figure 53 Seat Design in context with the full assembly.

The final detail design of the chassis is shown below. Because of the results of the final FEA simulation, 3 different tube profiles were selected for this design: 1in 2mm thickness, 0.75in 2mm thickness, and 1.25 1.5mm thickness. This were strategically placed to reduce the stress and strain of the frame. Also, this design includes all the proper mounts for the required components such as seat belt mounts, seat mounts, caliper mounts, free hub mounts and bottom bracket mount.



Figure 54 Final Chassis Design

Finite Elements Study

The Finite Element study was the most challenging task in the development of this design because of its importance to the performance of the vehicle and software limitations. Several finite elements packages were considered for this study, but ANSYS and SolidSims were used.

At the beginning, Inventor and Fusion 360 finite elements modules were tried. However, the limitations on mesh control proved this software not useful for our scenario. The problem relies on the tube notches required for the proper welding and assembly of the chassis. This induces several stress concentrations and contact points. When these features are not properly meshed, the computational error is considerable.

Then, Abaqus and Ansys were explored. The limitation with ABAQUS is the node limitations in the student version. For a complex model, to do a mesh convergence analysis of the plot is not plausible. ANSYS, however, allows up to 32000 nodes in the student version.

Nonetheless, the number of nodes is not enough for doing a full body analysis of the body. Therefore, simplifications must be made. A combination of shell and beam elements were used to achieved this.

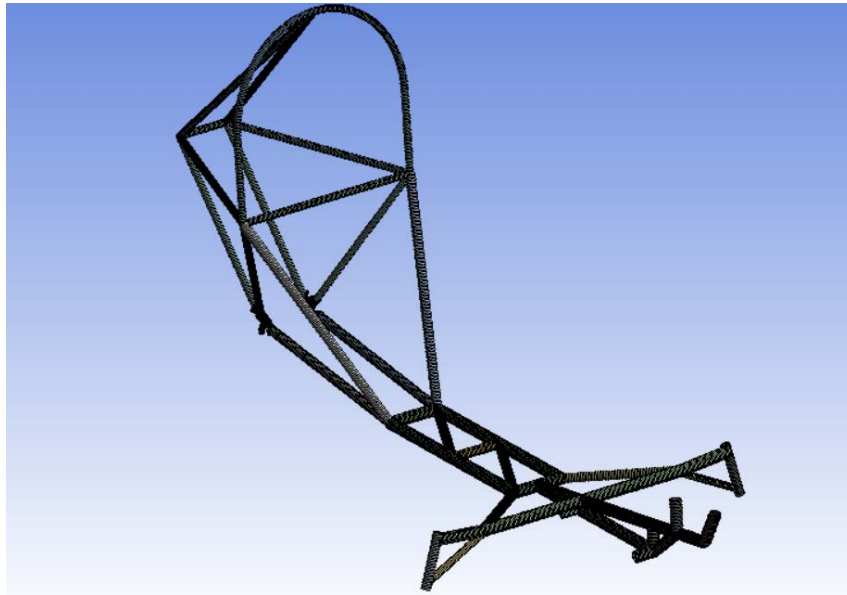
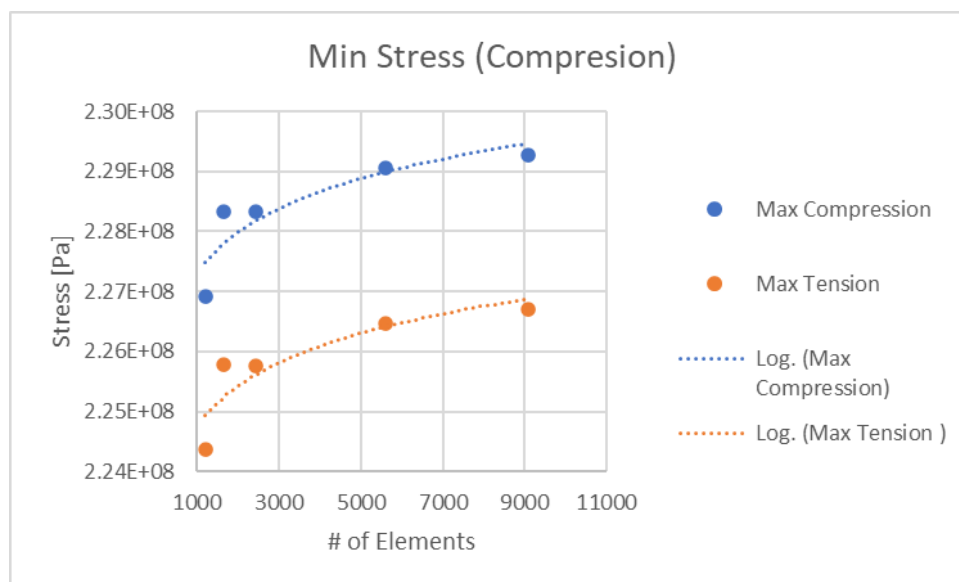


Figure 55 Final Chassis Mesh (9332 elements)



*Figure 56 Mesh Independence Identification.
Mesh independence is identified in over 9000 elements.*

Once the model was simplified, the set of 8 different load cases explain in the preliminary FEA section were run to understand the behavior of the detail chassis model. The most critical load scenario proved to be the drop test. This scenario was used to do the mesh convergence analysis. Then, the same mesh was applied to the remaining load scenarios. The following table shows the results of these set of simulations.

Table 7 ANSYS chassis FEA Analysis.

Two critical design scenarios were found in the Drop Test and Back Crash studies.

Critical Components 02				
Simulation	Component	Max Tension [Mpa]	Strain Energy [J]	Safety Factor
Drop Test	Horizontal Bar	166.6	0.023	1.0
Frontal Crash	Frontal Frame	247.88	0.018	1.2
Max Acceleration	Frontal Frame	223.85	0.036	1.3
Max Front Braking	MF	67.9	0.004	2.5
Max Turning	MF Joint w/ Horizontal	65.733	0.006	2.6
Roll Bar Vertical	Roll Bar	220.6	0.084	1.3
Roll Bar Horizontal	Cargo Space Bar	126.2	0.000	2.3
Back Crash	Main Frame	280.2	0.070	1.0

Although the simulation does not predict any security factors below 1. There were found two critical security factors just above one. This result can be consequence of the model simplification for being able to run the analysis in ANSYS. Beam elements are not a great simplification for short tubes and do not simulate properly the geometric effects of the joints. For this effect, shell elements or solid elements would have been better, but it will have caused to exceed the node numbers allowed by ANSYS student version. It is expected that the beam and shell element simplification will have computed an overestimate stress for the model. Also, the strain energy for the maximum acceleration case was significantly improved. This will give a better performance to the vehicle in power transmission.

Because of the two critical loading cases found with ANSYS, another simulation packaged was used to validate the design. SimSolid meshless method should be less

conservative, therefore it should compute a lower, more realistic, stress distribution of the model. The problem with this software is that it is still new in the market and the mathematical model that it uses to solve its simulations is not common knowledge yet.

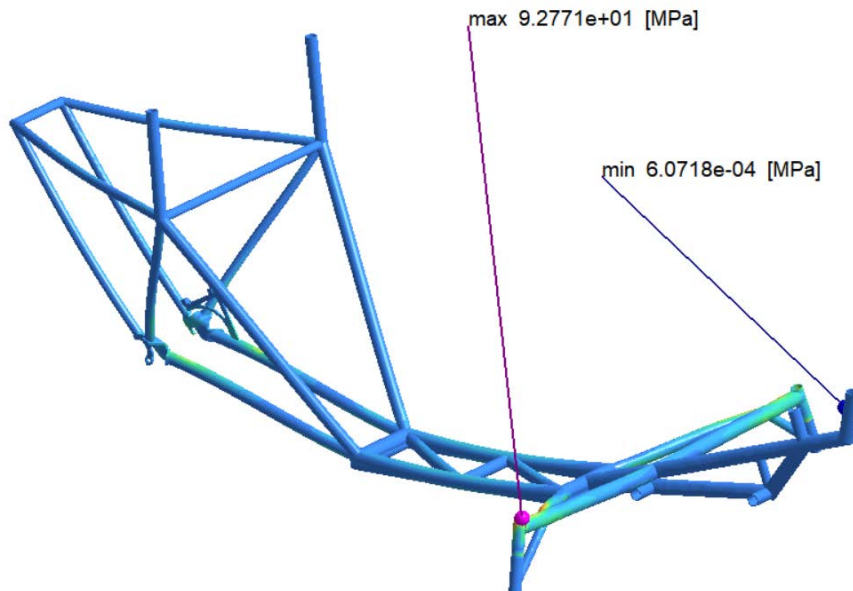


*Figure 57 SimSolid Drop Test Result.
The maximum Von Mises Stress is 92.7 [MPa]*

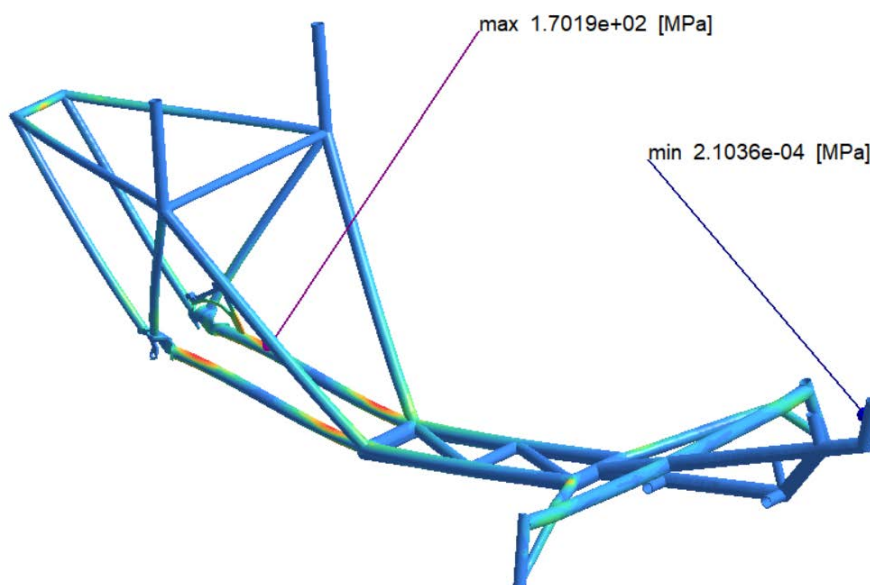


*Figure 58 SimSolid Back Crash Load Case Simulation.
Maximum Von Mises Stress is 170.2 MPa.*

The meshless method of computed a significantly lower stress than the one predicted by ANSYS. Both critical simulations were run, vertical drop and back crash, and it was found that the ANSYS error is consistent in about 40%. This yields safety factor of 1.8 and 1.7, respectively. Therefore, we are confident that the chassis design will perform as expected in real life conditions. Nonetheless, a significant amount of time in the test stage of this product development should focus in determining the actual loads the vehicle will be under.

Finally, with the beam results of ANSYS, the boundary conditions for the most critical component, the fork dropout, were found. This was used to do an independent FEA analysis of the component. The fork dropout is responsible for supporting more than 50% of the vehicle weight plus acceleration loads. The FEA analysis in ANSYS was used to find the critical loading scenario for this component which is the drop out load case. The boundary conditions computed from this scenario were imputed into the analysis of the fork dropout in SimSolid. The result of this simulations is shown below, and we are confident that the component will not fail under the expected circumstances with a fatigue safety factor for infinite life of 1.1.

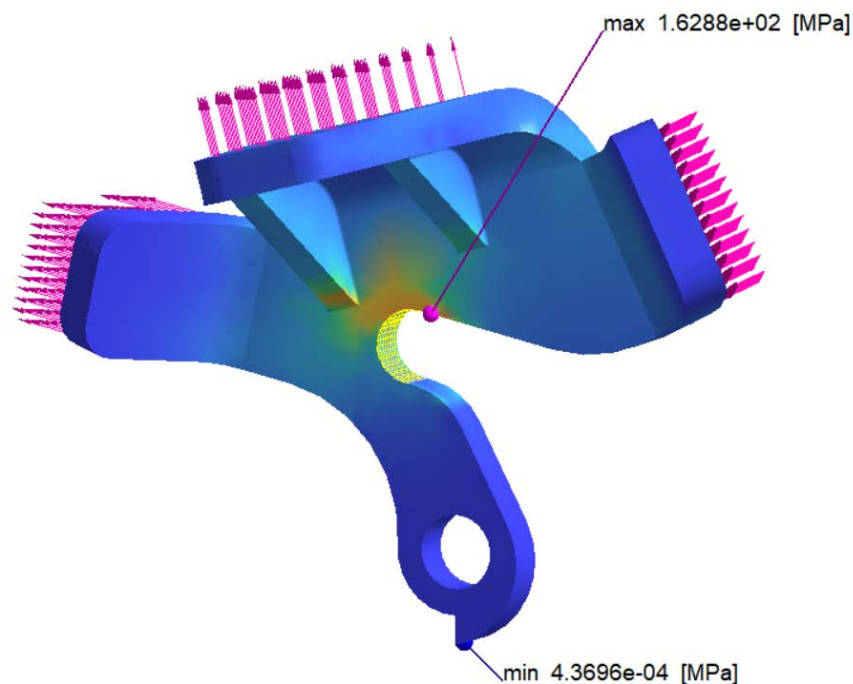


*Figure 59 Rear Wheel Dropout FEA Analysis.
Maximum Von Mises Stress is 162.9 MPa*

Finally, the brake mount support was analyzed to validate its detailed design. The simulated scenario was full braking only with the rear brake at 0.75G. The maximum Von Mises Stress was 262 MPa. This means a safety factor of 1.1 for this extreme braking condition.

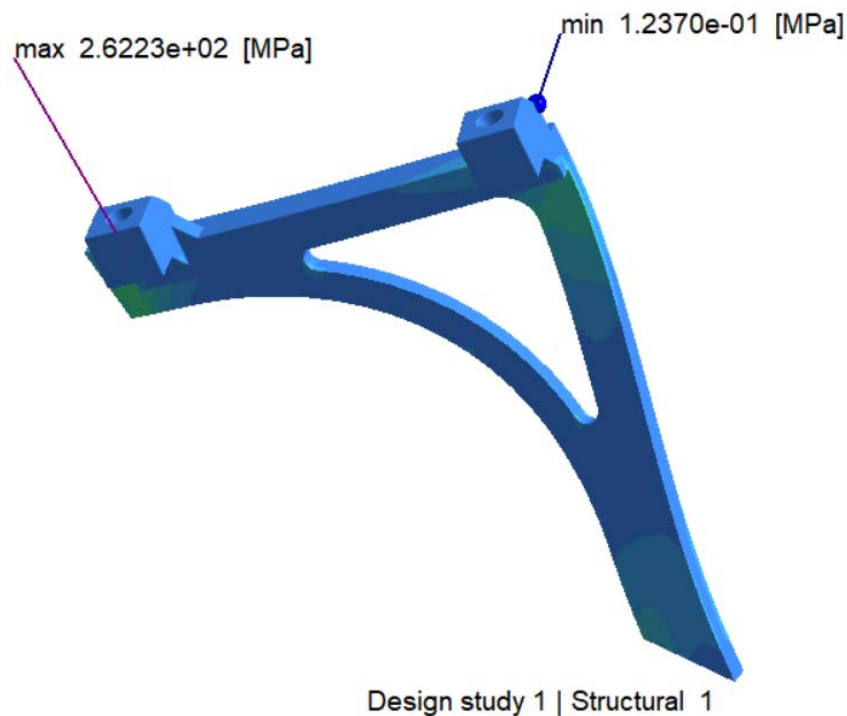


*Figure 60 Caliper Mount FEA.
Maximum Von Mises Stress is 262.23 [MPa].*

Weld Analysis

Finally, the critical joint weld analysis was performed to assure the vehicle will not fail in the weld. This analysis was performed using Shrigley's weld design method. The critical joint is the connection from the rear wheel dropouts with the chassis tubes. A simplification of the scenario is shown below.

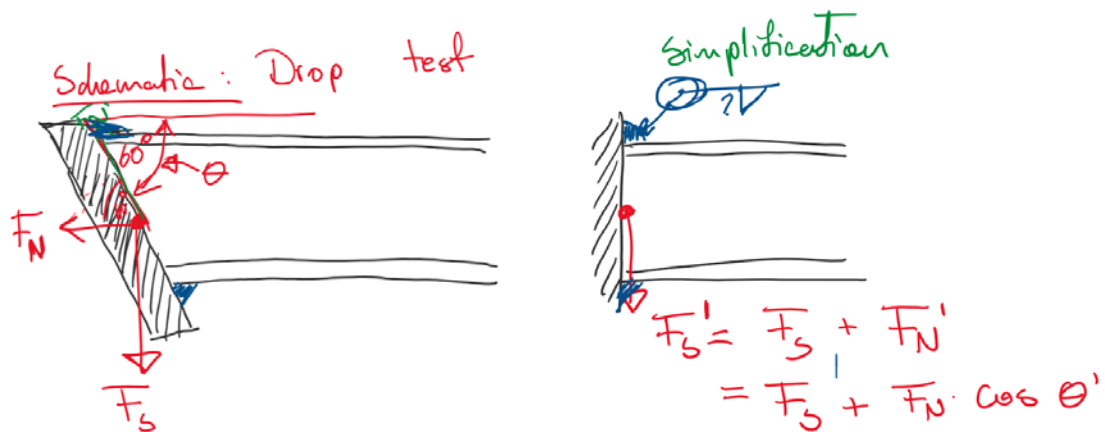


Figure 61 Critical Weld Scenario Simplification Sketch

The assumptions for this study are:

- Perfect 2mm thickness circular cross section, 1in tube
- Not significant material properties change in the manufacturing
- Electrode material AWS E60xx
- Base material ASTM A500
- No bending or torsional loads
- Uniform distribution of the stress with the contact surface
- $F_N = 2765$ [N] & $F_S = 36$ [N]
- $h = 2$ [mm]

Using the AISC norm from table 9.4 in Shrigley's, the maximum allowed stress in the weld is 116 MPa. This weld analysis was done for fatigue infinite life using the drop test criterium. Therefore, the stress in the weld is given by:

$$\tau = \frac{1.414 * K_{fs} * F_S'}{h * l}$$

Where K_{fs} is the stress concentration factors, F'_s is the effective shear load in the weld, h is the fillet weld dimension and l is the length of the weld.

$$\tau = \frac{1.414 * 1.2 * 1420}{\pi * 0.0254 * 0.002} = 15.1 \text{ MPa}$$

This gives a safety factor of 7.7. This is considered good for our design because there is no member of our manufacturing team certified in welding. Therefore, a high security factor will account for possible human error.

Direction Design

The design of the steering system was guided using chapter 10 and 11 of Design of Human-Powered Vehicles. The design methodology consists of defining the steering system to be used and the dimensions. Then, using a MATLAB code the steering dimensions were determined. This selection objective is to achieve a desired function to the steering angles of the wheels at different speeds and turning radius.

Definitions and Nomenclature

As a tadpole tricycle model was selected, several data are taken. The wheelbase L is the distance from the front axle to the rear axle. The CG, center of gravity, is located at a height h above the ground and a B distance from the rear axle. The caster angle is formed between the vertical pivot axis of the direction. The kingpin angle is the projected angle between the steering axis and a vertical plane. The camber angle is the inclination of the wheel plane from a vertical plane. Wheel track is the horizontal distance between the tire contact patches. The kinematic track is the horizontal distance between the intersection of the wheel axis and the steering axis.

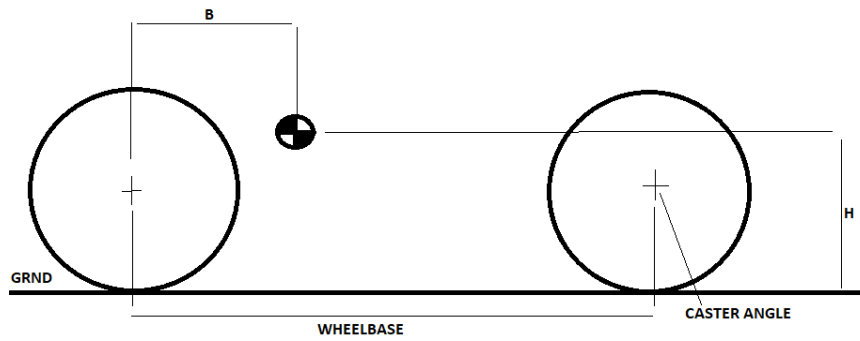


Figure 62 Side definition of the vehicle terms

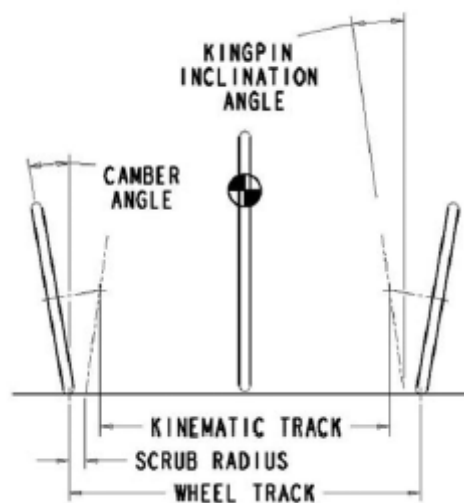


Figure 63 Front definition of the vehicle terms (Archibald, 2016)

Low Speed Cornering

At low speeds cornering, no lateral force is involved, so the wheels should roll with no slipping on the pavement, multi-track vehicles as a difference of single-track vehicles do not lean while turning.

For a Tadpole design vehicle, where two wheels are being steered, the inside and outside angles differ to prevent slip, understeer, and oversteer. The offset of the wheels determines the inside and outside angles, so the inside wheel should have a larger steer angle than the outside one. These angles are determined by

$$\delta_i = \tan^{-1} \left(\frac{L}{R - \frac{T}{2}} \right)$$

$$\delta_o = \tan^{-1} \left(\frac{L}{R + \frac{T}{2}} \right)$$

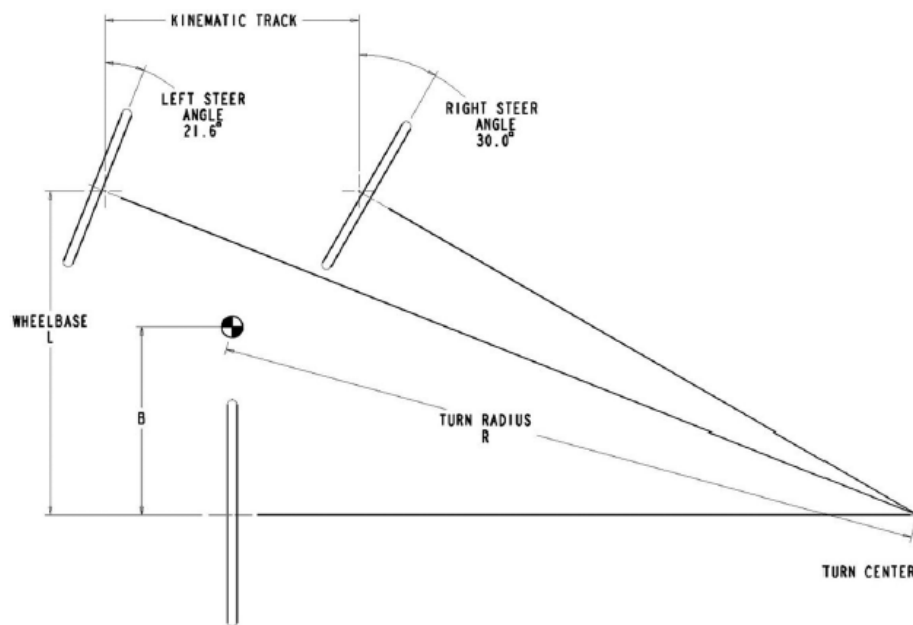


Figure 64 Ackerman Steering Angle for Tadpole Design (Archibald, 2016)

Steering Mechanism

There are a couple of steering mechanisms such as: Track rod, Six-bar linkage, and rack and pinion. All these systems are only precise for to scenario cases of, neutral steer when the wheels are straight, and one with a small turn radius. At the other scenarios, the angles are not the ideal ones. The deviation is acknowledged as steering error, this error can be minimized by using a well-designed steering system mechanism. The bigger error occurs at larger steer angle, small turning radius.



Figure 65 Track Rod Mechanism Neutral Steer (Archibald, 2016)



Figure 66 Track Rod Mechanism 30 degrees Steer (Archibald, 2016)

A track rod steering system is a mechanism with two steering arms connected to a track rod, for a first iteration a track rod system is the appropriate, because it is simple, has a good Ackerman compensation, and admits toe adjustments. In the track rod system both wheels will steer together, sharing the same Ackerman angles. A different steering linkage to control wheels turning. The track rod is commonly placed behind the axle.

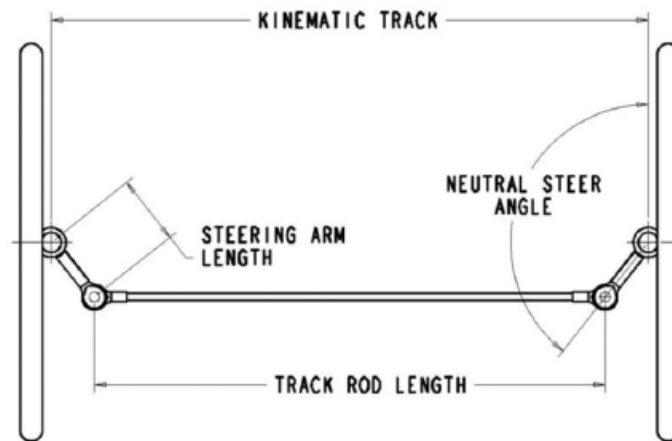


Figure 67 Track Rod Parameters (Archibald, 2016)

For determine the correct neutral steering angle, and the track rod arm, is that the neutral steering angle, the steering arm length must intersect the vehicle's center line at one third of its wheelbase, from the rear axle. This provides a mechanism with smaller errors, the neutral steer angle is determined by

$$\theta_0 = \tan^{-1} \left(\frac{4 * L}{3 * t} \right) + \frac{\pi}{2}$$

This angle is considered as a good and appropriated starting point. However, more variables need to be considered for dimension and weight changes of the rider, so it is recommended an adjustable mechanism. This will allow to tune the mechanism after a few tests. If the kinematic track and kingpin location are known parameters, then the steering arm length and neutral steer angle, are the only two parameters required.

The sensitivity of track rod depends on how the steering arms are connected. The steering bars are connected to the kingpins in the vehicle. This connection was made with the

purpose to have a better steering feeling. When the length of the steering arms is longer, the driver will have a better steering feeling.

Kinematic Analysis of Steering Mechanisms

A MATLAB code was developed to analyze the Ackerman and Track-rod mechanism. The purpose of the code is to determine the adequate inside and outside steer angle, $\delta_{i,o}$, and corresponding steering arm angle, θ_o . These were calculated for a range of turning radius, starting with the minimum turning radius of the vehicle, which is 2 m. The outside wheel arm is calculated based on the mechanism kinematics, and then evaluated for each position. The values will be compared with the correct angles corresponding to δ_i . Two figures that represent the steering accuracy will be presented.

The mean square error of steering provides an index for the whole turning radius. This is a criterion that will be used for optimization and is determined by:

$$MES = \frac{1}{n} * \sum_{i=1}^n (\theta_{o,true} - c)^2$$

The maximum deviation of the inside wheel from the one required for Ackerman steering is an index that shows the worst deviation from true steering, which is determined by:

$$MD = \max |(\theta_{o,true} - \theta_{o,actual})|$$

Where θ_o is the outside wheel steering arm angle, $\theta_{o,true}$ is the theoretical required angle, and $\theta_{o,actual}$ is the angle achieved in the real world by the mechanism.

Optimally the deviation should be located under one degree. The program will report the max deviation with the critical turning radius.

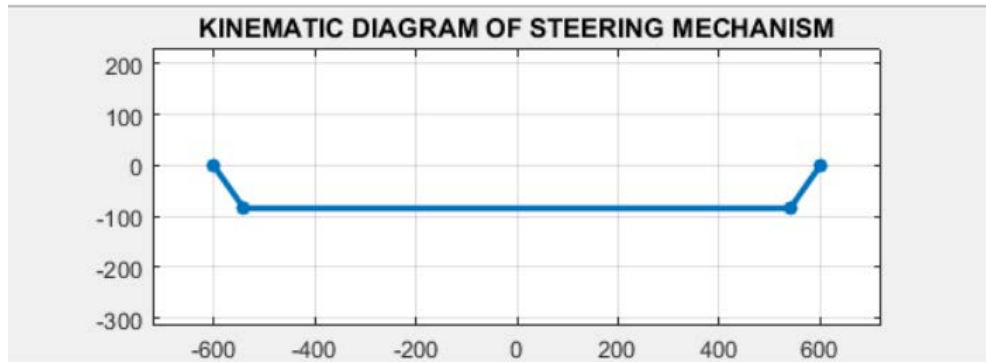


*Figure 68 Kinematic Diagram of Steering Mechanism.
1200 [mm] Track-Rod length.*

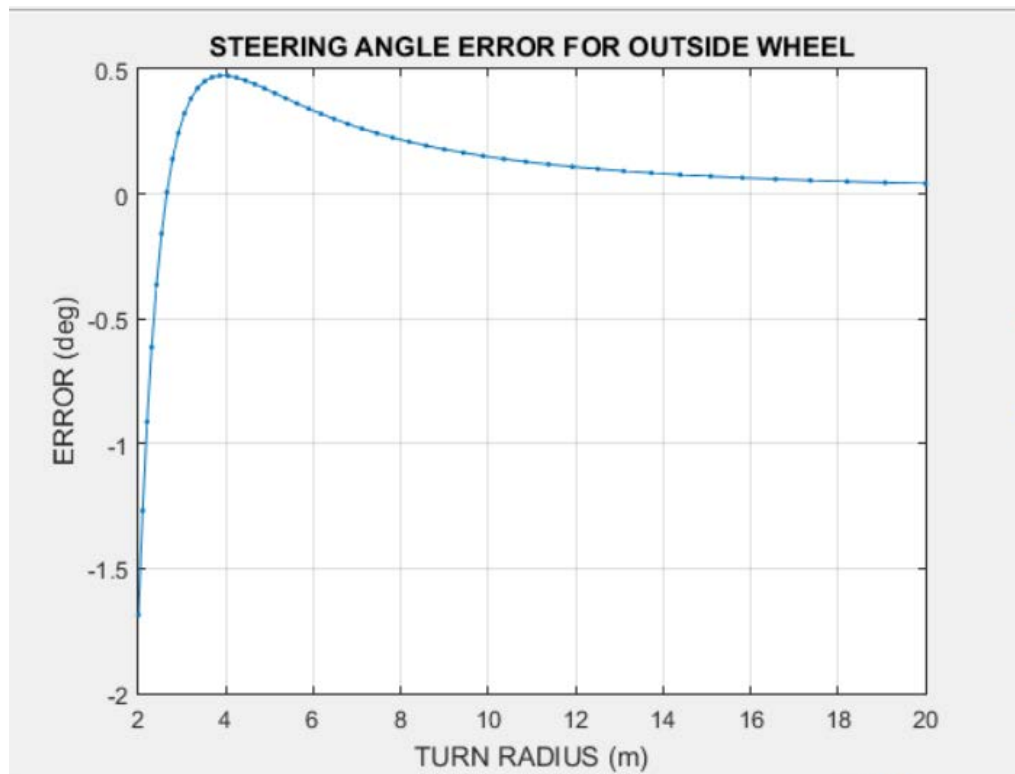


*Figure 69 Track Rod Steering Angle Error.
Maximum steering angle error: -2° at 2 [m].
Minimum steering angle error: 0.5° at 3.8 [m].*

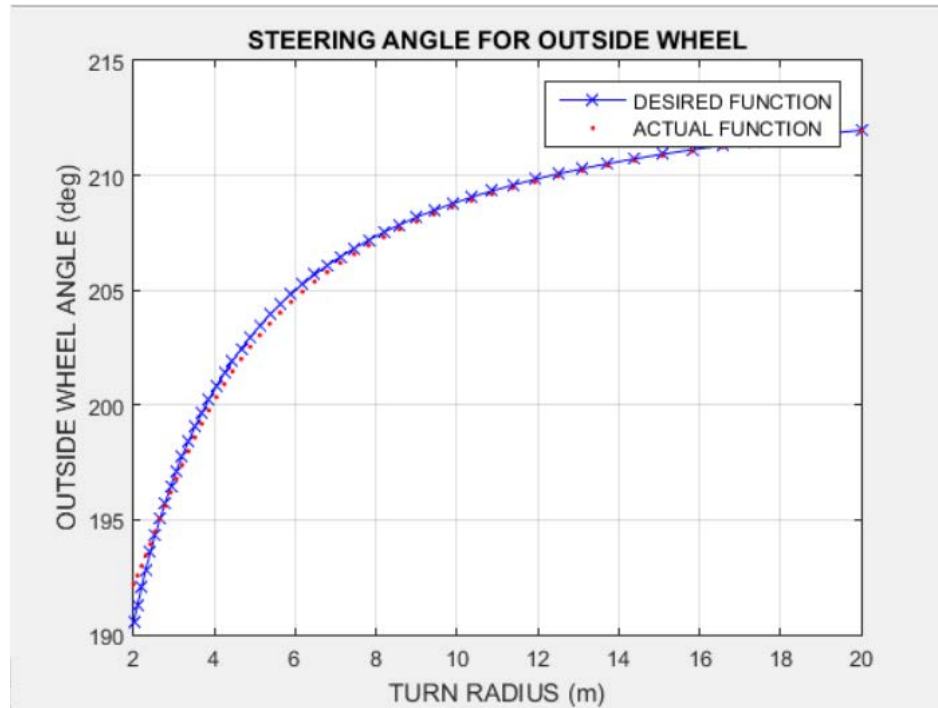


Figure 70 Track Rod Steering Angle.

The desire and actual function are similar, which means the selected system dimensions are correct.

Code Output

ACKERMAN STEERING ERROR

VEHICLE: ILALO

WHEELBASE: 1200.00 mm

TRACK: 1200.00 mm

TYPE OF STEERING MECHANISM: TRACK ROD

TRACK ARM LENGTH: 103.000 mm

STEERING ARM CENTERS: 1200.000 mm

TRACK ROD LENGTH: 1080.964 mm

NEUTRAL STEER ANGLE: 144.7 deg

MEAN SQUARE ERROR = 0.1855 deg²

MAX POS DEVIATION = 0.47 deg AT RADIUS = 3.86 m

MAX NEG DEVIATION = -1.69 deg AT RADIUS = 2.00 m

Lateral Load Transfer and Rollover Threshold

The lateral forces that acts on a vehicle in a high-speed turn produce a moment. This moment tends to shift the vehicle towards the outside of the turn. The inertial force acts through the center of gravity at a specified height from the ground. Tire forces acts at ground level, so a moment is caused. The lateral load transferred to the outside wheel is proportional to the ratio between the wheelbase and the wheel track, h/t . The lateral acceleration will be represented in G's, at a specific point the weight of the inside wheel will be zero, this will cause the vehicle to roll over, or capsizing. Rollover threshold is the point at which the inside wheel weight will be zero, and it is determined by:

$$RLT_{Tadpole} = \frac{b}{L} * \left(\frac{t}{2 * h} \right)$$

Sometimes, a vehicle rollover threshold can be different, due to road irregularities, causing an early rollover.

Longitudinal Load Transfer and Pitch Over Threshold

During braking, the rollover threshold is increased for tadpole vehicles. The opposite occurs for acceleration, but human-powered vehicles are most likely to achieve a greater braking deceleration.

Shifting vertical load from the rear/front axle to the front/rear, happens during braking and heavy acceleration. The pitch over threshold is like the rollover threshold. It is the condition in which the vertical load on one axle just becomes zero. Only pitch over due to braking is important for human-powered vehicles, where it is possible to lift the rear wheel off the ground while braking. This can be a real hazard on vehicles with high and forward centers of gravity like tadpole vehicles.

The pitch over threshold due to braking can be calculated by summing moments on the front wheel patch. The result is given by:

$$PT_{brk} = \frac{L - b}{h}$$

Understeer Gradient

The steering angle usually changes with lateral acceleration during high speed turns. Considering a steady-state high-speed turn, the tires must maintain a force that is equal to the vehicle mass times the lateral acceleration, or $m \cdot a_x$. This is accomplished with the combination of camber and slip forces.

As speed keep increasing and the vehicle is traveling a constant radius turn, the lateral acceleration increases as $a_y = \frac{V^2}{R}$. Tires should sustain a steadily increase on side loads. If the slip angle on an axle increases, the change in lateral load on each axle is unbalanced and a steering angle correction is required. The handle arm may need to be turned into or out of the turn. If the handle arm must be turned into the turn as speed increases, the vehicle is said to have understeer. If the handle arm must be turned out of the turn as speed increases, the vehicle is said to have oversteer.

While the vehicle experiences a high-speed turn, the steering angle δ is different than the Ackerman angle. This deviation depends on the lateral acceleration. The steering angle depends on the Ackerman angle and the front and rear slip angles:

$$\delta = \delta_a + \alpha_f + \alpha_r$$

Where:

$$\alpha_f = \left(\frac{W_f}{C_{af}} \right) * A_y$$

$$\alpha_r = \left(\frac{W_r}{C_{ar}} \right) * A_y$$

Knowing that the understeer gradient, K, is determined:

$$K = \left(\frac{W_f}{C_{af}} - \frac{W_r}{C_{ar}} \right)$$

If the value of K is positive, the vehicle experiences understeer, and if the value of K is negative the vehicle experiences oversteer.

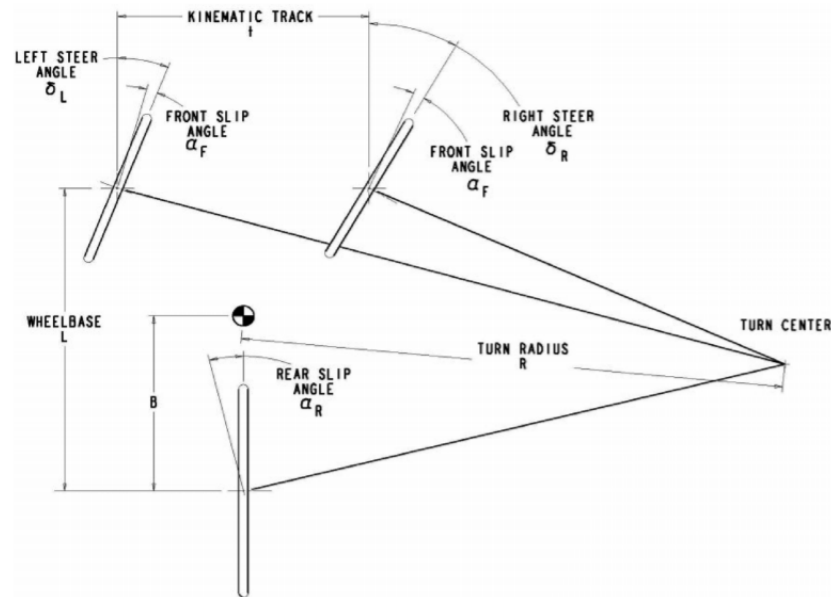


Figure 71 High Speed Cornering Parameters (Archibald, 2016)

It is important to use cornering tire properties, Mark Archibald, presents a table with the main values.

Table 8 Cornering Tire Properties (Archibald, 2016)

Cornering Tire Properties for Several Bicycle Tires

Tire	A	B
Schwalbe Durano 28-406 ¹	0.2718195	0.0000702
Ritchey Tom Slick 26 × 1.4 ¹	0.4214691	0.0002715
Tioga Comp Pool 20 × 1.75 ¹	0.4468100	0.0002787
Unspecified bicycle tire ²	.2532	.000211

¹Measured by the author

²Based on data from Cole and Khoo³

As the first model will be manufactured using unspecified tires the Properties chosen are:

$$A=0.2532$$

$$B=0.000211$$

The rear axle is not affected by lateral load transfer, and the axle stiffness is simply the stiffness of the tire. The front axle does experience lateral load transfer, and the stiffness is given. Substituting each equation in the general formula for understeer gradient, we have:

$$K_{Tadpole} = \left[\frac{W_f}{2 * (A_f * \left(\frac{W_f}{2}\right) - B_f * \left(\frac{W_f}{2}\right)^2 - B_f * (\Delta F_z)^2)} - \frac{W_r}{A_r W_r - B_r * (W_r)^2} \right]$$

A MATLAB code was developed to determine the high-speed forces and understeer gradient of the vehicle. The minimum turning radius used for these calculations is four meters because the ASME HPV challenge determined a minimum turning radius of eight meters. Thus, we worked with a half radius turning circle as a safety factor.

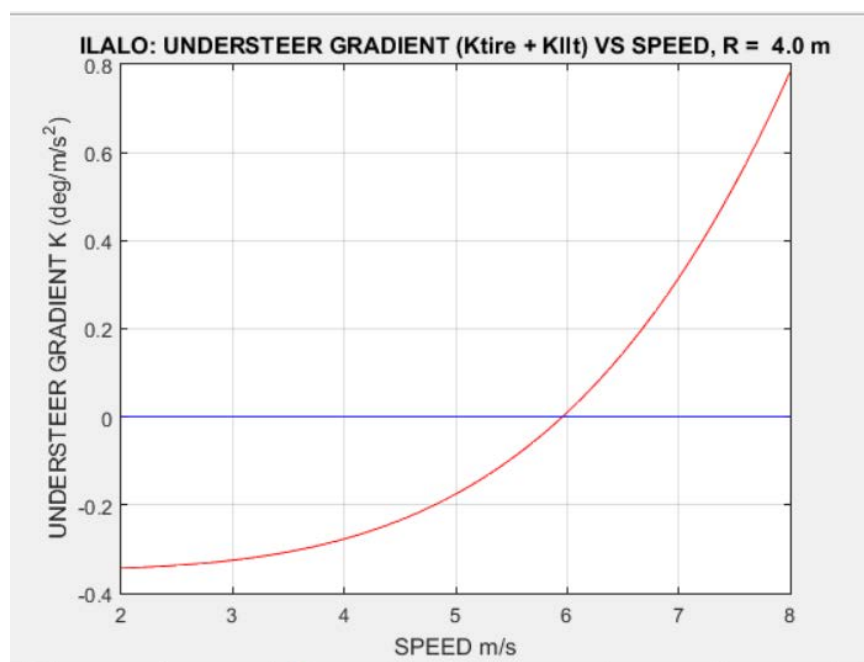
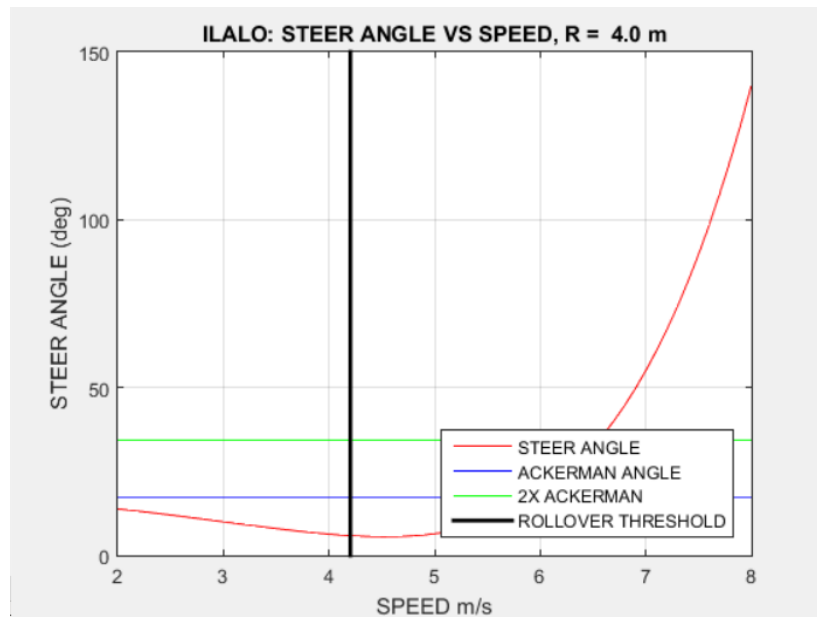


Figure 72 Understeer Gradient.

The speed limit to travel from understeer to oversteer is 6 [m/s].

In the figure, we can see that the vehicle will experience understeer above 6 m/s, and below 6 m/s will experience oversteer. 6m/s is approximately 21.6 km/h.



*Figure 73 Steer Angle vs Speed and Rollover Threshold.
The steer angle varies at different speeds.*

In the figure we can see how the rollover threshold is critical at a 4.2 m/s speed, which is 15.12 km/h, the blue and green line shows the inside and outside wheel angle, we can appreciate that are straight lines, so we can determine that the system is well designed.

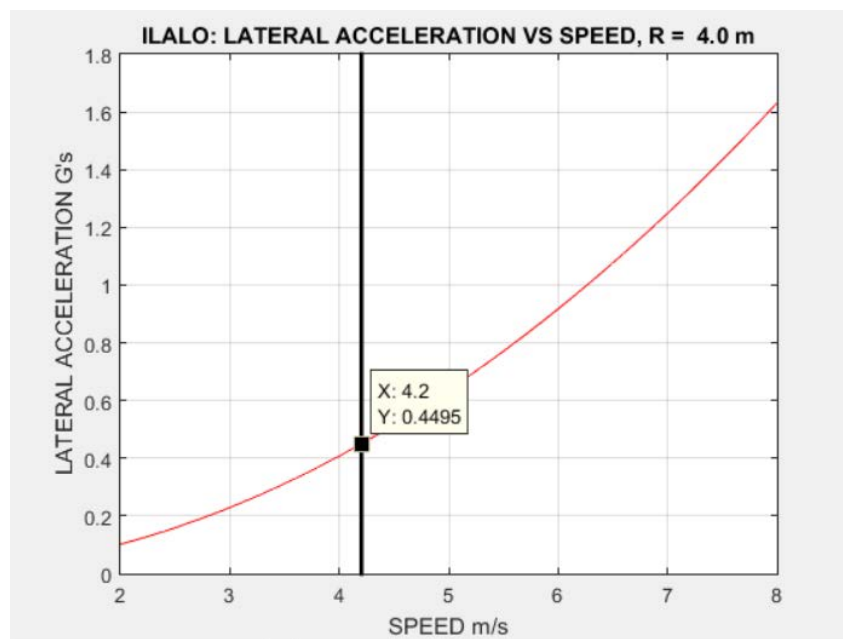


Figure 74 Lateral Acceleration vs Speed.

The critical threshold is a speed of 4.2 [m/s] and 0.4495 G of acceleration.

Code Output

TRICYCLE HANDLING EVALUATION

VEHICLE: ILALO

TYPE OF TRIKE: TADPOLE

TOTAL MASS: 100.00 kg

WHEELBASE: 1.200 m

TRACK: 1.200 m

CG HEIGHT: 0.500 m

CG LOCATION: 0.450 m

STATIC WEIGHT FRACTION, REAR: 62.5 %

ROLLOVER THRESHOLD: 0.450 G's

BRAKE PITCHOVER THRESHOLD: 1.500 G's

ACCELERATION PITCHOVER THRESHOLD: 0.900 G's

Six-bar steering

A six-bar steering system was considered as a possible new direction system, after doing all the calculations and the MATLAB codes the new system would have not be an upgrade of the old system because gains are minimal, and more weight will have been added with 6 bars instead of one used in the track-rod system.

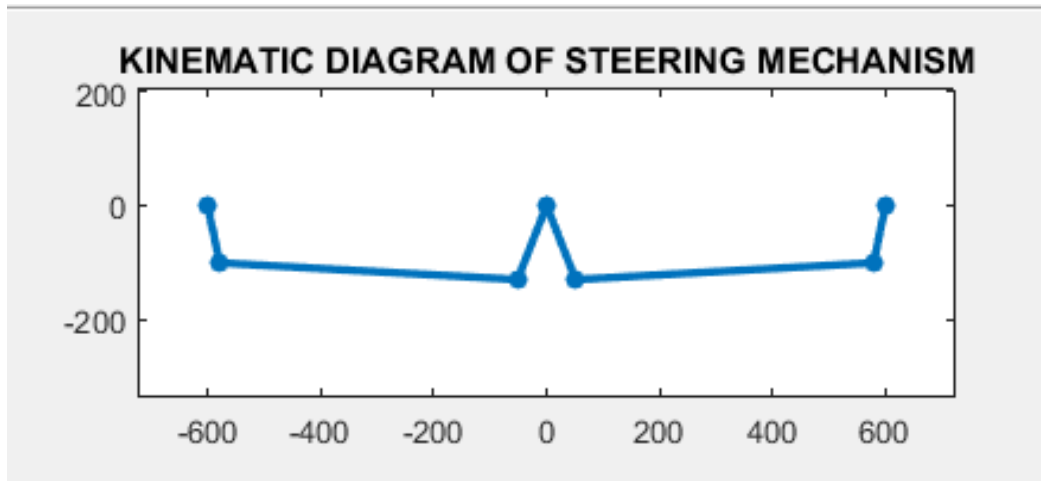


Figure 75 Kinematic Diagram of Six Bar Steering Mechanism.
Six-bar steering mechanism dimensions.

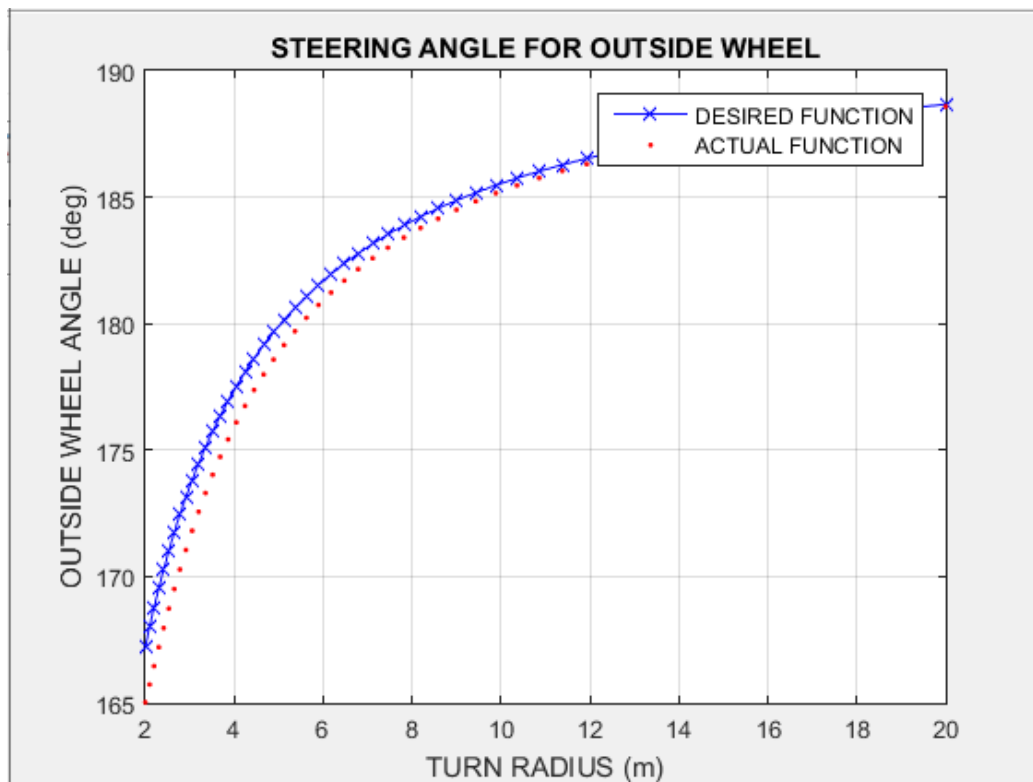
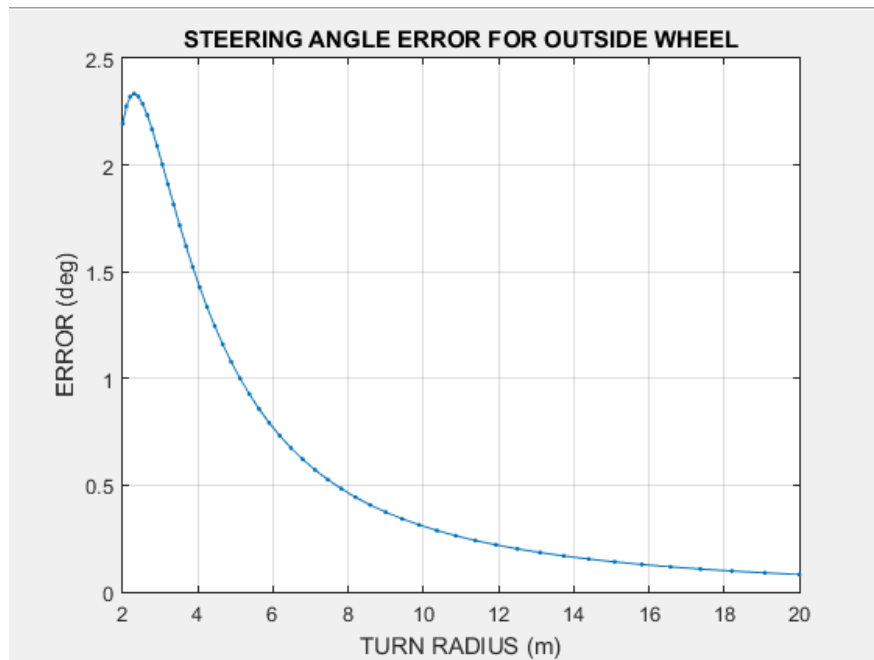


Figure 76 Six Bar steering Angle for Outside Wheel.
The six-bar and track-rod mechanism actual functions do not approximate to the desired function



*Figure 77 Six Bar Steering Angle Error for Outside Wheel.
 Maximum error: 2.3 ° at 2.2 [m].
 Minimum error: 0.12 ° at 20 [m].*

Code Output

ACKERMAN STEERING ERROR

VEHICLE: ILALO

TYPE OF STEERING MECHANISM: SIX-BAR TRAILING

FRAME LENGTH: 600.000 mm

FRAME ANGLE: 90.0 deg

TRACK ARM LENGTH: 103.000 mm

NEUTRAL STEER ANGLE: 168.0 deg

TIE ROD LENGTH: 528.000 mm

BELL CRANK LENGTH: 140.000 mm

BELL CRANK ANGLE: 201.5 deg

MAX INSIDE WHEEL ANGLE: 40.6 deg

MAX OUTSIDE WHEEL ANGLE: 27.0 deg

MAX ACKERMAN ANGLE: 31.0 deg

MAX STEERING INPUT: 23.2 deg

MEAN SQUARE ERROR = 1.5770 deg²

MAX DEVIATION = 2.33 deg AT RADIUS = 2.30 m

Automatic Control

Parking Brake

The implemented automatic control unit consists of a parking brake system. Its main purpose is to prevent the vehicle from moving after parking, especially when it is on sloped surfaces. The system could also aid in theft prevention since it allows driving capabilities to the owner alone. The blocking and unblocking capability of the brake is accessed by the owner of the vehicle through Bluetooth communications with their smartphone. The following section explains the setup, programming and use of the system.

Components

- Arduino Nano
- Bluetooth module HC-05
- 9V Battery
- Servo Motor M MG995
- Extended Door Side Lock

Schematic

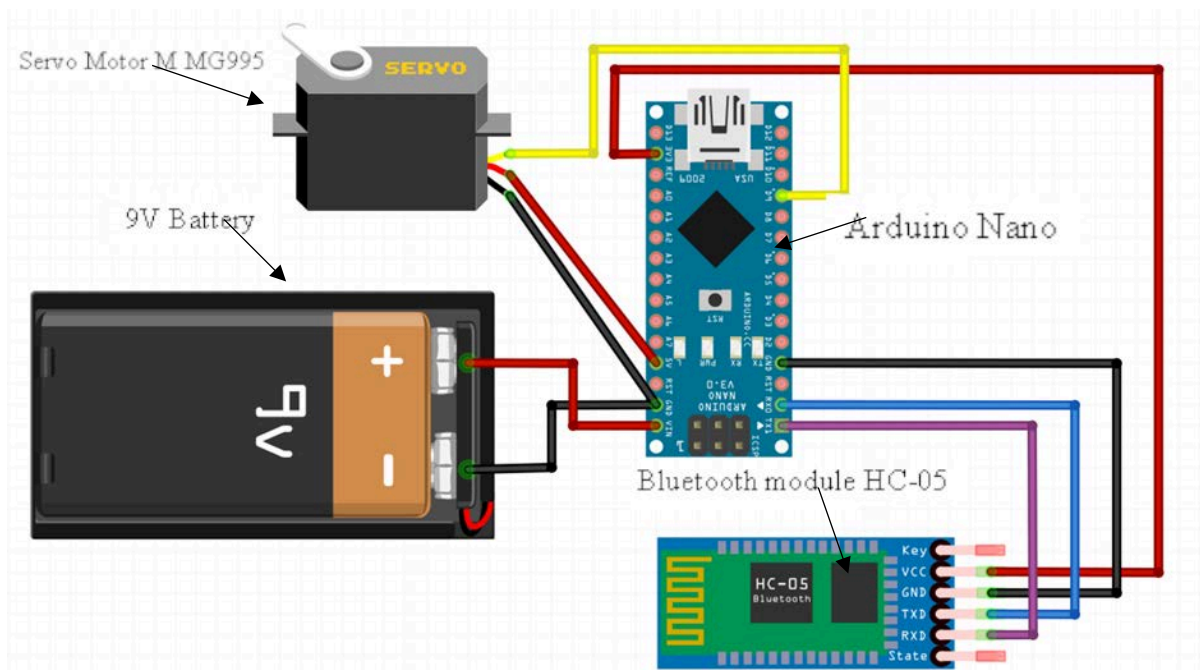


Figure 78 Automatic Control Schematic

As shown on the schematic on the figure 77, the setup is relatively simple. The 9V battery powers the Arduino Nano (chosen for its versatility when joining the system to the vehicle chassis) which drives the servomotor. The HC-05 Bluetooth module acts as an on/off switch for the system since there is no interest in managing varying degrees of rotation in the motor. The extended door side lock is in turn attached to the servomotor, which will alternate between 0 and 60 degrees to slide the lock in and out of position. The system locks the rear wheel by using the door side lock as an obstacle between its spikes. To ensure the durability and reliance of the system, the M MG995 servo motor was chosen since it has a powerful torque and premium components, such as metal gears.

Simulation

To test the system, the schematic was analyzed using the electronic circuit analyzer from the software *Fritzing*, which allows current and voltage simulations that verify the validity and resistance of the circuit. This proved that the used schematic manages the correct amount of power for its components, without short circuits or burnt components.

The used code was proved to be able to compile in the *Arduino* loading software, but, due to the physical testing limitations set by the Covid-19 pandemic, simulations had to be used to prove the validity of the system. The online platform *Autodesk TinkerCad* was used to emulate the use of the schematic with the code. Sadly, the platform does not support Bluetooth module testing, so a slide on/off switch was used to replace the Bluetooth operations for the simulation (the code had to be slightly modified for this effect). Figure 76 shows how the simulation was run successfully, with a 60 degrees motor position representing the open lock (on in the switch), and 0 degrees motor position representing the closed lock (off in the switch).

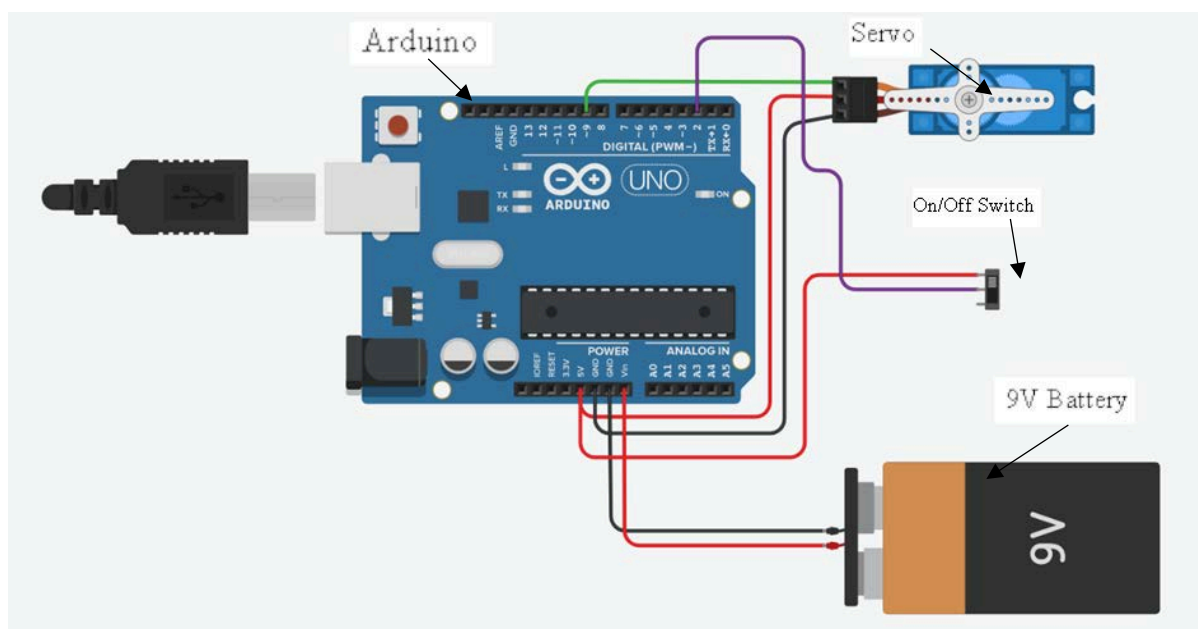


Figure 79 Switch Simulation

App Interaction

The *Romoremo* app (free in the Apple and Android app stores) was used as a remote control for the parking brake. The app is easy to set up through Bluetooth and includes the option to program buttons to use. In the case of this product, a simple two-button layout is used to lock and unlock. Pressing the *lock* button will send the *0* signal to the Bluetooth receiver, moving the motor to 0 degrees. Similarly, pressing the *unlock* button will send the *1* signal to the Bluetooth receiver, moving the motor to 60 degrees.

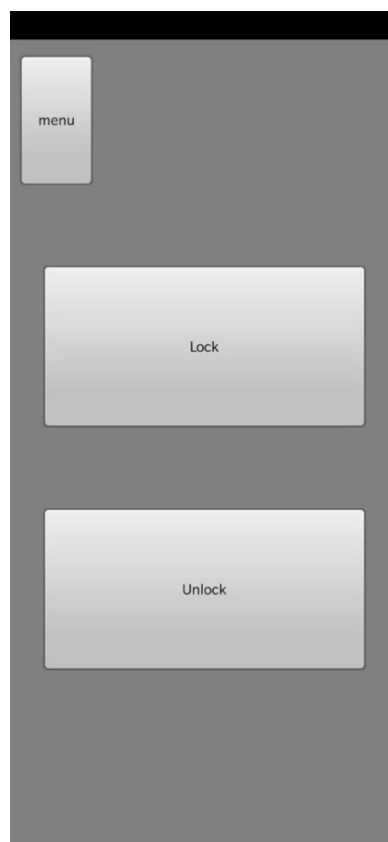


Figure 80 App Interface

Matlab Codes

Loading Scenarios

```

%% Weight Fraction Computation - pg 108. Overview Design of HPV Archibald
% By: Francisco Plaza
% 02/15/2020
clear all
close all
clc

% NOMENCLATURE
% CM - Center of Mass
% W - Weight
% R - Rear
% F - Front
% f - Weight Fraction
% G - grade

% Metodology:
% So far the values are assing randomly. There is no design objtive yet
% defined.

%% ##### Parameters #####
%***GEOMETRY***
m = 25 + 75; %kg Mass of the vehicle including the rider
L = 1.2; %m Wheel base / DEFINED by Design Parameters
b = 0.45; %m horizontal distance from Rear axis to CM
h = 0.50; %m vertical distance from the ground to the CM
h_b = h/b;

%***CONDITIONS***
g = 9.8; %ms-2 gravity
G = -0.15:0.01:0.15; %Slope grade
C_RR = 0.005; % Rollin Resistance Coefficient

%***DRIVE SYSTEM***
P = 200; %[W] Estimated human power input
w = 0; %[rad/s] Angular velocity
V_cruise = 8.333; %[m/s] Cruise target speed of the vehicle - 30
km/hr... kratos has 12.5 or 45 km/hr
d_DW = 0.6604; % [m] Diameter of the drive wheel
r_turning = 3; %[m] Minimum turning diameter from Krator design book

%***AERODYNAMICS
A_aero = 1.08; %[m2] Frontar area 1.2m*0.9m
rho = 1.2; %[kg/m3]
C_D = 0.5; %Drag Coefficient from Kratos design

%***TURN RADIUS
V_turn = 1:8; %[m/s] Turning velocity of the vehicle
r = 3; %[m] minimum requiere turn radius

%***BRAKING
V_brake = 7; %[m/s] Before breaking velocity
d_brake = 6; %[m] Maximum braking distance

%***POWER INPUT
P_input = 200; %[W] Human power input
eta_PT = 0.9; %Power train efficiency

```

```

eta_friction = 0.75; %Estatic friction coefficient for asphalt

%% ##### Computations #####
W = m*g; %N Full vehicle weight
theta = atan(G);

%% *****LEVEL GROUND STATIC LOAD*****
% Wheel Weight Computation
W_F = W*b/L; %Computation of Front wheel weight
W_R = W - W_F; %Computation of Real wheel weight
% Weight Fraction
f_R = W_R/W*100;
f_F = W_F/W*100;

%% *****GRADE STATIC LOAD*****
% Wheel Weight Computation
W_F_G = (W*(b*cos(theta)-h*sin(theta)))/L; %Computation of Front wheel
weight
W_R_G = (W*((L-b)*cos(theta)+h*sin(theta)))/L; %Computation of Real wheel
weight
% Weight Fraction
f_R_G = W_R_G/W*100;
f_F_G = W_F_G/W*100;

% Create table
[f_R f_F;...
W_F_G' W_R_G'];

% Create Plots
figure(1)
hold on
plot(G,W_R_G,'r')
plot(G,W_F_G,'k')
title('Estudio de Cargas Estatica para diferentes pendientes. It #01')
xlabel(sprintf('Slope Grade. For h/b = %.2f',h_b))
ylabel('Force [N]')
legend('Rear Wheel','Front Wheel')
hold off

%% *** STEADY MOTION LOADS ***
% For steady state motion at cruise
F_aero = rho/2*C_D*A_aero*V_cruise^2; %[Aerodynamic drag]
F_RR = W*C_RR; %[N] Rolling Resistance

F_x_ss = F_RR + F_aero + W*sin(theta); % [N] Drive force requiere for SS
grade motion

%Transformation to power
w_DW_ss = V_cruise*2/d_DW; %[rad/s] angular velocity of drive wheel at
cruise speed
T_DW_ss = d_DW/2*F_x_ss; %[Nm] Drive wheel steady state motion required
P_DW_ss = T_DW_ss*w_DW_ss; %[W] Drive wheel steady state power required

[(G*100)' F_x_ss' P_DW_ss']; %Steady motion loads data values

figure(2)
plot(G*100, P_DW_ss,'b')
title('Estudio de fuerza de traccion necesaria para S.S motion en
pendientes. It #01')
xlabel(sprintf('Slope Grade. For h/b = %.2f',h_b))
ylabel('Power [W]')

```

```

%% *** CURVATURE ***
for i = 1:length(V_turn)
    %Computations
    a_y = V_turn(i)^2/r;    %Centripetal Acceleration
    F_y = m*a_y;           %Centripetal Force
    F_yF = W_F_G*a_y/g;    %Turning Force Front Wheel
    F_yR = W_R_G*a_y/g;    %Turning Force Real Wheel

    %Start Plotting
    figure(4); %Front Wheel Turning Force for different turning velocities
    hold on
    plot(G, F_yF); %Front Wheel Plots
    hold off
    title('Turning Force at the Front Wheel for different turning
velocities. It #01');
    xlabel(sprintf('Slope Grade. For h/b = %.2f',h_b));
    ylabel('Turning Force [N]');

    figure(5); %Rear Wheel Turning Force for different Turning Velocities
    hold on
    plot(G, F_yR); %Real Wheel Plots
    hold off
    title('Turning Force at the Rear Wheel for different turning
velocities. It #01');
    xlabel(sprintf('Slope Grade. For h/b = %.2f',h_b));
    ylabel('Turning Force [N]');
end

%Centripetal Force Calculation
a_y = V_turn.^2/r;    %Centripetal Acceleration
F_y = m*a_y;         %Centripetal Force

figure(6); %Centripetal Force plot
    hold on
    plot(V_turn, F_y); %Real Wheel Plots
    hold off
    title('Centripetal Force for Different Turning Velocities. It #01');
    xlabel('Turning Velocity [m/s]');
    ylabel('Centripetal Force [N]');

figure(4); %Turning Force Front Wheel
legend(sprintf('V_(turn) = %.0f m/s',V_turn(1)),sprintf('V_(turn) = %.0f
m/s',V_turn(2)),...
    sprintf('V_(turn) = %.0f m/s',V_turn(3)),sprintf('V_(turn) = %.0f
m/s',V_turn(4)),...
    sprintf('V_(turn) = %.0f m/s',V_turn(5)),sprintf('V_(turn) = %.0f
m/s',V_turn(6)),...
    sprintf('V_(turn) = %.0f m/s',V_turn(7)),sprintf('V_(turn) = %.0f
m/s',V_turn(8)));

figure(5); %Turning Force Rear Wheel
legend(sprintf('V_(turn) = %.0f m/s',V_turn(1)),sprintf('V_(turn) = %.0f
m/s',V_turn(2)),...
    sprintf('V_(turn) = %.0f m/s',V_turn(3)),sprintf('V_(turn) = %.0f
m/s',V_turn(4)),...
    sprintf('V_(turn) = %.0f m/s',V_turn(5)),sprintf('V_(turn) = %.0f
m/s',V_turn(6)),...
    sprintf('V_(turn) = %.0f m/s',V_turn(7)),sprintf('V_(turn) = %.0f
m/s',V_turn(8)));

```

```

% figure(6); %Centripetal Force
% legend(sprintf('V_(turn) = %.0f m/s',V_turn(1)),sprintf('V_(turn) = %.0f
m/s',V_turn(2)),...
%     sprintf('V_(turn) = %.0f m/s',V_turn(3)),sprintf('V_(turn) = %.0f
m/s',V_turn(4)),...
%     sprintf('V_(turn) = %.0f m/s',V_turn(5)),sprintf('V_(turn) = %.0f
m/s',V_turn(6)),...
%     sprintf('V_(turn) = %.0f m/s',V_turn(7)),sprintf('V_(turn) = %.0f
m/s',V_turn(8)));

%% *** Braking ***
a_brake = -V_brake^2/(2*d_brake); %[m/s^2] Computation
for aceleration necessary to satisfy braking design parameter
F_brake = -F_aero-F_RR-W*sin(theta)-m*a_brake; %[N] Necessary force to
brake within the design parameter for diferente slopes
figure(3)
plot(G,F_brake)
title('Estudio de la fuerza de frenado necesaria para diferentes
pendientes. It #01')
xlabel(sprintf('Slope Grade. For h/b = %.2f',h_b))
ylabel('Braking Force [N]')
legend(sprintf('Braking Force @ level = %.0f [N]',F_brake(11)))

A_brake_max1 = -(L-b)/h %Pitchover limit
A_brake_max2 = - eta_friction

%% ***Acceleration***
P_prime = P_imput*eta_PT; %Actual power transmitted to the wheels.
Fx_max_traction = eta_friction*W; %[N] Max force possible to apply to the
vehicle wheel
V_PW = 0:0.2:9; %[m/s] ranges of velocity of the vehicle
Fx_max_power = P_prime./V_PW; %[N] Max force that can be imput to the
vehicle according to power available.
A = ones(1,length(V_PW))*Fx_max_traction;

%Plot of Force vs Vehicle Speed
figure(7)
plot(V_PW,A,'b');
hold on
plot(V_PW,Fx_max_power,'b');
hold off
title('Estudio de la fuerza de aceleracion maxima para plano. It #01')
xlabel('Vehicle Velocity [m/s]')
ylabel('Acceleration Force [N]')

%Computo de acceleration for level ground
ax_traction = 1/m *(Fx_max_traction - F_RR); %[m/s^2] max acceleration due
to traction
F_aero = rho./2.*C_D.*A_aero.*V_PW.^2; %[Aerodynamic drag] for different
velocities
ax_power = 1/m *(Fx_max_power - F_aero - F_RR); %[m/s^2] max acceleration
due to power imput
%Plot of acceleartion
A = ones(1,length(V_PW))*ax_traction;
figure(8)
plot(V_PW,A,'r');
hold on
plot(V_PW,ax_power,'r');
hold off
title('Estudio de la aceleracion maxima para plano. It #01')
xlabel('Vehicle Velocity [m/s]')

```

```
ylabel('Acceleration [m/s^2]')
```

Failure Criteria

```
% Code For computing the Failure Criteria of the Chassis Design
% Wrote By: Francisco X. Plaza
% Date: 03/05/2020

%% Input
% Material Selected: ASTM A500 Structural Steel
Sut = 350; %[MPa] Ultimate Strength
Sy = 290; %[MPa] Yield Strenth
    %For Ka Cold Drawn
    a = 4.51;
    b = -0.265;
    %For kb
    d = 0.0190; %[m]
% FEA Simulation Inputs Static
Sigma_VM = 63.5; %[Mpa] Von Mises Strength Computed by FEA Simulation

% FEA Fatigue Analysis

%% Static Analysis
eta_static = Sy/Sigma_VM;

%% Fatigue Analysis
ka = a*Sut^b;
kb = 0.879*d^-0.107;
kc = 1;
kd = 1;
ke = 0.814; % 99% of confidence
kf = 1;

% Endurance Limit
Se = 0.5*ka*kb*kc*kd*ke*kf*Sut;

%% Data Presentation
sprintf('Yield Strength is: %0.f MPa \nSafety Factor in Static Analysis is:
%.2f \nThe Endurance Limit is: %.2f MPa',...
        Sy, eta_static, Se)
```

Akerman Track Rod (Archibald, 2016)

```

clear;
close all;
clc;

% INPUT SECTION
vehicle = 'ILALO';

% Vehicle Parameters
r1 = 1.20;          % KINEMATIC TRACK
L = 1.20;          % WHEELBASE
Rmin = 2;          % MINIMUM TURN RADIUS

%Mechanism parameters
r2 = 0.103;        % STEERING ARM LENGTH
theta_o = (atand((4*L)/(3*r1))+(pi/2)+90)*pi/180; %144.7*pi/180; %
NEUTRAL STEER ANGLE

% Select Units
unit = 'm';        % Units, enter 'i' for inches or 'm' for meters

% Output switch
output = 'y';      % Set to 'N' to suppress graphical/text output
% END INPUT SECTION

% Type of mechanism
mech_type = 'TRACK ROD';

% Compute track rod length from given data
r3 = r1-2*r2*sin(theta_o);          % TRACK ROD LENGTH
t = r1;

% Compute minimum theta and R based on mechanism limit position
theta_min = acos((r2^2-r1^2-(r2+r3)^2)/(2*r1*(r2+r3))) + pi/2;
Rminmech = L/tan(theta_o-theta_min) + t/2;
if Rmin < Rminmech,
    fprintf(1,'MINIMIM TURN RADIUS NOT OBTAINABLE ON INSIDE WHEEL \n\n');
end;

```

```

% Establish turn radius vector R
Rmax = 20;
n = 50;
I = (Rmax/Rmin)^(1/(n-1)) - 1;
R = Rmin*(I+1).^(0:n-1)';

% Compute steer angles
if theta_o > 0,
    psi_o = 2*pi - theta_o;
else
    psi_o = -theta_o;
end;
theta = theta_o - atan2(L,(R-t/2)); % INSIDE WHEEL ANGLE
psi_p = psi_o - atan2(L,(R+t/2)); % THEORETICAL OUTSIDE WHEEL ANGLE

% Solve Chase equation
C = r2*exp(i*theta) - r1*exp(i*pi/2);
Ca = abs(C);
Cu = C./Ca;
Cuxk = (imag(Cu) - i*real(Cu));
T = (r2^2-r3^2+Ca.^2)./(2*Ca);
A1=sqrt(r2^2-T.^2).*Cuxk + T.*Cu;
A2=-sqrt(r2^2-T.^2).*Cuxk + T.*Cu;
if sign(imag(A1(1))*imag(A1(n))) > 0,
    psiA1 = angle(A1)+2*pi;
else
    psiA1 = unwrap(angle(A1));
end;
psiA2 = angle(A2);
if theta_o > 0,
    psi = psiA1;;
else
    psi = psiA2;
end;

% Compute Error
err = 180*(psi_p - psi)/pi;
MSE = mean(err.^2);
[max_dev, max_dev_idx] = max(err);
[min_dev, min_dev_idx] = min(err);

```

```

% Output Results
if (output == 'y') | (output == 'Y'),
    close ALL;
    clc;

    if lower(unit) == 'm',
        runit = 'm';
        munit = 'mm';
        r1 = r1*1000;    % convert kinematic dimensions to mm
        r2 = r2*1000;
        r3 = r3*1000;
        L = L*1000;
        t = t*1000;
        Rf = R;
    else
        runit = 'ft';
        munit = 'in';
        Rf = R/12;        % Radius in feet
    end

    % Plot results

    plot(Rf,psi_p*180/pi,'bx-',Rf,(psi)*180/pi,'r. '); %STEER ANGLES
    fig1 = gcf;
    set(fig1,'Position',[990 690 560 420]);
    set(fig1,'Position',[50 690 560 420])
    title('STEERING ANGLE FOR OUTSIDE WHEEL');
    str = sprintf('TURN RADIUS (%s)',runit);
    xlabel(str);
    ylabel('OUTSIDE WHEEL ANGLE (deg)');
    grid;
    legend('DESIRED FUNCTION', 'ACTUAL FUNCTION',0);

    fig2 = figure;        % ACKERMAN ERROR PLOT
    plot(Rf,err,'.-');
    set(fig2,'Position',[990 150 560 420])
        set(fig1,'Position',[50 50 560 420])
    title('STEERING ANGLE ERROR FOR OUTSIDE WHEEL');
    xlabel(str);
    ylabel('ERROR (deg)');
    grid;

```

```

fig3 = figure;          % GRAPHIC OF MECHANISM
QX = [-r1/2 -r1/2+r2*sin(theta_o) r1/2-r2*sin(theta_o) r1/2];
QY = [0 r2*cos(theta_o) r2*cos(theta_o) 0];
v = [-.6*r1 .6*r1 -1.5*r2 r2];
H = plot(QX,QY,'- .');
set(fig3,'Position',[15 375 560 200]);
set(H,'linewidth',2.5);
set(H,'markersize',21);
axis(v);
axis equal;
title('KINEMATIC DIAGRAM OF STEERING MECHANISM');
grid;
% Print Summary
fprintf(1,'\n\n ACKERMAN STEERING ERROR \n\n');
fprintf(1,'VEHICLE:   %s \n\n',vehicle);
fprintf(1,'WHEELBASE:   %5.2f %s \n',L,munit);
fprintf(1,'TRACK:         %5.2f %s \n\n',t,munit);
fprintf(1,'TYPE OF STEERING MECHANISM:   %s \n\n',mech_type);
fprintf(1,'TRACK ARM LENGTH:           %6.3f %s \n',r2,munit);
fprintf(1,'STEERING ARM CENTERS:        %6.3f %s \n',r1,munit);
fprintf(1,'TRACK ROD LENGTH:           %6.3f %s \n',r3,munit);
fprintf(1,'NEUTRAL STEER ANGLE:        %5.1f deg \n\n',theta_o*180/pi);
fprintf(1,'MEAN SQUARE ERROR = %7.4f deg^2 \n\n',MSE);
fprintf(1,'MAX POS DEVIATION = %4.2f deg AT RADIUS = %5.2f %s \n',...
        max_dev,Rf(max_dev_idx),runit);
fprintf(1,'MAX NEG DEVIATION = %4.2f deg AT RADIUS = %5.2f %s \n\n',...
        min_dev,Rf(min_dev_idx),runit);
end;

```

Six-bar trail (Archibald, 2016)

```

% 6B_trail.m Data file for 6-Bar trailing rod mechanism

mech_type = 'SIX-BAR TRAILING';
vehicle = 'ILALO';

% Vehicle parameters
L = 1.2;      % WHEELBASE
t = 1.2;      % KINEMATIC TRACK

```

```

Rmin = 2; % MINIMUM TURN RADIUS, in

% Mechanism parameters
r1 = 0.6; % BELL-CRANK PIVOT TO STEERING AXIS DISTANCE ON
FRAME
theta1 = 90*pi/180; % ANGLE OF VECTOR R1
r2 = 0.103; % STEERING ARM LENGTH
r3 = 0.528; % TIE ROD LENGTH
r4 = 0.14; % BELL-CRANK ARM LENGTH
theta_o = 168.0*pi/180; %151*pi/180; % NEUTRAL STEER ANGLE

```

Ackerman six-bar (Archibald, 2016)

```

function [err, MSE] = Ackerman_6B_f(varargin);
% Ackerman_6B --> computes steering error for 6-Bar steering
%
% Input Arguments
% fstr string % NAME OF SCRIPT FILE CONTAINING DATA
%
%
% DATA REQUIRED IN INPUT SCRIPT FILE:
% Vehicle Parameters
% vehicle string % NAME OF VEHICLE
% L scaler % WHEELBASE
% t scaler % KINEMATIC TRACK
% Rmin scaler % MINIMUM TURN RADIUS
%
% Mechanism parameters
% r1 scaler % BELL-CRANK PIVOT TO STEERING AXIS DISTANCE ON
% FRAME
% r2 scaler % STEERING ARM LENGTH
% r3 scaler % TIE ROD LENGTH
% r4 scaler % BELL-CRANK ARM LENGTH
% theta_o scaler % NEUTRAL STEER ANGLE FROM VEHICLE X-AXIS TO
% STEERING ARM WHEN WHEELS STRAIGHT AHEAD
% theta1 scaler; % ANGLE OF VECTOR R1 FROM BELL CRANK PIVOT TO
% KINGPIN AXIS
%
% unit char % INPUT LENGTH UNIT, EITHER 'M' OR 'I'
% output char % SWITCH TO SUPPRESS OUTPUT, EITHER 'Y' OR 'N'
%
%
% Written By Mark Archibald March, 2005
% Revised February 2012

clear;
% close all;

mech_type = 'SIX-BAR LINKAGE';

% Check for optional arguments

```

```

if nargin == 0,
    % SAMPLE FILES: (Matlab scripts that contain all parameter values)
    mnu = menu('SELECT VEHICLE', 'DEFAULT SIX BAR TRAIL', ...
              'ENTER OTHER FILENAME');

    switch mnu
    case 1,
        sixbar_trail;
    case 2,
        fprintf('\n\nACKERMAN STEERING PROGRAM -- SIX BAR LINKAGE \n\n');
        fstr = input('ENTER FILE NAME: ', 's');
        eval(fstr);
    end
else,
    % Data file passed to function
    fstr = varargin{1};
    eval(fstr)
end
unit = 'm';
output = 'y';
% END INPUT SECTION ..>.....

% Establish R vector
Rmax = 20;
n = 50;
I = (Rmax/Rmin)^(1/(n-1)) - 1;
R = Rmin*(I+1).^(0:n-1)';

% Compute steer angles
psi_o = 2*pi-theta_o;
theta = theta_o - atan2(L, (R-t/2)); % Inside Wheel Angle
psi_p = psi_o - atan2(L, (R+t/2)); % Theoretical Outside wheel angle

% Determine Neutral steer angle delta_o of bell crank
C = r2*exp(i*theta_o) - r1*exp(i*thetal);
Ca = abs(C);
Cu = C./Ca;
Cuxk = (imag(Cu) - i*real(Cu));
T = (r4^2-r3^2+Ca.^2)./(2*Ca);
A1=sqrt(r4^2-T.^2).*Cuxk + T.*Cu; % These are scalers corresponding
A2=-sqrt(r4^2-T.^2).*Cuxk + T.*Cu; % to the neutral steer position
delA1 = angle(A1);
delA2 = angle(A2);
if abs(theta_o) < pi/2, % If TRUE, choose solution with angle closest to 0
    if abs(delA1) < abs(delA2),
        delta_o = delA1;
    else
        delta_o = delA2;
    end
else % ELSE choose solution with angle closest to pi
    if abs(delA1) > abs(delA2),
        delta_o = delA1;
    else
        delta_o = delA2;
    end
end
delta_o = delta_o + (sign(delta_o)-1)*(-pi); % Convert from (-pi to pi) to
(0 to 2*pi)

% solve first Chase equation for del -- bell crank angle, inside wheel
C = r2*exp(i*theta) - r1*exp(i*thetal);

```

```

Ca = abs(C);
Cu = C./Ca;
Cuxk = (imag(Cu) - i*real(Cu));
T = (r4^2-r3^2+Ca.^2)./(2*Ca);
A1=sqrt(r4^2-T.^2).*Cuxk + T.*Cu;
A2=-sqrt(r4^2-T.^2).*Cuxk + T.*Cu;
delA1 = angle(A1);
delA2 = angle(A2);
if abs(theta_o) < pi/2, % If TRUE, choose solution with angle closest to 0
    if abs(delA1) < abs(delA2),
        deli = delA1; % deli = actual angle of bell crank (inside
    else % wheel
        deli = delA2;
    end
else % ELSE choose solution with angle closest to pi
    if abs(delA1) > abs(delA2),
        deli = delA1;
    else
        deli = delA2;
    end
end
delio = deli + (sign(deli)-1)*(-pi); % Convert from (-pi to pi) to (0 to
2*pi)
del = delta_o-deli; % del = relative angle of bell crank wrt neutral
steer
delo = delta_o+del; % delo = del reflected about delta_o (for
outside wheel)

% Solve second Chase eqn for outside wheel angle (actual)
C = r1*exp(i*theta1) + r4 *exp(i*delo);
Ca = abs(C);
Cu = C./Ca;
Cuxk = (imag(Cu) - i*real(Cu));
T = (r2^2-r3^2+Ca.^2)./(2*Ca);
A1=sqrt(r2^2-T.^2).*Cuxk + T.*Cu;
A2=-sqrt(r2^2-T.^2).*Cuxk + T.*Cu;
psiA1 = 2*pi - unwrap(angle(A1));
% % if (psiA1(1)-psi_p(1)) > pi*15/8,
% %     psiA1 = psiA1 - 2*pi;
% % elseif (psiA1(1)-psi_p(1)) < -pi*15/8,
% %     psiA1 = psiA1 + 2*pi;
% % end;
psiA2 = 2*pi - unwrap(angle(A2));
% psiA1 = angle(A1);
% psiA2 = angle(A2);
% psiA1 = psiA1 + (sign(psiA1)-1)*(-pi); % Convert from (-pi to pi) to (0
to pi)
% psiA2 = psiA2 + (sign(psiA2)-1)*(-pi);
if psiA1(n) < 2*pi,
    if psiA1(n) > psi_o,
        psi = psiA2;
    else
        psi = psiA1;
    end
else
    psiA1 = psiA1 - 2*pi;
    if psiA1(n) > psi_o,
        psi = psiA2;
    else
        psi = psiA1;
    end
end

```

```

end
if psi(n) > 2*pi,
    psi = psi - 2*pi;
end

% Compute Error
err = 180*(psi_p - psi)/pi;
MSE = mean(err.^2);
[max_dev, max_dev_idx] = max(abs(err));

% Compute steer angles and max steer angles
steer_i = theta_o - theta;           % Actual inside wheel steer angles
steer_o = psi_o - psi;              % Actual outside wheel steer angles
max_steer_Ack = atan2(L,R)          % Ackerman steering angles
max_steer_i = max(steer_i);         %
max_steer_o = max(steer_o);         % Steering angles at minimum turn radius
max_Ack = max(max_steer_Ack);       %
max_delta = (delta_o - delio(1));   %

% Output Results
if (output == 'y') | (output == 'Y'),
    close ALL;
    clc;
    if lower(unit) == 'm',
        runit = 'm';
        munit = 'mm';
        r1 = r1*1000; % convert kinematic dimensions to mm
        r2 = r2*1000;
        r3 = r3*1000;
        r4 = r4*1000;
        L = L*1000;
        t = t*1000;
        Rf = R;
    else
        runit = 'ft';
        munit = 'in';
        Rf = R/12; % Radius in feet
    end
end

% Plot results
Rf = R; % Radius in feet
plot(Rf, psi_p*180/pi, 'bx-', Rf, (psi)*180/pi, 'r. ');
fig1 = gcf;
set(fig1, 'Position', [990 200 560 420])
title('STEERING ANGLE FOR OUTSIDE WHEEL');
xlabel('TURN RADIUS (m)');
ylabel('OUTSIDE WHEEL ANGLE (deg)');
grid;
legend('DESIRED FUNCTION', 'ACTUAL FUNCTION', 0);

fig2 = figure;
plot(Rf, err, '-. ');
set(fig2, 'Position', [990 150 560 420])
title('STEERING ANGLE ERROR FOR OUTSIDE WHEEL');
xlabel('TURN RADIUS (m)');
ylabel('ERROR (deg)');
grid;

fig3 = figure; % GRAPHIC OF MECHANISM

```

```

    QX = [-r1*sin(thetal) -r1*sin(thetal)+r2*sin(theta_o)
r4*sin(delta_o)...
    0 -r4*sin(delta_o) r1*sin(thetal)-r2*sin(theta_o) r1*sin(thetal)];
    QY = [-r1*cos(thetal) -r1*cos(thetal)+r2*cos(theta_o)
r4*cos(delta_o)...
    0 r4*cos(delta_o) -r1*cos(thetal)+r2*cos(theta_o) -r1*cos(thetal)];
    v = [-1.2*r1 1.2*r1 -1.5*r2 r2];
    H = plot(QX,QY,'- .');
    set(fig3,'Position',[15 375 560 200]);
    set(H,'linewidth',2.5);
    set(H,'markersize',21);
    axis(v);
    axis equal;
    title('KINEMATIC DIAGRAM OF STEERING MECHANISM');

% Print Summary
fprintf(1,'\n\n ACKERMAN STEERING ERROR \n\n');
fprintf(1,'VEHICLE: %s \n\n',vehicle);
fprintf(1,'TYPE OF STEERING MECHANISM: %s \n\n',mech_type);
fprintf(1,'FRAME LENGTH: %6.3f in \n',r1);
fprintf(1,'FRAME ANGLE: %5.1f deg \n',thetal*180/pi);
fprintf(1,'TRACK ARM LENGTH: %6.3f in \n',r2);
fprintf(1,'NEUTRAL STEER ANGLE: %5.1f deg \n',theta_o*180/pi);
fprintf(1,'TIE ROD LENGTH: %6.3f in \n',r3);
fprintf(1,'BELL CRANK LENGTH: %6.3f in \n',r4);
fprintf(1,'BELL CRANK ANGLE: %5.1f deg \n\n',delta_o*180/pi);
fprintf(1,'MAX INSIDE WHEEL ANGLE: %5.1f deg \n',max_steer_i*180/pi);
fprintf(1,'MAX OUTSIDE WHEEL ANGLE: %5.1f deg \n',max_steer_o*180/pi);
fprintf(1,'MAX ACKERMAN ANGLE: %5.1f deg \n',max_Ack*180/pi);
fprintf(1,'MAX STEERING INPUT: %5.1f deg \n\n',max_delta*180/pi);
fprintf(1,'MEAN SQUARE ERROR = %7.4f deg^2 \n\n',MSE);
fprintf(1,'MAX DEVIATION = %4.2f deg AT RADIUS = %5.2f ft
\n\n',max_dev,Rf(max_dev_idx));
end;

```

High-speed cornering, rollover and pitchover (Archibald, 2016)

```

clc;
clear;
close all;

% INPUT SECTION
% Input Trike Data
vehicle = 'ILALO';
m = 100; % Total mass, kg
type = 'TADPOLE';
L = 1.2; % Wheelbase, m
t = 1.2; % Track, m
b = .45; % CG location from rear axle, m
h = .5; % CG height, m

```

```

% Input Tire Properties
Af = .2532;      % 1st Cornering stiffness coefficient, front
Bf = .000211;   % 2nd Cornering stiffness coefficient, front
Ar = .2532;      % 1st Cornering stiffness coefficient, rear
Br = .000211;   % 2nd Cornering stiffness coefficient, rear
mup = .95;      % Peak brake coefficient
mus = .8;       % Slide brake coefficient

% Input Test Radius
R = 4;          % Skid pad circle radius, m
Vmax = 8;       % Max test speed, m/s
% END INPUT SECTION
% Constants
g = 9.81;       % m/s^2

% Calculations
V = (2:.1:Vmax)'; % Test speed, m/s
ay = V.^2/R;

boL = b/L;      % Aft CG ratio, b/L
hoT = 2*h/t;    % Height over half track ratio
hoL = h/L;      % Height over Wheelbase ratio h/L

lay = length(ay);
% for i=1:lay,
%     say(i,:) = sprintf('LATERAL ACCEL = %5.2f G \n',ay(i)/g);
% end;

if type == 'TADPOLE';
    % Cornering Stiffness
    Wf = m*g*boL;
    Wr = m*g*(1-boL);
    Caf = 2*(Af*Wf/2-Bf*(Wf/2).^2);
    Car = Ar*Wr-Br*(Wr.^2);
    Ktire = Wf./Caf - Wr./Car;
    DFz = m*(hoT/2)*ay;
    Kllt = (Wf./Caf.^2)*(2*Bf*DFz.^2);
    K = Ktire + Kllt;

```

```

% Rollover Threshold
Rollg = boL/hoT;           % G's
Roll  = g*boL/hoT;       % m/s^2

elseif type == 'DELTA ',
    Wf = m*g*boL;
    Wr = m*g*(1-boL);
    Caf = Af*Wf-Bf*(Wf.^2);
    Car = 2*(Ar*Wr/2-Br*(Wr/2).^2);
    Ktire = Wf./Caf - Wr./Car;
    DFz = m*(hoT/2)*ay;
    Kllt = -(Wr./Caf.^2) * (2*Bf*DFz.^2);
    K = Ktire + Kllt;

% Rollover Threshold
Rollg = (1-boL)/hoT;      % for g's
Roll  = g*(1-boL)/hoT;   % for m/s^2

else
    fprintf('ERROR ! WRONG TYPE ENTERED \n\n');
    return;
end;

% Pitchover Threshold
Pitchacc = g*boL/hoL;
Pitchbrk = g*(1-boL)/hoL;

% Critical Speed
vcr = sqrt(-180*L*g./(pi*K));

% Characteristic Speed
vchar = sqrt(180*L*g./(pi*K));

% Steer Angle Delta
del = (180/pi)*(L/R) + K.*ay; % deg

% Prepare Reference Graph Data
delack = 180/pi*L/R*ones(1,2);
Vdelack = [V(1) V(length(V))];
delack2 = 2*delack;
rolltic = sqrt(R*Roll)*ones(1,2);

```

```

title1 = sprintf('%s: UNDERSTEER GRADIENT (Ktire + Kl1t) VS SPEED, R = %4.1f
m'...
    ,vehicle,R);
title2 = sprintf('%s: STEER ANGLE VS SPEED, R = %4.1f m',vehicle,R);
title3 = sprintf('%s: LATERAL ACCELERATION VS SPEED, R = %4.1f
m',vehicle,R);

% Output Results

fprintf(1, '\nTRICYCLE HANDLING EVALUATION \n\n');
fprintf(1, 'VEHICLE:      %s \n',vehicle);
fprintf(1, 'TYPE OF TRIKE: %s \n\n',type);

    fprintf(1, 'TOTAL MASS:      %5.2f kg \n',m);
    fprintf(1, 'WHEELBASE:      %5.3f m \n',L);
    fprintf(1, 'TRACK:          %5.3f m \n',t);
    fprintf(1, 'CG HEIGHT:      %5.3f m \n',h);
    fprintf(1, 'CG LOCATION:    %5.3f m \n\n',b);
    fprintf(1, 'STATIC WEIGHT FRACTION, REAR:      %4.1f %% \n',100*(1-boL));
    fprintf(1, 'CRITICAL SPEED:      %5.3f m/s \n',vcr);
    fprintf(1, 'ROLLOVER THRESHOLD:      %5.3f G's \n',Rollg);
    fprintf(1, 'BRAKE          PITCHOVER          THRESHOLD:      %5.3f          G's
\n',Pitchbrk/g);
    fprintf(1, 'ACCELERATION          PITCHOVER          THRESHOLD:      %5.3f          G's
\n\n',Pitchacc/g);

plot(V,K/g, 'r',Vdelack,zeros(1,2), 'b');
%plot(ay/g,K/g, 'r')
fig1 = gcf;
set(fig1, 'Position', [1200 50 560 420])
grid;
xlabel('SPEED m/s');
%xlabel('LATERAL ACCELERATION (G)');
ylabel('UNDERSTEER GRADIENT K (deg/m/s^2)');
title(title1);
% legend(say);

fig2 = figure;
plot(V,del, 'r',Vdelack,delack, 'b',Vdelack,delack2, 'g');
vax = axis;
hold on;

```

```

plot(rolltic,vax(3:4),'k','linewidth',2);
hold off
fig1 =(gcf);
set(fig1,'Position',[25 50 560 420])
grid;
xlabel('SPEED m/s');
ylabel('STEER ANGLE (deg)');
title(title2);
legend('STEER ANGLE','ACKERMAN ANGLE','2X ACKERMAN',...
       'ROLLOVER THRESHOLD','location','SouthEast')

fig3 = figure;
plot(V,ay/g,'r');
set(fig3,'Position',[600 50 560 420]);
vax = axis;
hold on;
plot(rolltic,vax(3:4),'k','linewidth',2);
hold off
xlabel('SPEED m/s');
ylabel('LATERAL ACCELERATION G's');
title(title3);
grid;

```

Gear Development (Archibald, 2016)

```

function G = gear_test(varargin)
% INPUT VARIABLES
% Units:'I' for gear-inches
%       'M' for meters development
%
% OUTPUT VARIABLES
% G = Matrix of gear development
%
% Calculates the gears for bicycle drivetrains. Gears are
% plotted on log scale to compare effort for each gear. Speeds
% corresponding to low, high, and medium cadence are also plotted for
% each gear.

clc;
close all;

```

```

fprintf('\n\nBICYCLE GEAR CALCULATOR \n\n');

% INPUT DATA
vehicle = "Ilalo"; % Vehicle name
sec_width = 54; % Tire Section Width [mm] or
[in]
BSD = 559; % Bead Seat Diameter [mm] or
[in]
chain = [40, 30, 22]; % Row Vector of chainring
sizes (may be scalar for single)
free = [25, 23, 21, 19, 17, 15, 13, 12, 11]; % Row Vector for number of
teeth on each freewheel cog
cad = [90,135, 50]; % Row vector for Cadence:
Nominal, Max, Min (rpm)

% Basic Calculations
nf = length(free);
wheel = (BSD+2*sec_width)/25.4; % Wheel diameter, inches
lc = length(chain);

% Calculate gearing
G = wheel*chain'./free;
LO = min(min(G));
HI = max(max(G));
RANGE = HI/LO;

% Convert Units if required
unit = 'meters';
units = 'm';
%if ~isempty(varargin) % Check for optional argument
% units = varargin{1}; % Store unit switch
% if lower(units) == 'm'
% unit = 'meters';
conv = pi/39.37; % conversion factor from gear-inches to meters
dev.
G = G*conv;
LO = LO*conv;
HI = HI*conv;
% end

```

```

%end

% OUTPUT RESULTS .....
clc;
fprintf('\n\nBICYCLE GEAR CALCULATOR \n\n');
fprintf(1,'    VEHICLE:  %s \n',vehicle);
fprintf(1,'DRIVE WHEEL:  %2i-%3i ISO\n',sec_width,BSD);
fprintf(1,'    LOW GEAR:  %4.1f %s \n',LO,unit);
fprintf(1,'    HIGH GEAR:  %5.1f %s \n',HI,unit);
fprintf(1,'        RANGE:  %4.2f \n\n',RANGE);
fprintf('CHAINRING TOOTH NUMBERS: \n');
disp(chain);
fprintf('CASSETTE TOOTH NUMBERS: \n');
disp(free);

fprintf(1,'\nGEARS (%s) \n\n',unit);
if lc == 1
    fprintf('    %5.1f \n',G);
elseif lc == 2
    fprintf('    HIGH        LOW \n');
    fprintf('    %5.1f        %5.1f \n',G);
elseif lc == 3
    fprintf('    HIGH        MID        LOW \n');
    fprintf('    %5.1f        %5.1f        %5.1f \n',G);
end

close;
gear_plot(G,chain,free,vehicle,unit);

fig2 = figure;
[Vnom, Vmin, Vmax] = gear_speed(G,cad,vehicle,units);
set(gcf,'Position',[20 400 750 500]);

function [Vnom,Vmin,Vmax] = gear_speed(G,cad,vehicle,units)
%
% Computes speeds for bicycle with gearing specified
%
% INPUT VARIABLES
% Variable      Size      Description
% G              (i,j)      Gear inches i = # chainrings, j = # sprockets
% cad            (3)        Cadence [nominal, max, min]

```

```

% vehicle      string      Name of vehicle
% units        string      System of Units for G: 'I' for inches,
%                                     'M' for meters
%
%
% OUTPUT VARIABLES
% Vnom         (i,j)       Bike speed in each gear for nominal cadence
% Vmax         (i,j)       Bike speed in each gear for maximum cadence
% Vmin         (i,j)       Bike speed in each gear for minimum cadence

[i,j] = size(G);

% F is a conversion factor for speed
if lower(units) == 'm'
    F = 1/(60);           % m/s
    vunit = 'm/s';
    unit = 'm';
else
    F = pi*60/(12*5280); % mph
    vunit = 'mph';
    unit = 'in';
end

Vnom = G*cad(1)*F;
Vmax = G*cad(2)*F;
Vmin = G*cad(3)*F;

% Plotting matrices
hold off;
p = ['bx-' ; 'gx-' ; 'rx-' ; 'kx-' ; 'cx-' ; 'mx-'];
for k = 1:i
    V1 = [Vmin(k,:);Vnom(k,:);Vmax(k,:)];
    G1 = [G(k,:); G(k,:); G(k,:)];
    plot(G1,V1,p(k,:), 'linewidth',2, 'markersize',12);
    hold on
end

% Axis values
LL = min(min(G));
HL = max(max(G));
wG = size(G);

```

```

wG = min(wG);
lG = length(G);
v2 = 10*ceil(HL/10);
if LL < 20
    v1 = floor(LL);
else
    v1 = 10*floor(LL/10);
end
vm = max(max(Vmax));
avm = 10*(floor(vm/10) + 1);
A = [v1 v2 0 avm];
axis(A);

grid;
xstr = sprintf('Gear Development (%s)',unit');
ystr = sprintf('Speed (%s)',vunit');
xlabel(xstr);
ylabel(ystr);
titstr = sprintf('%s\nSPEED RANGES FOR EACH GEAR',vehicle);
title(titstr);
ax = gca;
ax.FontSize = 16;

function gear_plot(G,chain,free,vehicle,unit)
% gear_plot(G) Plot options for gearing programs
%
% Input Variables
%
% G Matrix Matrix of gear numbers
% chain Vector of chainring tooth numbers
% free Vector of freewheel tooth numbers
% vehicle Vehicle name

LL = min(min(G));
HL = max(max(G));
wG = size(G);
wG = min(wG);
lG = length(G);

str1 = sprintf('%2.0f ',chain);
titstr = sprintf('%s \nEQUIVALENT CHAINRING SIZES: %s TEETH',vehicle,str1);

```

```

o = ones(lG,1)*(1:wG);
cf = semilogx(G',o);

set(gcf, 'Position',[20 100 750 200])
h = findobj('Type','Line');
switch wG
    case 1
        set(h(1), 'Marker', 'o');
        legstr = ['SPEED 1'];
    case 2
        set(h(1), 'Marker', 'o');
        set(h(2), 'Marker', 's');
        legstr = ['SPEED 1'; 'SPEED 2'];
    case 3
        set(h(1), 'Marker', 'o');
        set(h(2), 'Marker', 's');
        set(h(3), 'Marker', 'd');
        legstr = ['SPEED 1'; 'SPEED 2'; 'SPEED 3'];
    case 4
        set(h(1), 'Marker', 'o');
        set(h(2), 'Marker', 's');
        set(h(3), 'Marker', 'd');
        set(h(4), 'Marker', 'v');
        legstr = ['SPEED 1'; 'SPEED 2'; 'SPEED 3'; 'SPEED 4'];
    case 5
        set(h(1), 'Marker', 'o');
        set(h(2), 'Marker', 's');
        set(h(3), 'Marker', 'd');
        set(h(4), 'Marker', 'v');
        set(h(5), 'Marker', '*');
        legstr = ['SPEED 1'; 'SPEED 2'; 'SPEED 3'; 'SPEED 4'; 'SPEED 5'];
end

set(cf, 'LineStyle', 'none');
set(cf, 'MarkerSize', 10);
set(cf, 'LineWidth', 2);
grid;

title(titstr);
xstr = sprintf('Gear Development (%s) (Log Scale)',unit);
xlabel(xstr);

```

```

ylabel('Chainring');
ax = gca;
ax.FontSize = 16;

v2 = 10*ceil(HL/10);
if LL < 20
    v1 = floor(LL);
    xtic = v1:2:20;
else
    v1 = 10*floor(LL/10);
    xtic = v1;
end
end
v = [v1 v2 0 wG+1];
axis(v);
ha = gca;
if v2 <= 100
    if xtic >= 30
        xtic = (30:10:v2);
    else
        xtic = [xtic 30:10:v2];
    end
else
    xtic = [v1:10:100 120:20:v2];
end

set(ha,'XTick',xtic);
set(ha,'YTick',1:wG);

cogs = sprintf('Cassette Cogs: %s ',num2str(free));
text(v1+1,.3,cogs,'backgroundColor','White','Edgecolor','k');
legend(legstr);

```

Arduino Codes

Parking Brake (Roumega, 176)

```
#include <Servo.h>
Servo myservo;
int pos = 0;
int state; int flag=0;
void setup()
{
myservo.attach(9);
Serial.begin(9600);
myservo.write(60);
delay(1000); }
void loop()
{
if(Serial.available() > 0)
{
state = Serial.read();
flag=0;
} // if the state is '0' the DC motor will turn off
if (state == '0')
{
myservo.write(8);
delay(1000);
Serial.println("Break Locked");
}
else if (state == '1')
{
myservo.write(55);
delay(1000);
Serial.println("Break Unlocked");
}
}
```

Appendix B – Project Management

Material and Component Selection Tables

Material Selection Table

Materials						
Cost > Manufacturability > Weight>Durability						
CRITERIA	Cost	Manufacturability	Weight	Durability	$\Sigma+1$	Weighted Value
Cost	-	1	1	1	4	0.40
Manufacturability	0	-	1	1	3	0.30
Weight	0	0	-	1	2	0.20
Durability	0	0	0	-	1	0.10
				TOTAL	10	1

Cost > Manufacturability > Weight>Durability						
Cost	AISI 1020	AISI 4130	Aluminum	Bamboo	$\Sigma+1$	Weighted Value
AISI 1020	-	1	1	0	3	0.33
AISI 4130	0	-	1	0	2	0.22
Aluminum	0	0	-	0	1	0.11
Bamboo	0	1	1	-	3	0.33
				TOTAL	9	1

Cost > Manufacturability > Weight>Durability						
Manufacturability	AISI 1020	AISI 4130	Aluminum	Bamboo	$\Sigma+1$	Weighted Value
AISI 1020	-	1	1	1	4	0.40
AISI 4130	0	-	1	1	3	0.30
Aluminum	0	0	-	0	1	0.10
Bamboo	0	0	1	-	2	0.20
				TOTAL	10	1

Cost > Manufacturability > Weight>Durability						
Weight	AISI 1020	AISI 4130	Aluminum	Bamboo	$\Sigma+1$	Weighted Value
AISI 1020	-	0	0	0	1	0.13
AISI 4130	0	-	0	0	1	0.13
Aluminum	1	1	-	0	3	0.38
Bamboo	1	1	0	-	3	0.38
				TOTAL	8	1

Cost > Manufacturability > Weight>Durability						
Durability	AISI 1020	AISI 4130	Aluminum	Bamboo	$\Sigma+1$	Weighted Value
AISI 1020	-	0	1	0	2	0.25
AISI 4130	1	-	1	1	4	0.50
Aluminum	0	0	-	0	1	0.13
Bamboo	0	0	0	-	1	0.13
				TOTAL	8	1

TOTAL	Cost	Manufacturability	Weight	Durability	Weighted
AISI 1020	0.13	0.12	0.03	0.03	0.30
AISI 4130	0.09	0.09	0.03	0.05	0.25
Aluminum	0.04	0.03	0.08	0.01	0.16
Bamboo	0.13	0.06	0.08	0.01	0.28

Automatic Control Selection Table

Cost > Manufacturability > Maintenance > Weight > User Benefit							
CRITERIA	Cost	Manufacturability	Maintenance	Weight	U. Benefit	$\Sigma+1$	Weighted Value
Cost	-	1	1	1	1	5	0.33
Manufacturability	0	-	1	1	1	4	0.27
Maintenance	0	0	-	1	1	3	0.20
Weight	0	0	0	-	1	2	0.13
User Benefit	0	0	0	0	-	1	0.07
TOTAL						15	1

Cost > Manufacturability > Maintenance > Weight > User Benefit						
Cost	Safety Brake	A. Gear Shifts	Slope Assistance	Electric Motor	$\Sigma+1$	Weighted Value
Safety Brake	-	0	1	1	3	0.33
A. Gear Shifts	0	-	1	1	3	0.33
Slope Assistance	0	0	-	1	2	0.22
Electric Motor	0	0	0	-	1	0.11
TOTAL					9	1

Cost > Manufacturability > Maintenance > Weight > User Benefit						
Manufacturability	Safety Brake	A. Gear Shifts	Slope Assistance	Electric Motor	$\Sigma+1$	Weighted Value
Safety Brake	-	0	1	1	3	0.38
A. Gear Shifts	0	-	0	1	2	0.25
Slope Assistance	0	0	-	1	2	0.25
Electric Motor	0	0	0	-	1	0.13
TOTAL					8	1

Cost > Manufacturability > Maintenance > Weight > User Benefit						
Maintenance	Safety Brake	A. Gear Shifts	Slope Assistance	Electric Motor	$\Sigma+1$	Weighted Value
Safety Brake	-	0	1	1	3	0.33
A. Gear Shifts	0	-	1	1	3	0.33
Slope Assistance	0	0	-	1	2	0.22
Electric Motor	0	0	0	-	1	0.11
TOTAL					9	1

Cost > Manufacturability > Maintenance > Weight > User Benefit						
Weight	Safety Brake	A. Gear Shifts	Slope Assistance	Electric Motor	$\Sigma+1$	Weighted Value
Safety Brake	-	0	1	1	3	0.33
A. Gear Shifts	0	-	1	1	3	0.33
Slope Assistance	0	0	-	1	2	0.22
Electric Motor	0	0	0	-	1	0.11
TOTAL					9	1

Cost > Manufacturability > Maintenance > Weight > User Benefit						
User Benefit	Safety Brake	A. Gear Shifts	Slope Assistance	Electric Motor	$\Sigma+1$	Weighted Value
Safety Brake	-	0	0	0	1	0.10
A. Gear Shifts	1	-	1	0	3	0.30
Slope Assistance	1	0	-	0	2	0.20
Electric Motor	1	1	1	-	4	0.40
TOTAL					10	1

TOTAL	Cost	Manufacturability	Maintenance	Durability	Efficiency	Weighted Value
Safety Brake	0.11	0.10	0.07	0.04	0.01	0.33
A. Gear Shifts	0.11	0.07	0.07	0.04	0.02	0.31
Slope Assistance	0.07	0.07	0.04	0.03	0.01	0.23
Electric Motor	0.04	0.03	0.02	0.01	0.03	0.13

Drive Train Selection Table

Cost > Manufacturability > Maintenance > Durability > Weight = Efficiency								
CRITERIA	Cost	Manufacturability	Maintenance	Durability	Weight	Efficiency	$\Sigma+1$	Weighted Value
Cost	-	1	1	1	1	1	6	0.29
Manufacturability	0	-	1	1	1	1	5	0.24
Maintenance	0	0	-	1	1	1	4	0.19
Durability	0	0	0	-	1	1	3	0.14
Weight	0	0	0	0	-	0.5	1.5	0.07
Efficiency	0	0	0	0	0.5	-	1.5	0.07
						TOTAL	21	1

FWD > SRWD > CRWD > AWD						
Cost	FWD	SRWD	CRWD	AWD	$\Sigma+1$	Weighted Value
FWD	-	1	1	1	4	0.40
SRWD	0	-	1	1	3	0.30
CRWD	0	0	-	1	2	0.20
AWD	0	0	0	-	1	0.10
				TOTAL	10	1

SRWD > CRWD > FWD > AWD						
Manufacturability	SRWD	CRWD	FWD	AWD	$\Sigma+1$	Weighted Value
SRWD	-	1	1	1	4	0.40
CRWD	0	-	1	1	3	0.30
FWD	0	0	-	1	2	0.20
AWD	0	0	0	-	1	0.10
				TOTAL	10	1

SRWD > CRWD > FWD > AWD						
Maintenance	SRWD	CRWD	FWD	AWD	$\Sigma+1$	Weighted Value
SRWD	-	1	1	1	4	0.40
CRWD	0	-	1	1	3	0.30
FWD	0	0	-	1	2	0.20
AWD	0	0	0	-	1	0.10
				TOTAL	10	1

CRWD > SRWD = FWD > AWD						
Durability	CRWD	SRWD	FWD	AWD	$\Sigma+1$	Weighted Value
CRWD	-	1	1	1	4	0.40
SRWD	0	-	0.5	1	2.5	0.25
FWD	0	0.5	-	1	2.5	0.25
AWD	0	0	0	-	1	0.10
				TOTAL	10	1

FWD > SRWD > CRWD > AWD						
Weight	FWD	SRWD	CRWD	AWD	$\Sigma+1$	Weighted Value
FWD	-	1	1	1	4	0.40
SRWD	0	-	1	1	3	0.30
CRWD	0	0	-	1	2	0.20
AWD	0	0	0	-	1	0.10
				TOTAL	10	1

FWD = CRWD > SRWD > AWD						
Efficiency	FWD	CRWD	SRWD	AWD	$\Sigma+1$	Weighted Value
FWD	-	0.5	1	1	3.5	0.35
CRWD	0.5	-	1	1	3.5	0.35
SRWD	0	0	-	1	2	0.20
AWD	0	0	0	-	1	0.10
				TOTAL	10	1

TOTAL	Cost	Manufacturability	Maintenance	Durability	Weight	Efficiency	Weighted Value
SRWD	0.09	0.10	0.08	0.04	0.02	0.01	0.33
CRWD	0.06	0.07	0.06	0.06	0.01	0.03	0.28
FWD	0.11	0.05	0.04	0.04	0.03	0.03	0.29
AWD	0.03	0.02	0.02	0.01	0.01	0.01	0.10

Steering System Selection Table

Cost > Manufacturability > Weight > Maintenance > Stability							
CRITERIA	Cost	Manufacturability	Weight	Maintenance	Stability	$\Sigma+1$	Weighted Value
Cost	-	1	1	1	1	5	0,33
Manufacturability	0	-	1	1	1	4	0,27
Weight	0	0	-	1	1	3	0,2
Maintenance	0	0	0	-	1	2	0,13
Stability	0	0	0	0	-	1	0,07
					SUM	15	1

FWS > RWS > AWS					
	FWS	RWS	AWS	$\Sigma+1$	Weighted Value
Cost					
FWS	-	1	1	3	0,5
RWS	0	-	1	2	0,33
AWS	0	0	-	1	0,17
			SUM	6	1

FWS > RWS > AWS					
	FWS	RWS	AWS	$\Sigma+1$	Weighted Value
Manufacturability					
FWS	-	1	1	3	0,5
RWS	0	-	1	2	0,33
AWS	0	0	-	1	0,17
			SUM	6	1

FWS > RWS > AWS					
	FWS	RWS	AWS	$\Sigma+1$	Weighted Value
Weight					
FWS	-	1	1	3	0,5
RWS	0	-	1	2	0,33
AWS	0	0	-	1	0,17
			SUM	6	1

FWS = RWS > AWS					
	FWS	RWS	AWS	$\Sigma+1$	Weighted Value
Maintenance					
FWS	-	0,5	1	2,5	0,5
RWS	0,5	-	1	1,5	0,3
AWS	0	0	-	1	0,2
			SUM	5	1

AWS > FWS > RWS					
	AWS	FWS	RWS	$\Sigma+1$	Weighted Value
Stability					
AWS	-	0,5	1	3	0,5
FWS	0,5	-	1	2	0,33
RWS	0	0	-	1	0,17
			SUM	6	1

CRITERIA	Cost	Manufacturability	Weight	Maintenance	Stability	Weighted Value
AWS	0,06	0,04	0,03	0,03	0,03	0,19
FWS	0,17	0,13	0,1	0,07	0,02	0,49
RWS	0,11	0,09	0,07	0,04	0,01	0,32

Steering Input Selection Table

Handlebar > Steering Levers > Steering Wheel					
Cost	Handlebar	Steering Levers	Steering Wheel	$\Sigma+1$	Weighted Value
Handlebar	-	1	1	3	0,5
Steering Levers	0	-	1	2	0,33
Steering Wheel	0	0	-	1	0,17
			SUM	6	1

Steering Levers > Handlebar > Steering Wheel					
Manufacturability	Steering Levers	Handlebar	Steering Wheel	$\Sigma+1$	Weighted Value
Steering Levers	-	1	1	3	0,5
Handlebar	0	-	1	2	0,33
Steering Wheel	0	0	-	1	0,17
			SUM	6	1

Steering Wheel = Handlebar > Steering Levers					
Weight	Steering Wheel	Handlebar	Steering Levers	$\Sigma+1$	Weighted Value
Steering Wheel	-	0,5	1	1,5	0,38
Handlebar	0,5	-	1	1,5	0,38
Steering Levers	0	0	-	1	0,25
			SUM	4	1

CRITERIA	Cost	Manufacturability	Comfort	Weight	Weighted Value
Handlebar	0,2	0,1	0,03	0,06	0,38
Steering Wheel	0,07	0,05	0,05	0,06	0,22
Steering Levers	0,13	0,15	0,08	0,04	0,4

Chassis Selection Table

Cost > Manufacturability > Weight = Stability						
CRITERIA	Cost	Manufacturability	Weight	Stability	$\Sigma+1$	Weighted Value
Cost	-	1	1	1	4	0.4
Manufacturability	0	-	1	1	3	0.3
Weight	0	0	-	1	2	0.2
Stability	0	0	0	-	1	0.1
				TOTAL	10	1

Tadpole = Delta > Quad					
Cost	Tadpole	Delta	Quad	$\Sigma+1$	Weighted Value
Tadpole	-	0.5	1	2.5	0.42
Delta	0.5	-	1	2.5	0.42
Quad	0	0	-	1	0.17
			TOTAL	6	1

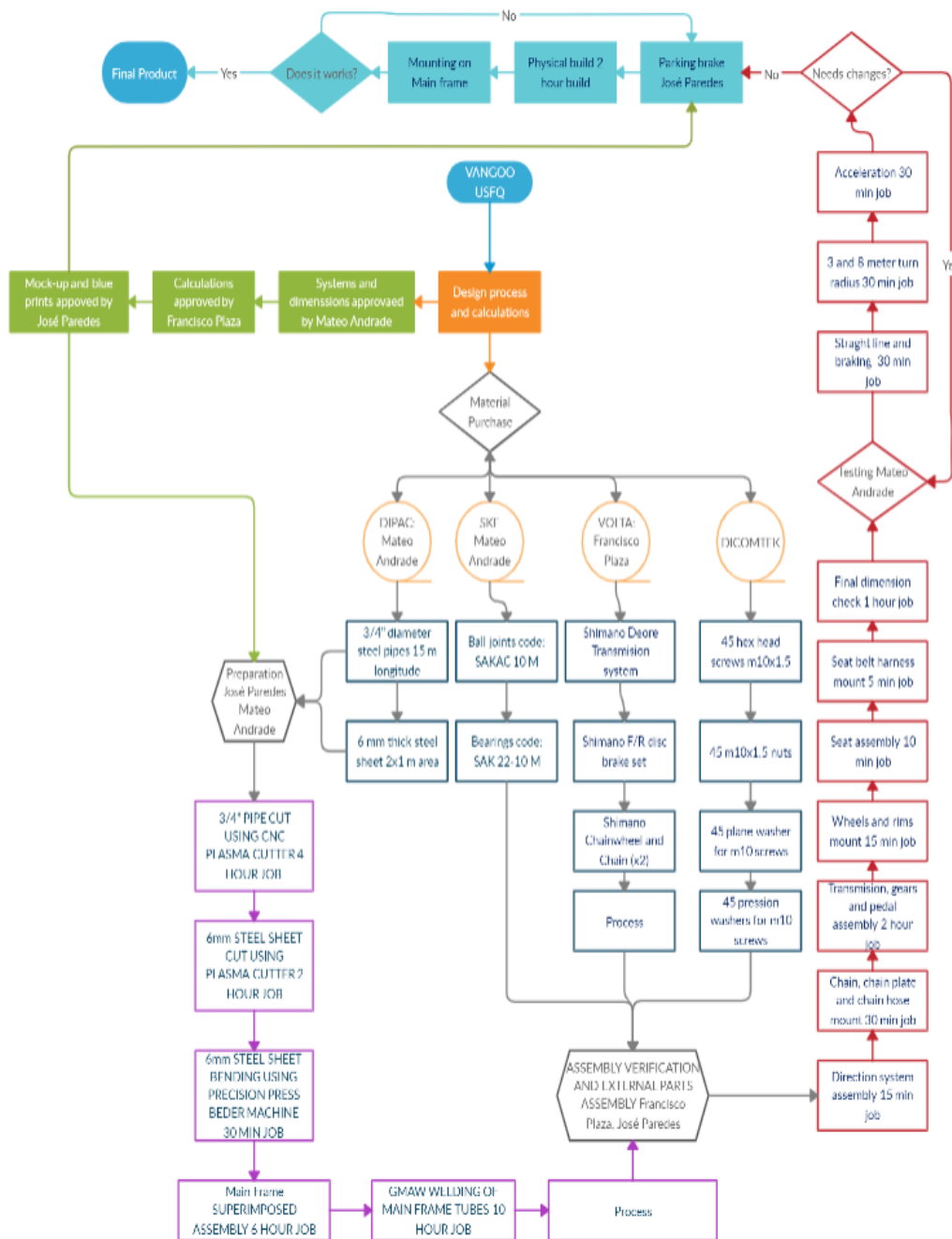
Tadpole = Delta > Quad					
Manufacturability	Tadpole	Delta	Quad	$\Sigma+1$	Weighted Value
Tadpole	-	0.5	1	2.5	0.42
Delta	0.5	-	1	2.5	0.42
Quad	0	0	-	1	0.17
			TOTAL	6	1

Tadpole = Delta > Quad					
Weight	Tadpole	Delta	Quad	$\Sigma+1$	Weighted Value
Tadpole	-	0.5	1	2.5	0.42
Delta	0.5	-	1	2.5	0.42
Quad	0	0	-	1	0.17
			TOTAL	6	1

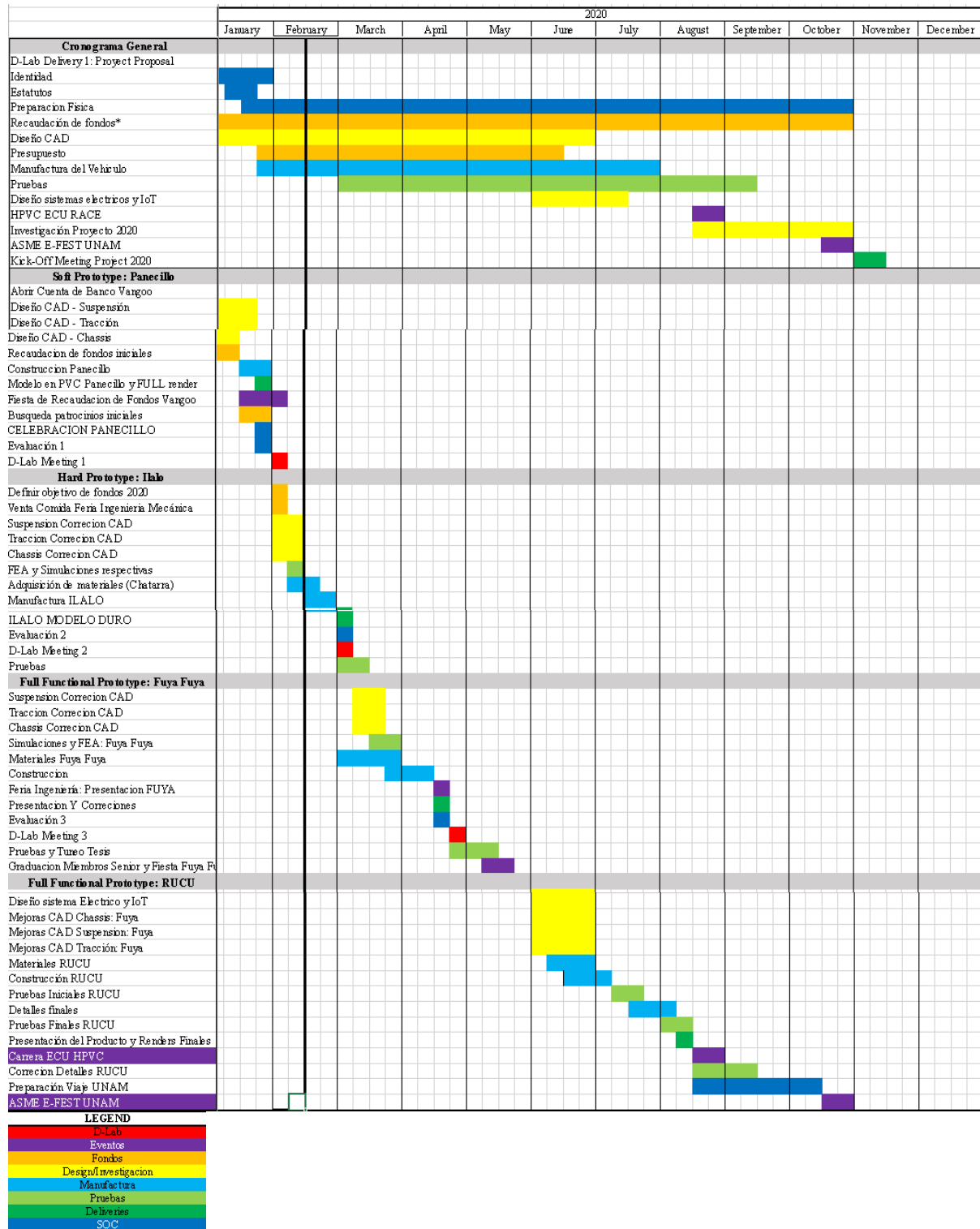
Quad > Tadpole > Delta					
Stability	Quad	Tadpole	Delta	$\Sigma+1$	Weighted Value
Quad	-	1	1	3	0.50
Tadpole	0	-	1	2	0.33
Delta	0	0	-	1	0.17
			TOTAL	6	1

TOTAL	Cost	Manufacturability	Weight	Stability	Weighted Value
Tadpole	0.17	0.13	0.08	0.05	0.43
Delta	0.17	0.13	0.08	0.03	0.41
Quad	0.07	0.05	0.03	0.02	0.17

Design for Manufacturing



Gantt Chart



Budget and Expenses Report

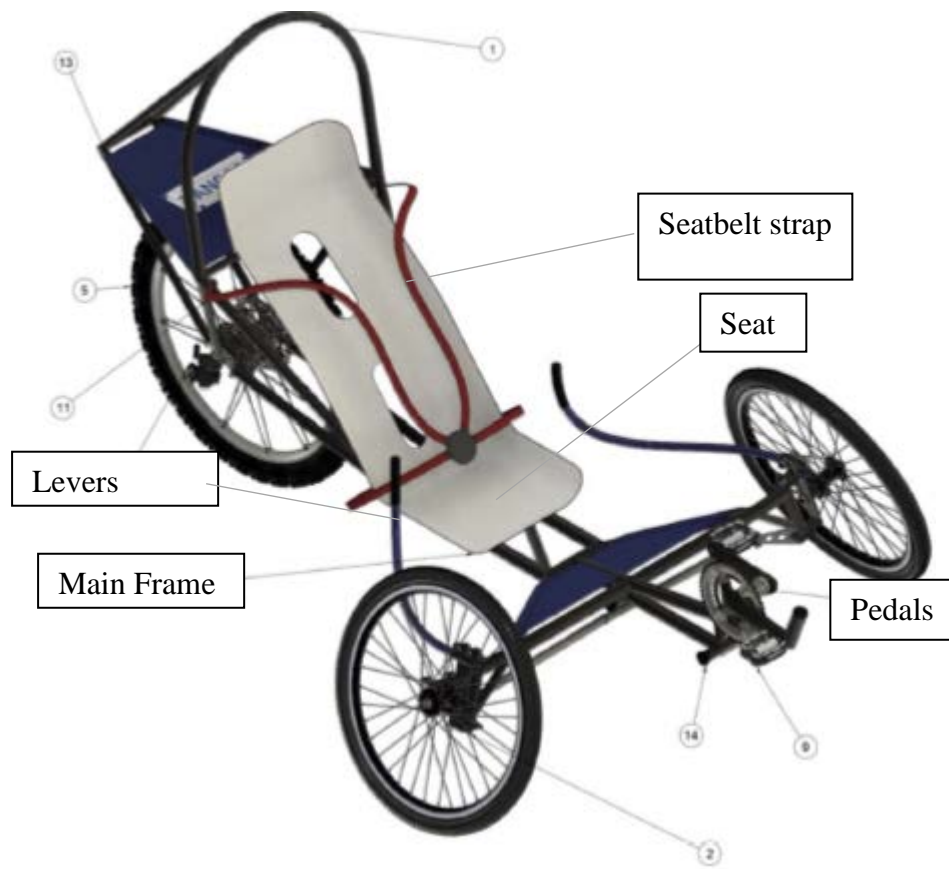
VANGOO ILALO BUDGET				
Concept	Description	Quantity	Unit Price	Total Price
3/4in 2mm Tubes	Chassis	3	12	\$ 36.00
1in 2mm Tube	Chassis	1	12	\$ 12.00
6mm platine	Chassis	1	12	\$ 12.00
Seat	Chassis	1	30	\$ 30.00
Crankset	Transmission	1	60	\$ 60.00
Bottom braket	Transmission	1	20	\$ 20.00
180mm Disk	Brakes	1	30	\$ 30.00
160mm Disk	Brakes	2	20	\$ 40.00
Hidraulick Disk Calliper	Brakes	3	35	\$ 105.00
Brakes Lever	Brakes	2	0	\$ -
Shifters	Transmission	2	15	\$ 30.00
Rear Derailleur	Transmission	1	42	\$ 42.00
Front Derailleur	Transmission	1	30	\$ 30.00
Rear Cassettes	Transmission	1	25	\$ 25.00
Chain	Transmission	3	25	\$ 75.00
Chain Tensors	Transmission	3	10	\$ 30.00
Front hub	Direction	2	40	\$ 80.00
Rear freehub	Transmission	1	40	\$ 40.00
26in wheel	Transmission	3	30	\$ 90.00
Paint	Finishes	1	20	\$ 20.00
Uniball		4	46	\$ 184.00
Rodamientos 22DO y 10ID		6	26	\$ 156.00
Vehicle Assembly	Manufacturing	1	50	\$ 50.00

Subtotal	\$ 1,197.00
Risk Factor	30.00%
Iva 12%	\$ 186.73

Total	\$ 1,742.83
--------------	--------------------

Appendix C – Maintenance and Operating Manual

Operation Manual



1. Place the vehicle on a leveled surface.
2. Put on a protective helmet (preferably a DOT approved one).
3. Pass one leg over the main frame and in front of the seat.
4. Place your body on the seat.
5. Secure the seat belt properly by tightening the straps.
6. Take your cell phone and turn the Bluetooth on. Then, secure the phone into a safe place.
8. Place your feet over the pedals.
9. Using Romoremo app, unlock the parking brake (this will give you 2 seconds to push the pedals).

10. Grab the levers placed to your side and Start pedaling.
11. Select the gear you feel comfortable pedaling with.
12. To steer right, bring the right arm closer to your body.
13. To steer left, bring the left arm closer to your body.
14. To brake with the rear wheel, pull the brake lever on the right handle.
15. To brake with the front wheels, pull the brake lever on the left handle. Be careful when using this break at turns or high speeds, as it can destabilize the vehicle.
16. Before exiting the vehicle, while at a full stop, use the Romoremo app to lock the parking brake.
17. To exit the vehicle, unbuckle the seat belt and proceed to remove one leg from the vehicle first, and then use it to balance yourself while you pull outwards.

Caution - Operational Warnings 
Warning

- Never expose a limb outside of the vehicle frame while in movement.
- Always secure a proper fit of the helmet and seat belt.
- Be careful when using the front brake at turns or high speeds, as it can destabilize the vehicle.
- Be aware of your surroundings always.
- Do not attempt to operate the vehicle with headphones, since it reduces awareness of the surroundings.
- Never use the cell phone or other distracting objects while riding the vehicle.
- In case of collision or roll:
 - Try to keep all the limbs inside the frame of the vehicle.
 - Reduce the neck injury risk by using your hands to emulate a neck brace.
 - Exit the vehicle moving slowly, being extra careful with debris.

- Reduce speeds in wet conditions.

Maintenance Manual

Readjustments after the first outing

- Bolt and screws tightening once the first outing is complete the tightening of the screws should be checked using a 10 mm Allen wrench and a 13mm and 14 mm hexagonal wrenches.

Cleaning and Greasing

- Cleansing: This process should be using a 100% cotton wipe that will be moisturized just with water, if you prefer to use a small amount of soap. If the vehicle is very dirty or covered in mud, use a garden hose with a powerful but tight water jet.



Warning

Make sure to not point the waterjet to the wheel bushings, chain or direction bearings and rods, if these elements get wet their lifetime will be decreased.

- Once the vehicle is clean, proceed to drying with a clean and dry wipe, if dispoible use an air compressor to accelerate the drying step.
- Degrease: Before proceeding to grease certain mechanical parts of the vehicle, it is necessary to degrease them thoroughly. In the case of the chain, it will be degreased with a specific product, or with a brush soaked in gasoline. Other items likely to degrease are the pinions and chainrings. After degreasing, a clean cloth should be passed to remove all product residue. There is no need to degrease indiscriminately, there are bearings that are self-lubricated, and a degreasing product could make them lose their qualities. It must be done individually and carefully.



Warning

To clean the chain and other fine components, cotton ear buds must be used.

- Grease: The same type of lubricant is not used for all components. For the steering and hubs solid grease is used, while for the chain it is liquid petroleum jelly or special chain oil.



Warning

Do not use 3 in 1 oil, this type of oil will dry immediately and that is not convenient.

The use of WD-40 is not recommended for the chain because dirt will stick to it and the chain will end up destroyed, and the pinions and chainrings will be damaged as well. WD-40 is useful in drive shafts. Oil and spray must be applied close to the target point.

Brakes

- Removing the brakes: To clean and adjust the brakes, it is necessary to follow the following steps to remove them:
 - a. The cable is loosened in the handle (with the relevant wheel), then the cam cable is released that does not have a screw, it is pressed, and the other screw is loosened. Now it will be removed with an Allen key, you should look at how the springs are because there is one longer than the other. the short anger inserted in the cam, and the length in the frame. also note which hole the cables were in. finally remove the shoes, to change or clean them, with an Allen key and a flat one.
- Cleansing: The cleansing process is very similar to the other components. Clean with a cloth slightly moistened with water or degreaser. It is convenient to clean the internal springs well, because a lot of dirt is stored there.
- Grease: Solid grease will be made inside the spring, and the bolts will also be coated.
- Mounting: The cams will be mounted without the shoes first. The springs are placed on the cams (the longest spout outwards) and will fit naturally into the stud of the frame.

- The shoes: When a shoe is new it has a small shiny layer in the braking zone that does not give very good performance at first. The same occurs when it is used and there is a crystallization of the rubber on its surface. In both cases, it is solved by gently sanding the rubber to leave it virgin.
- The cables: It is recommended to change the cables every two brake changes, including the covers. The small tension wheels on the handles are loosened two or three turns, to tighten the cable further, and the cam cable that does not have a screw is put on. Then the cams are brought together with one hand and the screw is tightened with the other hand. **The vehicle will be fully braked, now the small wheel is released one turn at a time to adjust the brake.**